The Effects of Integrated Chemical Catalysis and Reductive Pretreatment on Hydrothermal Liquefaction Derived Bio-oil Yield, Composition, and Stability

A THESIS
SUBMITTED TO THE FACULTY OF THE
UNIVERSITY OF MINNESOTA
BY

GLEN PETERSON

IN PARTIAL FULFUILLMENT OF THE REQUIREMENTS
FOR THE DEGREE OF
MASTER OF SCIENCE

Ulrike Tschirner

July, 2018

Acknowledgements

I would be remiss to suggest starting this acknowledgements section any other way than by thanking Dr. Ulrike Tschirner. Her tireless support and continuous feedback allowed me to reach heights that I didn't think I was capable of. She gave me an opportunity to do what I love in academia and research, and for that I will always be grateful. I wish I were better at articulating my appreciation in a more coherent manner, so I will just say, thank you Dr. Tschirner.

I would also like to thank my examination committee: Dr. Ulrike Tschirner, Dr. Shri Ramaswamy, and Dr. William Tze. Your patience and feedback was greatly appreciated during the process of writing and completing my research project.

There are other faculty, staff, and colleagues I would also like to recognize. Foremost, Leonard Reynolds for being a friend and mentor throughout my entire graduate school career, especially for the summer of 2017. Dr. Roger Ruan along with his Ph.D. candidate Liangliang Fan were instrumental, as they aided me in establishing the foundation for the analytical section of my research. Adam Talajkowski also deserves

recognition for his assistance during the summer. He did a respectable portion of the repetitious work that needed to get done. Without him, I would probably still be in the lab to this day.

In addition, I would also like to show my gratitude to Stephen Harvey, Sean Murray, Lucas Stolp, William Dean, Lenilton Vidal, Stephanie Harris, and Sean Bartz, who all in some manner aided me in my research. We never accomplish things on our own, and these people helped me along every step of the way.

Finally, as with all acknowledgements sections, I am legally obligated to thank my parents and family. Mom and Dad, I suppose you did an okay, albeit passable job of raising me and supporting me through these tumultuous times. Phil and Lauren, many times you teased me or actively rooted against me, but I know it was because you cared (somehow). Genuinely, I want to thank you all for your care and support through this journey, I really do appreciate it.

Sincerely,

Glen Peterson

Abstract

Bio-oil is a viscous mixture of aldehydes, ketones, organic acids, furans, phenolics, etc. It can be used for many different applications such as chemical generation, fuels, or can be upgraded to higher value products. However, due to its acidic nature and high oxygen content, bio-oil is very unstable. Integrated chemical catalysis and reductive pretreatment of the biomass feedstock were performed in an effort to stabilize the resultant bio-oil from hydrothermal liquefaction (HTL).

Various control (water), acidic (sulfuric acid), basic (sodium hydroxide), and reductive (sodium dithionite) solutions were added to the reaction chamber directly as the HTL solvents with the biomass (corn stover and 2-year hybrid poplar) for integrated chemical catalysis trials. Conversely, reductive pretreatments with sodium borohydride and sodium dithionite were completed separately, using DI water as the hydrothermal liquefaction solvent. The feedstocks were heated to 100°C for 30 min, then heated to 350°C, and finally quenched in a cool water bath.

Yield, composition, and stability analysis were conducted using fractionation and GC-MS techniques. Overall phase distribution was

relatively unaffected by varying integrated catalysis treatments i.e. solids, liquids, gases. Acidic integrated catalysis increased furan derivative relative abundance in the resulting bio-oil, while alkaline integrated catalysis and reductive pretreatments decreased furan derivative content. Also, reductive pretreatments increased double bonded γ-carbon large aromatic fragments such as eugenol. CHOS elemental composition of the bio-oil was largely unaffected by the varying treatments. Reductive pretreatments and alkaline catalysis trials increased resultant bio-oil pH and subsequently bio-oil stability, whereas acidic catalysis lowered bio-oil pH and destabilized the product. Reductive catalysis integrated many sulfur compounds in the bio-oil, causing many analysis difficulties.

Table of Contents

List of Tables

List of Figures

Chapter 1 Introduction

Due to the increase in global demand for energy and chemicals, a diversification in processing technologies will have to occur. With concerns about climate change, many sources of raw materials such as crude oil and coal are being considered to be phased out for greener technologies that have less of an impact on the world ecology (Azadi, Malina, Barrett, & Kraft, 2017). Biomass thermochemical conversion is not a new technology, however it has become more economically viable over the past 30 years (Bridgwater, 2012). One example of this technology, pyrolysis, has been used for thousands of years for the creation of charcoal via slow pyrolysis of wood.

Hydrothermal liquefaction is another thermochemical conversion process that is similar to pyrolysis in that it utilizes high temperatures to generate a versatile product called bio-oil. Bio-oil can be used as a fuel or a source of chemicals through many post-processing upgrading techniques, of which many will be discussed below. This carbon-neutral type of processing is necessary as the world develops cleaner, more efficient technologies to tackle global problems such as energy demands and climate change.

While other methods of biomass conversion are in use today, such as corn conversion to ethanol, most of the processes focus on generating transport fuels. These chemical and biochemical processes are inherently restrictive due to processing requirements for optimal production. Corn is a very pliable feedstock that can be converted via these chemical and biological pathways much easier than herbaceous or woody materials. These low value biomasses have a higher recalcitrance to conversion due to their high cellulose content, as opposed to corn which has much more starch and is thus easier to convert. This makes biological conversion problematic, as microbes and fermentation require readily digestible feedstocks. Also, chemical conversion can lead to yield loss, especially in lignin-rich materials, which are especially difficult to convert.

Thermochemical conversion of these recalcitrant biomasses can open the door to many other product types i.e. platform chemicals. Platform chemicals such as hydroxymethylfurfural and levulinic acid have diverse applications for use in fuels, solvents, pharmaceuticals, cosmetics, plastics, and more (Caretto & Perosa, 2013). While green fuel and energy generation are fundamental and necessary for a sustainable future, renewable sources of chemicals are just as important. That is why bio-oil

production and development of more efficient thermochemical conversion pathways is of paramount concern in the fast-changing industrial sectors.

This thesis will quantify the mechanism of hydrothermal liquefaction and the varying effects of integrated chemical catalysis and biomass reductive pretreatments on the yield, composition, and stability of the resulting bio-oil.

Chapter 2 Literature Review

2.1 Biomass Structure and Composition Overview

Biomass, generally defined, is renewable organic material that comes from plants or animals. This material includes numerous resources, such as agricultural residues, woody materials, herbaceous grasses, etc. The cellular structures of plant materials, and more specifically the cell walls, is a combination of primary and secondary wall configurations. Primary walls surround growing cells whereas secondary walls surround mainly specialized cells and contain thickened structures containing lignin (Keegstra, 2010). These plant walls, shown in Figure 2.1 (Plomion, Leprovost, & Stokes, 2001), are principally composed of cellulose, hemicellulose, and lignin. These three building blocks are the main reactants in biomass conversion to upgraded products.

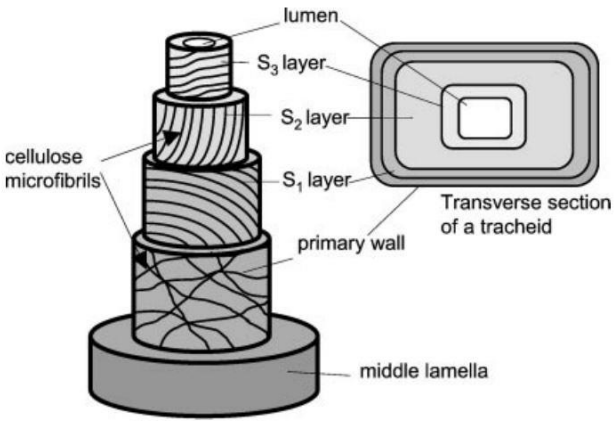

Figure 2.1 Plant wall structure (Plomion, Leprovost, & Stokes, 2001)

Cellulose, the main biopolymer found in plant material, is composed of glucose monomers linked into chains by the β-1-4 bond.

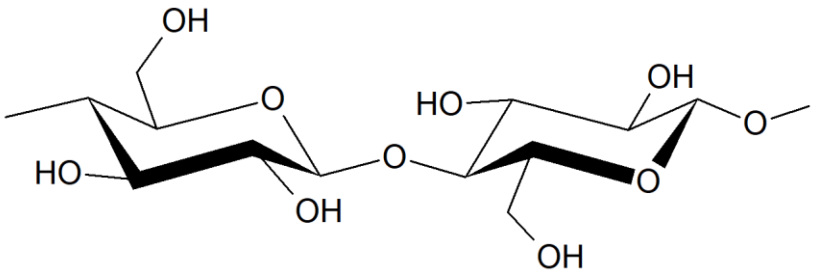

Figure 2.2 Cellulose structure and linkage

These chains interact with each other via hydrogen bonding to form microfibrils, a subset of its overall crystalline structure (Somerville, 2006). There are also intermolecular interactions between cellulose and hemicellulose or lignin. Cellulose has high recalcitrance due to the strong β-1-4 bond and its crystalline structure. This recalcitrance makes cellulose a difficult biopolymer to convert to fuels and other bioproducts without pretreatment (chemical, physical, thermochemical etc.).

Hemicellulose is composed of polysaccharide chains containing either hexose and/or pentose sugars. Common hemicelluloses include xylans, mannans, and glucomannans. A segment of hemicellulose is displayed in Figure 2.3.

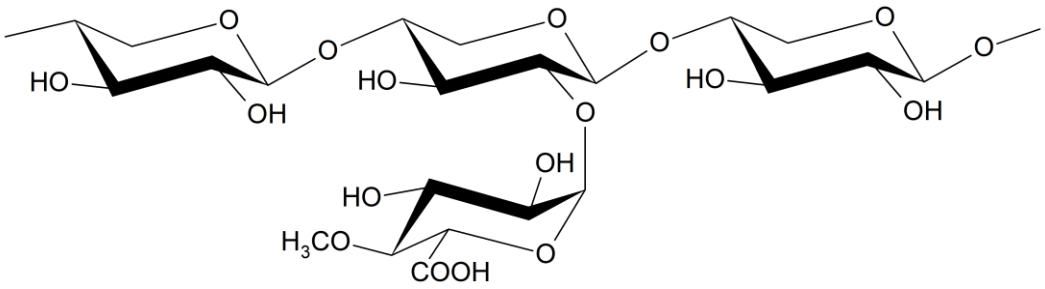

Figure 2.3 Common hardwood hemicellulose: 4-O-Methyl-D-glucouronoxylan

These chains form large, branching polymers that do not contribute to a crystalline structure, making them more susceptible to thermal or chemical degradation compared to cellulose (Mohan, Pittman, Jr., & Steele, 2006). In addition, hemicellulose also contains a significant number of acetyl groups that can hinder such processes as enzymatic hydrolysis from breaking down cellulose (Li, Thompson, & Thompson, 2016). As such, biological and chemical processing often requires purer feedstocks to increase product yield, whereas thermochemical treatment can utilize whole biomass more efficiently.

The final main constituent of biomass is lignin. Lignin is a large macromolecule composed of many cross-linked phenolic polymers (Figure 2.4).

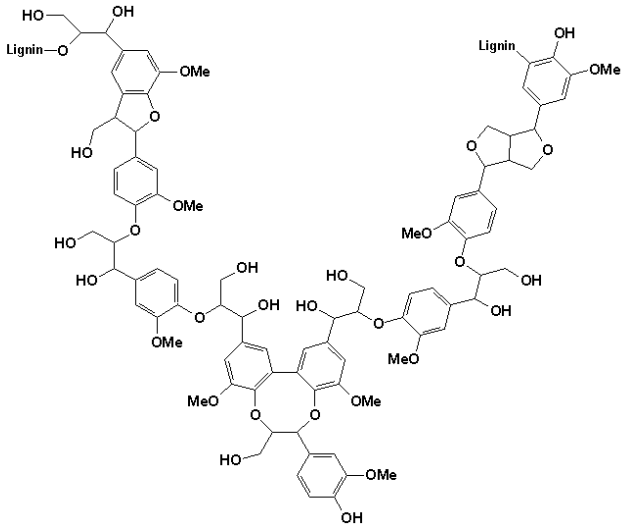

Figure 2.4 Small section of lignin structure

Lignin is a carbon dense material, containing many phenols and methyl groups. As will be discussed, limiting oxygen content in a biofuel (such as bio-oil) increases its overall value. Also, lignin contains many carbon-carbon bonds, making the degradation and/or removal of lignin from biomass difficult.

There are three lignols that are the building blocks of the large lignin macrostructures. From Figure 2.5, (1) p-coumaryl alcohol, (2) coniferyl alcohol, and (3) sinapyl alcohol when incorporated into the lignin molecule form p-hydroxyphenyl **H**, guaiacyl **G**, and syringyl **S** (Boerjan, Ralph, & Baucher, 2003).

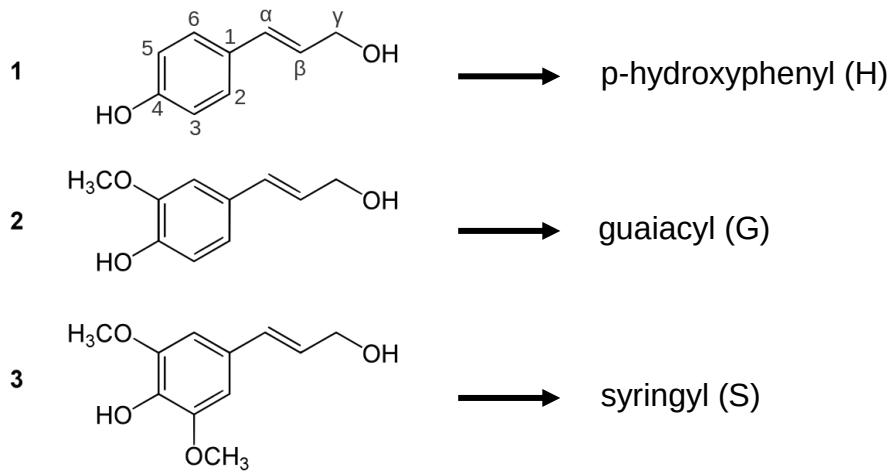

Figure 2.5 Lignol structures (Boerjan, Ralph, & Baucher, 2003)

Hardwood lignins, such as those in hybrid poplar, incorporate G and S lignin units and only traces of H units. Softwood lignins utilize mostly G units with low levels of H units. Grasses (herbaceous biomass) utilize G and S units with more H units than hardwood (Boerjan, Ralph, & Baucher, 2003). In addition of forming a sort of glue for holding the biomass together, lignin forms lignin-carbohydrate complexes, attaching to cellulose or hemicellulose chains. This, in turn, again increases the difficulty of removing lignin from raw biomass.

Biomass is diverse in composition appropriation among taxa. Herbaceous materials tend to have higher cellulose and hemicellulose content, whereas woody materials, especially softwoods, are rich in lignin. Table 2.1 summarizes the cellulose, hemicellulose, and lignin contents of

varying biomass types (Vassilev, Baxter, Andersen, Vassileva, & Morgan, 2012).

Table 2.1 Cellulose, hemicellulose, and lignin content of varying biomass and normalized to 100% (Vassilev, Baxter, Andersen, Vassileva, & Morgan, 2012)

Type of Biomass	Species	Cellulose	Hemicellulose	Lignin
Woody Biomass	Pine	48.1	23.5	28.4
Woody Biomass	(General) Hardwood	46.8	30.4	22.8
HAB[1]	Elephant grass	31.5	34.3	34.2
HAB[1]	Switchgrass	48.7	38.4	12.9
Other Residues	Corn stover	47.4	30.3	22.3

[1] Herbaceous and agricultural biomass

Choosing biomass species is integral when working with biomass conversion processes of any sort. In regards to thermochemical conversion, cellulose, hemicellulose, and lignin content of the feedstock will have a large impact on the effectiveness of the degradation, the operating conditions necessary to convert the biomass, and the products formed. Also, biomass composition will dictate chemical catalytic effectiveness.

2.2 Bio-Oil Overview

One of the most important issues facing the world is the use of fossil fuels and the resulting environmental consequences. Conventional fuels such as coal and oil generate the majority of the world's energy and are used as the raw materials for many chemicals. These chemicals are converted into the everyday products that we use, such as plastics, cleaners, and food. To create a sustainable society, not only does renewable energy need to be implemented on a massive scale, but renewably sourced chemicals for these essential products must also be developed.

Bio-oil is a viscous mixture of many different chemicals that are generated from rapid and simultaneous depolymerizing and fragmenting of cellulose, hemicellulose, lignin due to a fast increase in temperature (Mohan, Pittman, Jr., & Steele, 2006). The intermediates (bio-oil) formed are then quenched to prevent further degradation (gas formation). This complex product is composed of varying compounds including organic acids, ketones, aldehydes, phenols, furans, hydrocarbons, and more. This versatile product has many uses, such as chemical generation, energy, and biomass densification.

However, there are some logistical barriers that must be overcome to increase bio-oil production. Economic feasibility relies heavily on the development of low cost biomass feedstocks, including feedstock consistency (tonnage/composition), transportation, and storage (Carpenter, Westover, Stefan, & Jablonski, 2014). In addition to feedstock hurdles, the thermochemical conversion process needs to be studied further to ascertain the optimum operating conditions and to fully understand the effects of biomass composition and pretreatment.

This section will overview bio-oil composition and yield and how they are effected by biomass type, production techniques, and bio-oil's use.

2.2.1 Yield, Composition, and Stability

Bio-oil composition and yield is reliant on the type of feedstock used in the thermochemical degradation. Cellulose, hemicellulose, and lignin have different intermediates that are a result of thermal fractionation, generating different products when the bio-oil is quenched. The overall yield of usable bio-oil is also greatly affected by the type and initial composition of the biomass. Table 2.2 shows the effect of varying feedstocks on the overall yield of bio-oil from hydrothermal liquefaction (HTL) (Xue, et al., 2016).

Table 2.2 Effect of biomass composition on bio-oil yield (%) from HTL (Xue, et al., 2016)

Biomass	Hemicellulose	Cellulose	Lignin	Bio-oil
White pine bark	29.19	21.14	49.67	36
White spruce bark	38.72	35.10	26.18	58
White birch bark	28.00	37.98	34.02	67
Empty fruit bunch	26.9	26.6	18.6	15.72 ± 1.05
Palm mesocarp fiber	22.2	23.1	30.6	16.40 ± 0.21
Palm kernel shell	22.9	24.5	33.5	22.83 ± 0.56

As shown, the type and composition of the feedstocks greatly impacts the yield of bio-oil from HTL. Depending on the specific HTL operating conditions and the type of feedstock used, biomass cellulose, hemicellulose, and lignin content greatly effects bio-oil yield and composition (Jindal & Jha, 2016). The direct impact each constituent has on bio-oil production is a difficult, widely studied topic that has yet to be explained fully. Trends point to *either* higher or lower bio-oil yields based on initial cellulose content. Truly the interactions of each biomass constituent is complex and should be considered on a case by case basis.

General kinetic models have been developed to further visualize the thermal degradation of cellulose, hemicellulose, and lignin. Figure 2.6 shows the three kinetic models for each of the main biomass building blocks (Jindal & Jha, 2016).

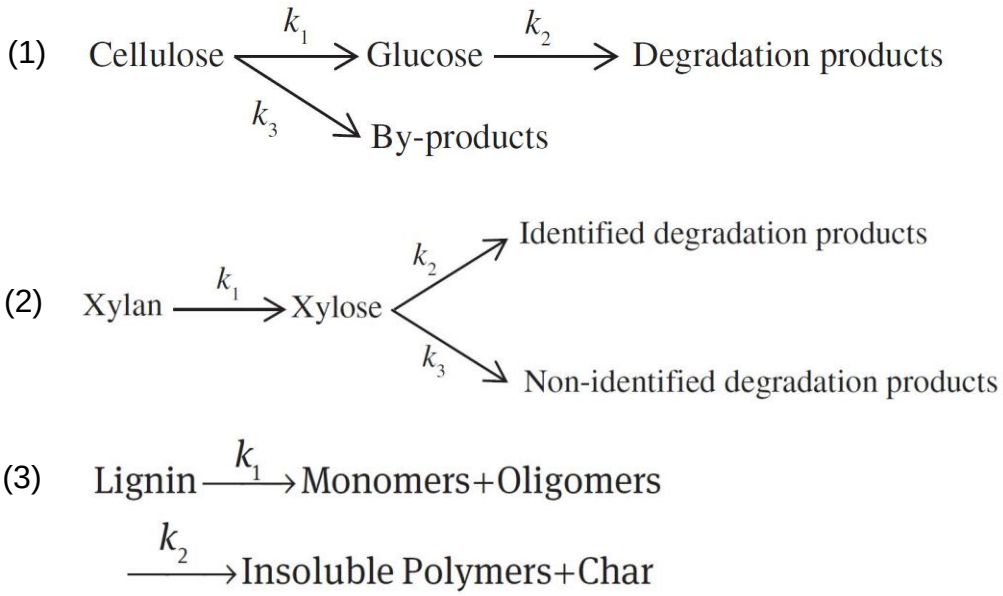

Figure 2.6 Generalized cellulose (1), hemicellulose (2), and lignin (3) thermal degradation kinetic models (Jindal & Jha, 2016)

Depolymerization of cellulose chains into glucose monomers and by-products is shown to be a simultaneous reaction in the proposed, generalized model. Glucose is then further degraded into other products such as furans (furfural, hydroxymethylfurfural). Xylan, a common hemicellulose polymer, is degraded into xylose monomers, similarly to cellulose degradation. From there, common, identified products and

uncommon, unidentified products are simultaneously formed via further degradation.

The lignin reaction model is very complicated and there is no current consensus on the reaction mechanisms of lignin thermal degradation due to the diverse structure of lignin (Jindal & Jha, 2016). The rate constants of the two-phase model refer to fast (k_1) and slow (k_2) thermal degradation reactions. The fast reaction degrades lignin into monomers and shorter oligomer chains, whereas the slow reaction yields insoluble polymers due to condensation reactions between soluble and insoluble species (Jindal & Jha, 2016).

A comprehensive and systematic study of HTL products from different feedstocks must be further developed to understand fully what the reaction pathways truly are.

The final aspect of bio-oil is its inherent instability. Bio-oil is a highly oxygenated, acidic mixture of a variety of compounds. These characteristics lead to a highly unstable product that is prone to secondary polymerization and condensation reactions that generally increase viscosity and lower the quality of the bio-oil. Studies have shown that low

pH bio-oil ages much faster than more neutral bio-oil. Meng et al. studied the effects of accelerated aging under varying pH conditions. At 2.5 pH the molecular weight increase in bio-oil was much higher than in pH 7.0 bio-oil (Meng, Moore, Tilotta, Kelley, & Park, 2014). This signifies the importance of mitigating (or at least controlling) highly acidic bio-oil fractions. However, while the pH of bio-oil is a good marker to understanding product stability, there are many other factors to consider such as bio-oil composition, temperature, and storage procedures.

2.2.2 Hydrothermal Liquefaction (HTL)

Bio-oil, as stated above, is formed through thermochemical degradation of biomass, followed by a rapid temperature reduction via quenching to condense or freeze the valuable liquid product intermediates. There are two main approaches to the thermal treatment of the biomass: hydrothermal liquefaction and pyrolysis. Using thermochemical techniques for converting biomass, many issues such as feedstock purity and feedstock chemical recalcitrance are avoided as the biomass is thermally degraded rather than by biological or chemical pathways. This also improves the economics of biomass conversion as there are less pretreatment steps needed to thermally degrade whole lignocellulosic biomass. Gasification is another main thermochemical process, however

its main products are gases, not bio-oil. Therefore, gasification will not be covered in this review.

HTL Operating Conditions

The first consideration that must be made when undergoing HTL is the operating temperature of the reaction. Moderate temperatures of 200–400°C have been shown to be optimal temperatures for HTL (Dimitriadis & Bezergianni, 2017). There are two main competing reactions that temperature has direct influence over: hydrolysis and repolymerization. Initial reactions decompose biomass into low molecular weight compounds. These compounds can then rearrange via condensation, cyclization, and polymerization reactions to form new compounds (Qian, Zuo, Tan, & He, 2007). As temperature increases, there is a promotion of either gasifying the products, or repolymerization/condensation reactions to form char. Generally, maximum bio-oil yields are found to be within the range of 250–350°C as shown by Figure 2.7 (Jindal & Jha, 2016).

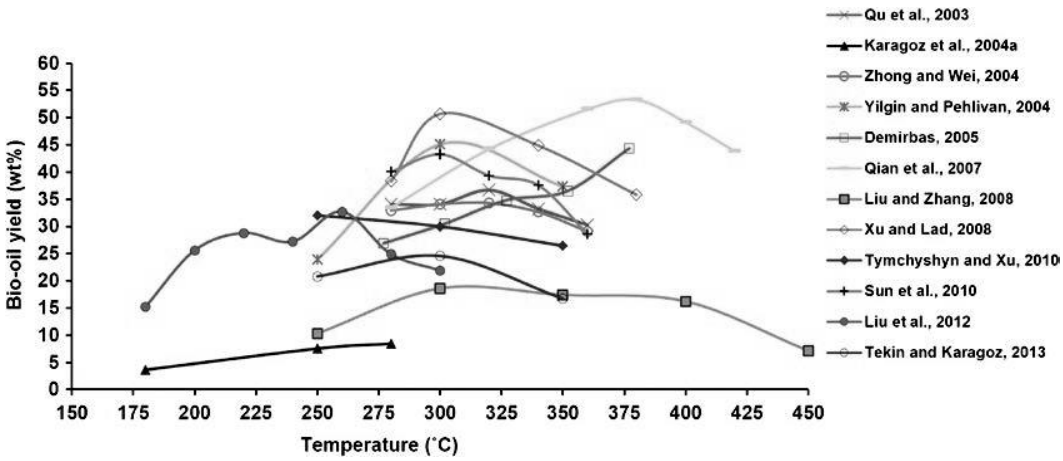

Figure 2.7 Bio-oil yields as a function of HTL operating temperature (Jindal & Jha, 2016)

Another important aspect of HTL is the operating pressure of the reaction. Water or other solvents are used as solvent, reactant, and catalyst in HTL. In the case of water, when undergoing subcritical HTL the pressure must be maintained at 5–40 MPa to ensure the water is in its liquid phase at the elevated temperatures (Williams, Westover, Emerson, Tumuluru, & Li, 2016). At supercritical water levels, pressure plays little role in bio-oil yield (Kabyemela, Takigawa, Adschiri, Malaluan, & Arai, 1998). Solvent cage effects slow free-radical reactions, which consequently favors the water-gas shift reaction rather than decomposition reactions (Jindal & Jha, 2016).

The final joint parameter that is paramount to HTL is residence time and heating rate. These two factors are directly related; with increasing heating

rates, residence time is decreased. Increased residence times showed higher yields of gaseous and char products due to the cracking of bio-oil intermediates and the condensation/carbonization reactions, respectively. Shorter residence times saw increased bio-oil reaction yields (Jindal & Jha, 2016).

The heating rate of the HTL also has a large impact on product distribution. Slow heating rates show increases in char products due to intermediate secondary reactions. Fast heating rates also show secondary reactions of the intermediates into gaseous products (Akhtar & Amin, 2011). Therefore, there needs to be a balance between residence time and heating rate. The residence time must be long enough to fully react the biomass, but not long enough to form char and gas products. Whereas, the heating rate needs to be fast enough to avoid carbonization reactions, but slow enough to avoid gasifying the feedstock.

Both these parameters are very much dependent on the biomass used, the products desired, and the operating temperature of the process. Therefore, there is no “standardized” residence time or heating rate, as they need to be considered with the other main operating conditions.

There are many more parameters that should be considered when designing a HTL process, including biomass to solvent ratio, initial pH, biomass particle size, and reducing gas environment i.e. decreasing the oxygen content of the reacting chamber to avoid combustion reactions. Along with these operating parameters, the general considerations of biomass composition and reactor type must also be weighed to fully understand what the variables are, and what the inevitable product will be.

HTL Process

There are three main processing types that will be discussed: batch (stirred and non-stirred), semi-continuous, and continuous. Due to pressure requirements of hydrothermal liquefaction, the actual chamber is most commonly a high pressure vessel.

Batch processing is the simplest form of HTL in which the entire process runs until completion, independent from other trials. Non-stirred batch reactors warm the outside of the chamber quickly to conductively heat the biomass. Induction heating and hot sand conduction have both been used in literature as batch processing styles (Zhang, Keitz, & Valentas, 2008), (Xu & Lad, 2008). Figure 2.8 shows the apparatus schematic used by Xu and Lad.

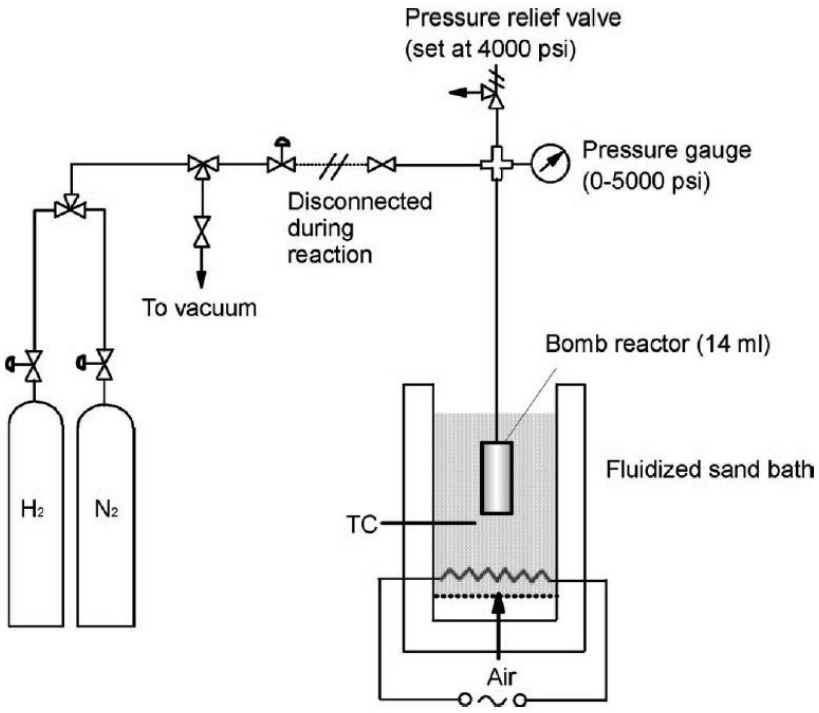

Figure 2.8 Bomb reactor schematic (Xu & Lad, 2008)

A correct biomass-to-water ratio is imperative when working with non-stirred batch processing. High heat and mass transfer is necessary to optimize bio-oil production from HTL. Having a dry biomass with little solvent water can result in unfavorable heat transfer, reducing bio-oil yield (Jindal & Jha, 2016). Stirred batch processing increases the heat transfer of the chamber to the biomass. When mixing, stirred processing evenly distributes the heat energy throughout the biomass, allowing for precise measurement and control of the reaction temperature (Zhong & Wei, 2004).

A semi-continuous processing experiment was developed by Hashaikeh et al. A set amount of biomass set in a stainless-steel tube reactor was thermally treated by preheated hot water (200–300°C) which was pumped using an HPLC pump at a flow rate of 3–8 mL/min. The outlet stream was filtered and analyzed as well as the residue left in the chamber (Hashaikeh, Fang, Butler, Hawari, & Kozinski, 2007). Increasing bio-oil throughput via continuous and semi-continuous processing is paramount to creating an economically viable system for creating renewably sourced chemicals.

Compared to batch and semi-continuous processing, continuous processing is the most economically feasible option. It provides the most throughput of the three and requires less hands-on maintenance or adjustment. A bench-scale tubular continuous HTL unit was used by Goudriaan and Peferoen. Figure 2.9 is the schematic this particular unit from feedstock slurry to product gases and liquids (Goudriaan & Peferoen, 1990).

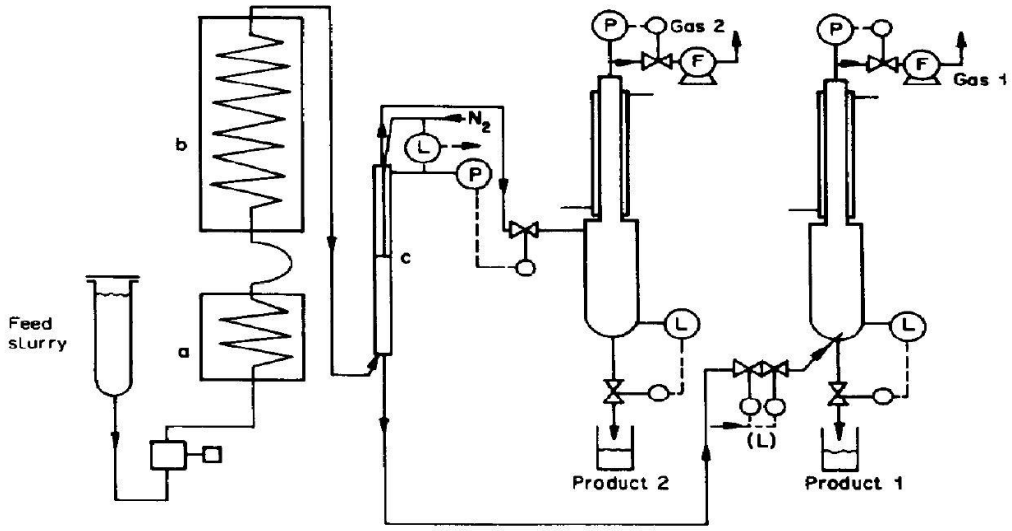

Figure 2.9 Continuous HTL bench-scale unit schematic (Goudriaan & Peferoen, 1990)

This process pumps a slurry of feedstock and water through a tubular, upflow reactor to convert the biomass. The liquid and gas phases are then separated and isolated.

HTL processing, using any of the aforementioned tactics, faces considerable obstacles such as upscaling of the process. Increased throughput requires larger pressure vessels. With larger pressure vessels, heat transfer becomes a greater issue i.e. how to heat a large volume of biomass quickly with limited chamber surface area (square-cube law). Increasing surface area while maintaining an acceptable volume is key to efficient HTL processing. While the processing fundamentals of this

experiment are something to look at, bio-oil production specifically is not part of the scope of the project.

HTL Products

Depending on the initial biomass composition, operational parameters, and processing scheme, the products from HTL are varied. Bio-oil is a mixture of many large compounds such as organic acids, ketones, aldehydes, phenols, alcohols, furans, aromatic hydrocarbons, and aliphatic hydrocarbons (Demirbas, 2011).

Compared to pyrolysis thermochemical conversion, HTL renders a higher quality product in terms of water content, oxygen content, and heating value (Dimitriadis & Bezergianni, 2017). Less water in the bio-oil, due to its reactant and penetrating nature at subcritical temperatures (Ramirez, Brown, & Rainey, 2015), increases the heating value of the product and decreases the amount of post-processing needed to upgrade the bio-oil if it were to be used in specific applications such as burning for energy. Decreased oxygen content is another favorable attribute of HTL derived bio-oil. High oxygen content signifies an acidic, unstable product that is prone to repolymerization.

Comparing the chemical composition of HTL and pyrolysis further provides evidence that HTL yields a more carbon rich and oxygen deficient product. Table 2.3 compares the elemental composition of bio-oil derived from HTL and pyrolysis (Gollakota, Kishore, & Gu, 2018).

Table 2.3 Elemental composition of bio-oil derived from HTL and pyrolysis (Gollakota, Kishore, & Gu, 2018)

Elemental Composition	HTL	Pyrolysis
C (wt%)	73	58
H (wt%)	8	6
O (wt%)	16	36
S (ppm)	< 45	29

Product elemental and composition distribution proposes that HTL derived bio-oil is more economically favorable compared to pyrolysis derived bio-oil. The only main, obvious drawback for HTL is the need for sealed high pressure vessels, which can cause difficulties when trying to create a continuous processing system that necessitates elevated pressures.

HTL Catalytic Approach

All previous descriptions of HTL have been under the assumption of non-catalytic HTL i.e. HTL using water as the solvent/catalyst. Catalytic HTL

uses varying solvents and catalysts to either shift product distribution or increase bio-oil yields. Char suppression while enhancing liquid product yield are the main objectives of catalysts in the HTL process. Catalysts can also be used to reduce repolymerization reactions of the bio-oil intermediates formed (Dimitriadis & Bezergianni, 2017).

Alkali salts (Na_2CO_3, K_2CO_3, etc.) are common catalysts used to increase bio-oil yields by reducing char/tar formation and accelerating the water-gas shift reaction (Kumar, Oyedun, & Kumar, 2018).

Alkali solutions such as NaOH and KOH solutions also affect bio-oil compositional and yield effects. Table 2.4 shows selected data of bio-oil % and CHNO content of bio-oil generated via NaOH and KOH catalyzed HTL (Khampuang, Boreriboon, & Prasassarakich, 2015).

Table 2.4 Select data of yield and compositional effects of NaOH and KOH catalyzed HTL (Khampuang, Boreriboon, & Prasassarakich, 2015)

Parameter	No Catalyst	NaOH	KOH
Amount (%)	-	5	5
Ethanol: water (v/v)	1:1	1:1	1:1
Oil %	49.0	52.3	53.3
C (%)	56.2	54.1	55.1
H (%)	6.9	7.8	7.2
N (%)	0.8	1.0	0.6
O (%)	36.1	37.1	37.1

As shown, NaOH and KOH have positive impacts on bio-oil yield. Alkali catalysts weaken the C-C bond resulting in lower activation energies regarding lignocellulose cleavage. Biomass swelling also increases internal surface area and causes wider separation of the linkages between cellulose and lignin (Khampuang, Boreriboon, & Prasassarakich, 2015). These effects allow for greater thermodegradation of the biomass into the constituent bio-oil compounds.

H_2SO_4 has also investigated as a viable catalyst to increase biomass conversion. Ye et al. 2014 studied the effects of catalyst loading during

low-heat (150°C) HTL. Liquefaction percentage increased significantly with catalyst percentage, from 44.99% with 1% catalyst to 92.86% with 2% catalyst (Ye, Zhang, Zhao, & Tu, 2014). Bio-oil yield was also shown to increase with H_2SO_4 addition according to Li et al. 2017. The general trend shown was increasing liquefaction and bio-oil yields with increasing sulfuric acid content (Li, Hu, & Xiao, 2017). These increases in liquefaction products indicates that integrated catalysis with H_2SO_4 aids in the breaking of biomass recalcitrance and formation of smaller molecular weight compounds.

Catalytic experimentation with HTL is not a new study and there are many papers regarding the effects of various catalysts including alkali salts, acid solutions, and physical zeolite addition. However, during the course of this literature review, no study was found dictating the effects of reduction agents such as sodium dithionite and sodium borohydride on the HTL process. Sodium dithionite is a common reducing agent used in pulp bleaching. Sodium dithionite, as well as sodium borohydride, being a reducing agent, reacts with carbonyl groups and other chromophoric systems in lignin. We hypothesize that the reduction process will assist in reducing oxygen content in the resulting bio-oil. High oxygen content

reduces bio-oil heating value, increases its acidity, and decreases the overall value of the product (Gollakota, Kishore, & Gu, 2018).

Comparison of HTL with Pyrolysis

Another major thermochemical reaction that is used in industry is pyrolysis. The process is very similar to hydrothermal liquefaction, such as the heating of carbon based material to volatize the feedstock into condensable vapors to obtain bio-oil. However, the major difference between pyrolysis and HTL is in operating parameters of the actual process. This leads to different product characteristics and processing/reactor schemes.

Reactor temperatures and retention time are the two major operating differences between HTL and pyrolysis. While HTL operates at temperatures ranging from 200–400°C for long residence times to volatilize biomass, pyrolysis reactor temperatures are higher at 450–550°C, with very short residence times of only 1–3 seconds. This relatively small temperature range enables the reactor to volatilize the feedstock, while avoiding unwanted reactions. If the temperature is too low carbonization reactions will increase solid yields, while if the temperature is too high there will be secondary reactions that further degrade the

condensable vapors into their constituent gases. Figure 2.10 shows this interaction of temperature discrepancy (Bridgwater, 2012).

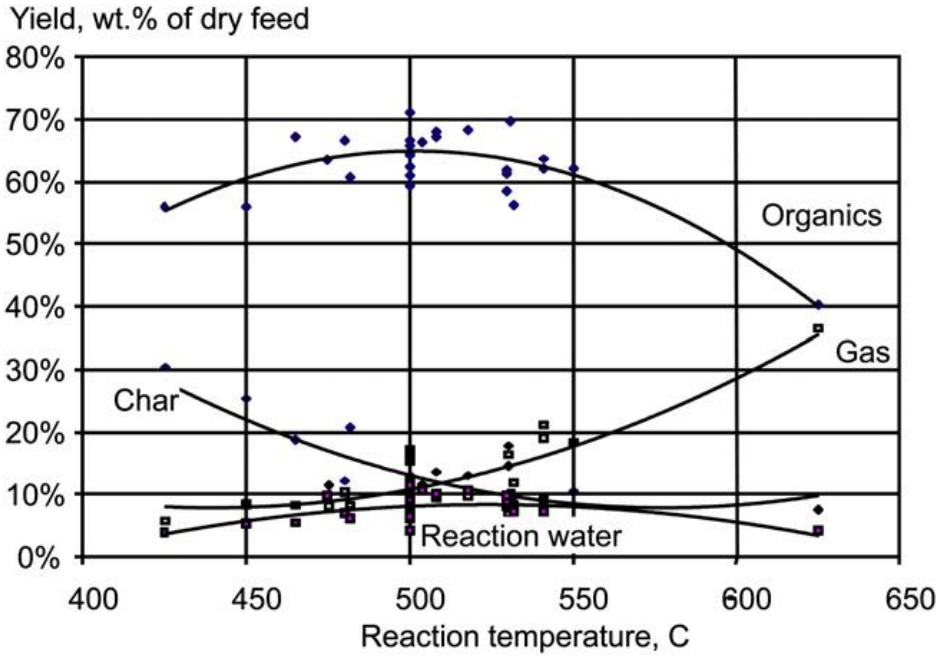

Figure 2.10 Reaction temperature effects on multi-phase yield of pyrolysis (Bridgwater, 2012)

As for residence times, a balance must also be maintained to optimize bio-oil yield. Fast-pyrolysis is a commonly researched type of pyrolysis that has retention times of only <1–3 seconds (Bridgwater, 2012). This is to increase condensable vapor production while avoiding carbonization or gasification reactions. Intermediate-pyrolysis uses retention times of 10 – 30 seconds. This approach has a reduced liquid yield and more char formation compared to fast-pyrolysis (Bridgwater, 2012). However, the

complexity and assumed capital cost of fixed bed reactors are lower than the fluidized bed reactors necessary for fast-pyrolysis. Truly even intermediate pyrolysis is a much faster process than HTL.

Reactor types for pyrolysis range from HTL-similar configurations i.e. fixed bed reactors, to very different configurations. One of these unique reactors is the bubbling fluidized bed reactor. This reactor uses a hot, gaseous medium to fluidize the feedstock and increase the heat transfer rate. The hot gas quickly volatilizes the biomass. The mixture of char, gas, and vapors are sent through a series of cyclones to separate the char. The vapors and gases are then quenched to condense the bio-oil out, which can then be separated from the fluidizing gases. The gas phase is then recycled through the system. This generates three outputs of bio-oil, char (which can be burned), and excess gas. Figure 2.11 shows a typical bubbling fluidized bed reactor configuration (Bridgwater, 2012).

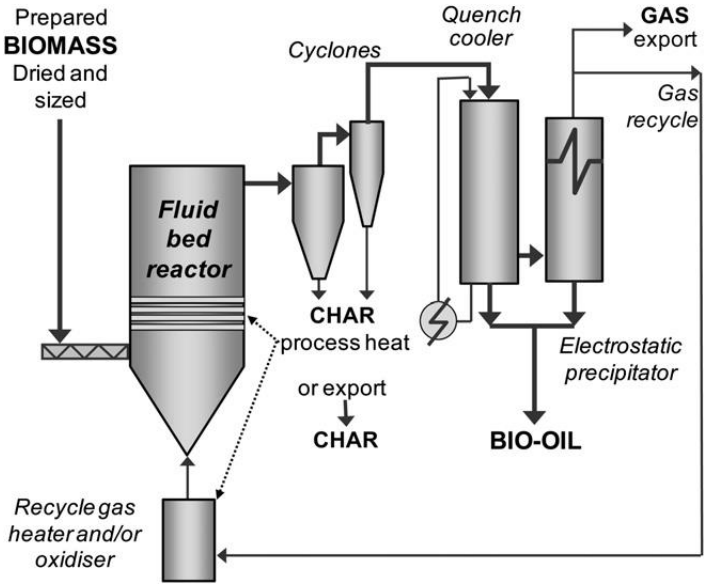

Figure 2.11 Common bubbling fluidized bed pyrolysis reactor configuration (Bridgwater, 2012)

Industrial examples of bubbling fluidized bed reactors include Dynamotive, who have created two plants which have throughputs of 100 t/d and 200 t/d. There are also many demonstration plants running around the world that range from 250 kg/d to 600 kg/d (Bridgwater, 2012). Since HTL is a slower process than pyrolysis, there is no requirement for fluidized bed reactors with extremely fast heating rates which are needed for pyrolysis.

The bio-oil products also differ between HTL and pyrolysis processing schemes. Bio-oil generated from pyrolysis is of lower quality in terms of oxygen content, heating value, and moisture content compared to the bio-

oil generated from HTL (Dimitriadis & Bezergianni, 2017). Table 2.5 shows the comparison in physical characteristics between bio-oil derived from HTL and pyrolysis (Gollakota, Kishore, & Gu, 2018).

Table 2.5 Bio-oil characteristic comparison between HTL and pyrolysis processes (Gollakota, Kishore, & Gu, 2018)

Characteristic	HTL	Pyrolysis
Moisture	5.1%	24.8%
HHV (MJ/kg)	35.7	22.6
Viscosity (cPa)	15,000	59

Water content in pyrolytic bio-oil is higher due to high dehydration reactions; compared to HTL bio-oil which is lower in water content due to water's reactant and feedstock-penetrating nature at subcritical conditions (Ramirez, Brown, & Rainey, 2015). While HTL has lower moisture content and a higher heating value, viscosity also greatly increases compared to pyrolytic bio-oil.

2.2.3 Bio-oil Use and Upgrading

Bio-oil has few direct uses due to its intrinsic complexity and composition. The most prevalent use for bio-oil production is the densification of biomass. Feedstocks such as switchgrass and corn stover have low

density and therefore increase transportation costs. Decentralizing biomass conversion is one valid economic solution to decreasing biomass transportation costs. Local farms would transport low density (high cost) biomass to a localized pyrolysis/HTL densification plant. The resulting bio-oil is then dense enough to be economically transported to a centralized conversion facility. Figure 2.12 visually shows the comparison between centralized and decentralized biomass conversion facilities (Braimakis, Atsonios, Panopoulos, Karellas, & Kakaras, 2014).

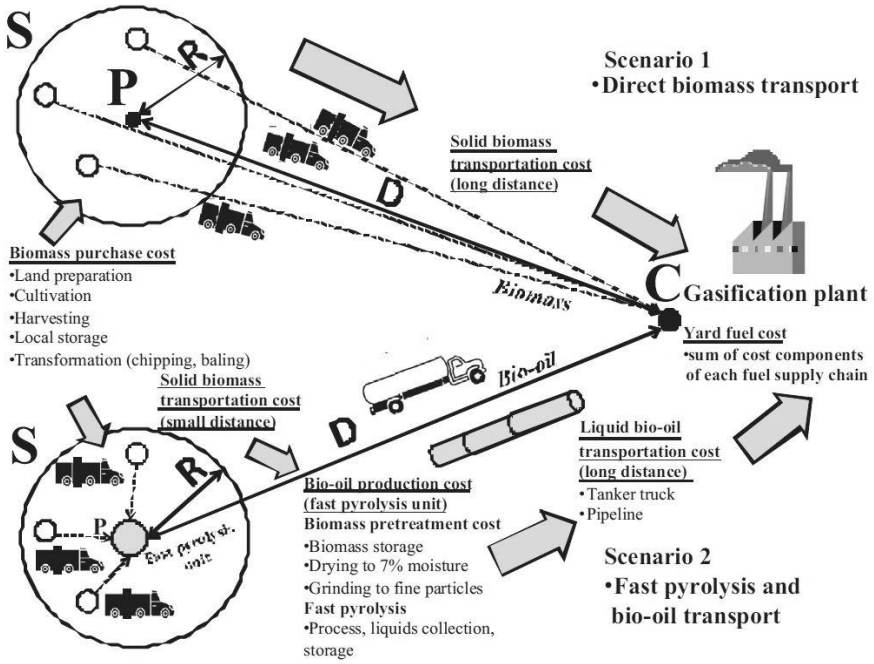

Figure 2.12 Visual comparison between centralized and decentralized biomass conversion (Braimakis, Atsonios, Panopoulos, Karellas, & Kakaras, 2014)

As shown, by transporting low density materials only short distances to be densified into bio-oil, the cost of transportation could be reduced.

Another direct use of bio-oil is chemical generation. Levoglucosan, resins, and adhesives are viably sourced, along with liquid smoke and wood flavorings, which are very popular bio-oil derivatives (Xiu & Shahbazi, 2012). Also, platform chemicals such as levulinic acid and methyl levulinate can be derived from bio-oil. These platform chemicals are especially valuable due to their diverse industrial applications such as conversion to fuels, plastics, pharmaceuticals, etc.

Bio-oil has also been used as a fuel for static energy applications such as boilers, burners, and furnaces. The high heating value and viscosity of HTL bio-oil is comparable to other fuel oil products, allowing it to be used in such applications. Other energy applications involve engines and turbines (Xiu & Shahbazi, 2012).

Although there are viable direct uses for bio-oil, much research has been done studying bio-oil upgrading techniques to increase the value of the product. Most fuels and chemicals produced by petroleum sources are able to be converted into useful forms and purified easily. Bio-oil

upgrading works on the same principle of taking a raw material and converting it into a product of greater value in a cost effective way. There are many bio-oil upgrading techniques including hydrotreating, emulsification, and steam reformation.

Hydrotreating tries to increase the hydrogen content of the bio-oil thus increasing the overall value. Hydrogenation, in practice, would saturate olefins and/or convert aromatics into naphthenes, etc. (Xiu & Shahbazi, 2012). The process requires high hydrogen pressure and high temperature, typically in an autoclave. Hydrogenation is a non-destructive treatment and should not greatly affect the boiling range while increasing the combustibility of the bio-oil. Catalysts are used to promote hydrogenation, of which there are many including Pt/Al_2O_3, Ni/HZSM-5, and $Ni36.5Cu2.3/ZrO_2$-SiO_2-La_2O_3 (Xian, Zhao, Xu, Han, & Yu, 2017). While hydrogenation can be effective, char, coke, and tar can be produced in relatively large quantities, causing catalyst deactivation and reactor fouling (Xiu & Shahbazi, 2012).

Another bio-oil upgrading technique is emulsification. The goal of emulsification is to create a fuel with bio-oil that can be used as a transport fuel with no engine modifications necessary (Bridgwater, 2012).

Bio-oil is not miscible with hydrocarbon fuels due to its high oxygen content and overall composition. When mixed thoroughly using both a mixing system (stirring or ultrasonic) and the addition of a surfactant, a stable emulsion can be produced from bio-oil (5%) and diesel fuel (Xian, Zhao, Xu, Han, & Yu, 2017). Current challenges with emulsification are the high cost of surfactants and energy needed for the emulsification. Also, engine corrosion and erosion have been shown to increase with emulsified fuels compared to the constituents by themselves (Bridgwater, 2012).

The final upgrading technique that will be discussed is steam reformation. Hydrogen gas is a green energy source that can cleanly combust with a great amount of energy. Therefore, there has been much research into hydrogen production via steam reformation of the aqueous phase of bio-oil. This requires bio-oil be separated into the water-soluble and water-insoluble phases. Steam reformation also requires rare/expensive catalysts that can passivate relatively easily (Xian, Zhao, Xu, Han, & Yu, 2017). Hydrogen gas, along with methane and carbon monoxide, was formed via steam reformation at high temperatures using a Ni-based catalyst. Acetic acid and hydroxyacetaldehyde were the main constituents

in the water-phase that decomposed into the high value gases (Wang, Montane, & Chornet, 1996).

Bio-oil is a valuable product in its own right and when upgraded to higher quality products. Biomass conversion pathways to these useful compounds have been widely studied and quantified. Acidic, basic, and reduction pathways are all used in industry as catalysts or for product formation. The next section will review some important chemical reaction pathways and their products.

2.3 Biomass Primary Reactions

Since we are proposing treatment of biomass in aqueous systems, some basic biomass reactions will be discussed here. Biomass can be directly converted in a wide range of products via chemical reactions. Many studies have been done researching and optimizing these reactions for industrial use. Acidic pretreatment is commonly used to break down the recalcitrant nature of biomass, remove or solubilize hemicelluloses for enzymatic biofuel production, and to convert the carbohydrate sugars into varying compounds such as hydroxymethylfurfural (HMF) and levulinic acid (Elumalai & Pan, 2011). Alkaline pretreatment, on the other hand, is

mainly used in the pulping/bleaching industry to remove lignin from lignocellulosic biomass (Wang, Xu, & Cheng, 2011). Reducing agents are also used in the pulping/bleaching industry to brighten the products via removal of lignin chromophores while maintaining pulp yield (Ellis, 1996).

2.3.1 Acidic Reactions

Cellulose and Hemicellulose Conversions

The pathways of cellulose and hemicellulose conversion to furans and then eventually to levulinic acid is a cornerstone to understanding acid-carbohydrate interactions. Figure 2.13 shows an adapted hydrolytic pathway of cellulose and hemicellulose to their respective furan derivatives (Elumalai & Pan, 2011).

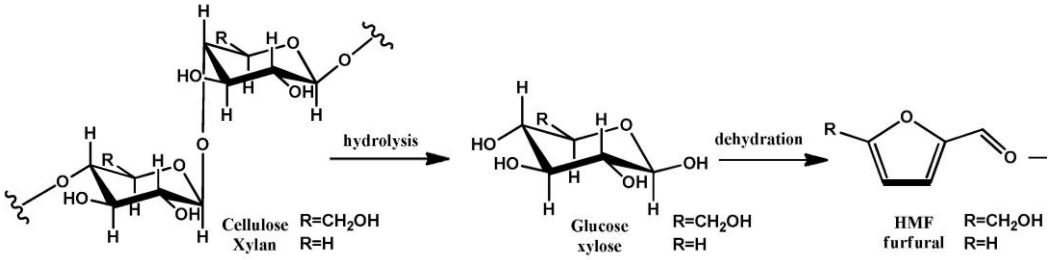

Figure 2.13 HMF and furfural conversion pathway from cellulose and hemicellulose, respectively (Elumalai & Pan, 2011)

The respective polymer is cleaved into glucose or xylose monomers via acid hydrolysis. H_2O attacks the β-1-O-4 linkage to depolymerize the

carbohydrate. Glucose (or an isomer) or xylose then undergoes dehydration to hydroxymethylfurfural or furfural, respectively. An H^+ ion catalyzes this reaction.

Levulinic acid is an important platform chemical that can be formed from HMF through a simple rehydration reaction. Figure 2.14 shows the full conversion process of cellulose hydrolysis to formation of levulinic acid from HMF (Chiappe, et al., 2018).

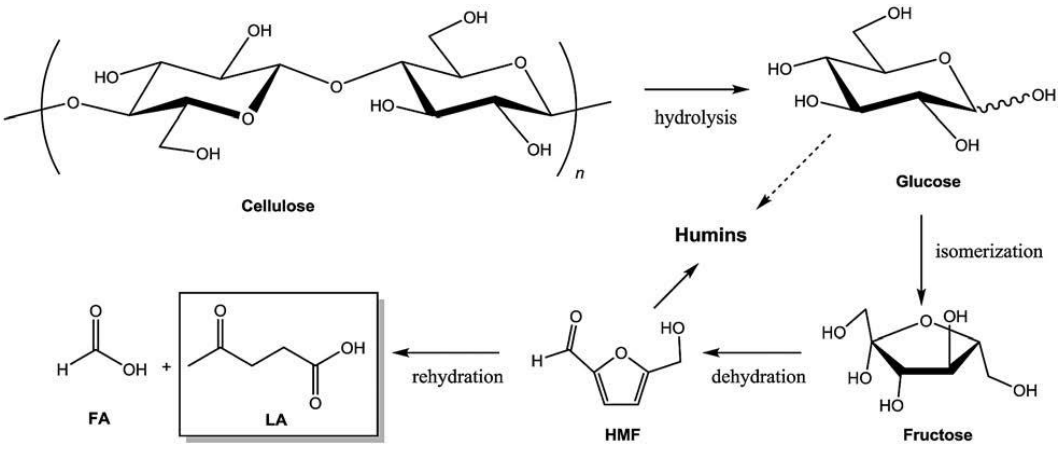

Figure 2.14 Cellulose to levulinic acid reaction pathway via acid catalysis (Chiappe, et al., 2018)

After HMF is formed via the hydrolysis and dehydration reaction, levulinic acid is formed by adding two water molecules to HMF. An acid catalyst must be present for cellulose to be converted into levulinic acid. High temperatures and long residence times result in the highest yields for

levulinic acid (Chiappe, et al., 2018). One major drawback for this process is that pure cellulose is assumed. Lignocellulosic biomass is a much more complex structure containing hemicelluloses and lignin-carbohydrate complexes. These impurities cause inhibition in the levulinic acid formation, and therefore much lower yields (Yoon, Han, & Shin, 2014).

Lignin Acid Reactions

Lignin is difficult to break down or convert due to its recalcitrant and varied structure. Acid catalyzed reactions generally focus on fragmentation via the α-ether linkage of a larger lignin macromolecule. Figure 2.15 shows this fragmentation of lignin under dilute acid conditions (Fengel & Wegener, Wood: chemistry, ultrastructure, reactions, 1983).

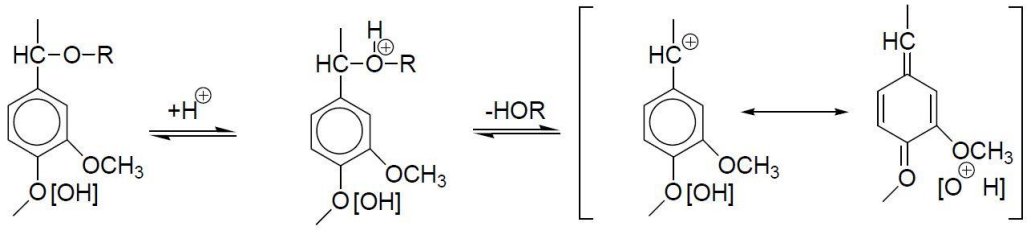

Figure 2.15 Lignin degradation under acidic conditions (Fengel & Wegener, Wood: chemistry, ultrastructure, reactions, 1983)

The H^+ ion interacts with the oxygen linkage between the two lignin components, cleaving the bond. This acid cracking leads to the formation

of a benzylic carbonium ion intermediate which can lead to further reactions (Elumalai & Pan, 2011). Phenolic derivatives are a commonplace when lignin undergoes acid catalysis, especially under high temperature conditions.

Strong acid treatment of lignin can lead to condensation reactions in which lignin fragments recombine with C-C linkages that are very difficult to break. Figure 2.16 shows a condensation pathway of two lignin fragments under strong acid conditions (Elumalai & Pan, 2011).

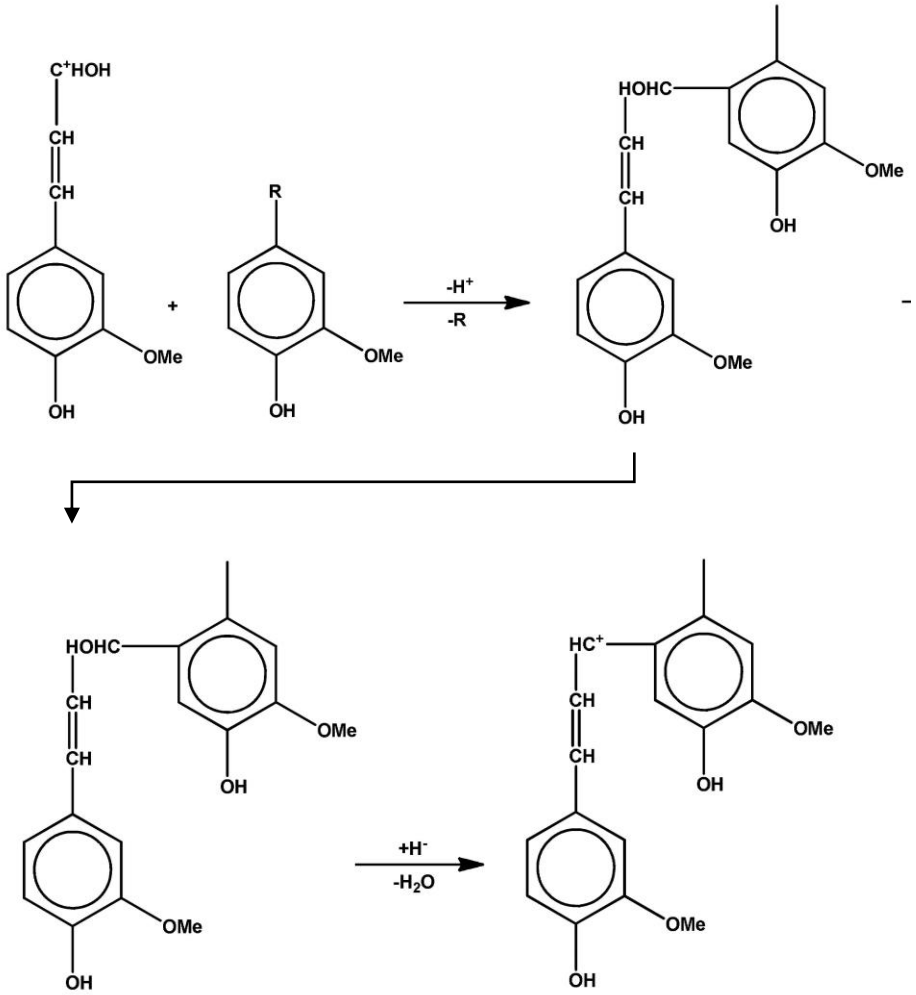

Figure 2.16 Lignin condensation reaction pathway (Elumalai & Pan, 2011)

The rate and frequency of these condensation reactions depend of the species involved and the environmental conditions (Elumalai & Pan, 2011). With strong acid conditions H^+ ions continuously drive the reaction forward, combining lignin fragments together via a C-C bond.

2.3.2 Basic Reactions

Peeling Reaction

The peeling reaction is the main pathway cellulose (or any other polysaccharide) takes when under alkaline conditions. The main emphasis of the reaction is the shedding of glucose monomers from the ends of the cellulose polymer chains. The peeled monomers can then undergo further conversion reactions, such as benzylic acid rearrangement to form a glucoisosaccharinic acid. This pathway is shown in Figure 2.17 (Elumalai & Pan, 2011).

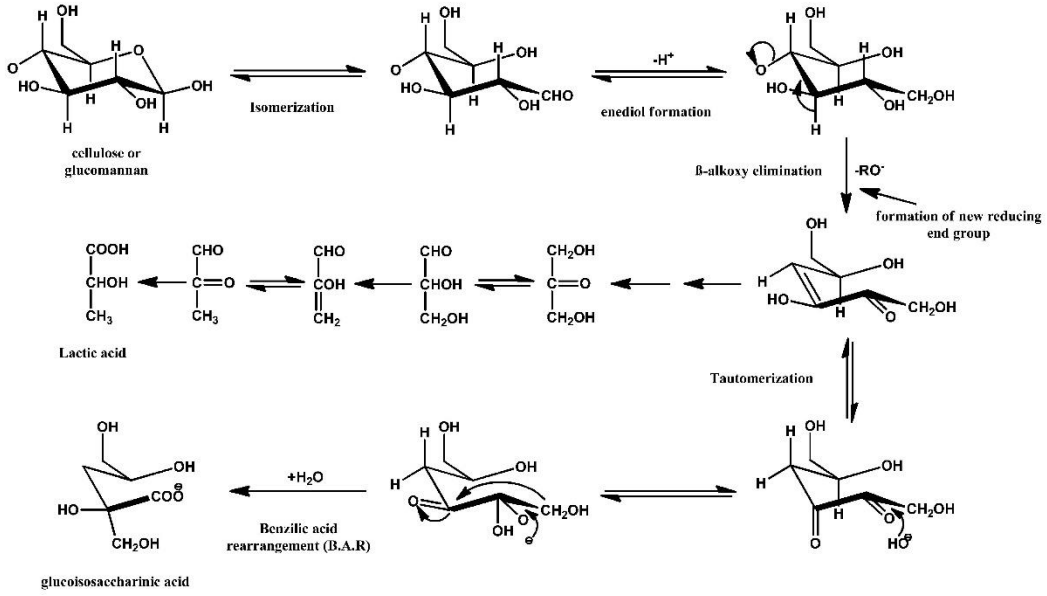

Figure 2.17 Peeling reaction pathway (Elumalai & Pan, 2011)

This reaction only peels monomers from the reducing end of the cellulose chain, and is therefore relatively ineffective at depolymerizing the biomass. The peeling reaction continues until the stopping reaction occurs on the reducing end, where the hexose monomer stays attached to the cellulose chain, preventing further depolymerization.

Alkaline Hydrolysis

As previously stated, the peeling reaction only functions from the reducing end of the cellulose chain. Depolymerization is slow under these conditions. However, if the temperature of the system is elevated, alkaline glycosidic hydrolysis can occur, greatly increasing the number of reducing ends in a cellulose chain, thus speeding the rate of depolymerization. Figure 2.18 shows the alkaline hydrolysis reaction (Elumalai & Pan, 2011).

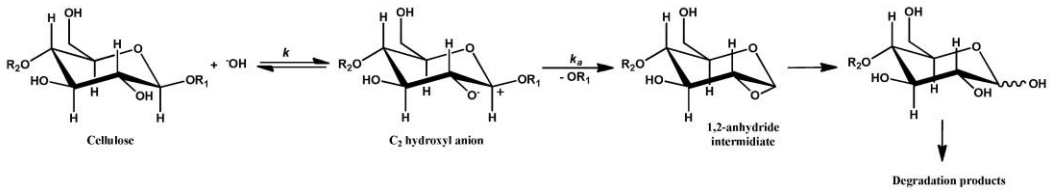

Figure 2.18 Alkaline hydrolysis at elevated temperatures (Elumalai & Pan, 2011)

Generally, alkaline hydrolysis is considered a slow reaction that requires high temperatures at or above 180°C. However, due to their effect of

increasing the number of reducing ends in a cellulose chain, this reaction can have a significant impact on the degree of biomass depolymerization.

Lignin Alkaline Reactions

There are two main lignin reactions that happen under alkaline conditions. One is a β-O-4 side chain elimination reaction, and the other is a condensation reaction. The β-O-4 linkage is cleaved under alkaline conditions after a rearrangement of a phenolic fragment to a quinone methide intermediate. Other cleavages include a γ-C elimination, releasing formaldehyde. Figure 2.19 shows the varying pathways a lignin segment can take under these conditions (Elumalai & Pan, 2011).

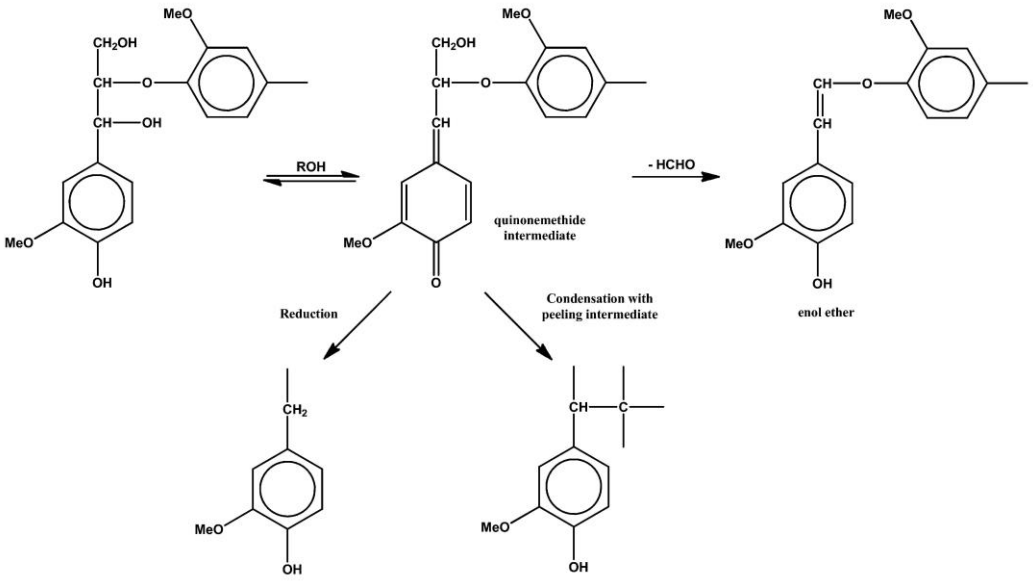

Figure 2.19 Lignin degradation under alkaline conditions (Elumalai & Pan, 2011)

These elimination reactions greatly reduce the degree of polymerization of the lignin in the biomass feedstock. Side chain cleavage can also reduce biomass recalcitrance and allow for easier reactivity/degradation.

Alkaline conditions can also lead to lignin condensation reactions, as shown in Figure 2.20 (Elumalai & Pan, 2011).

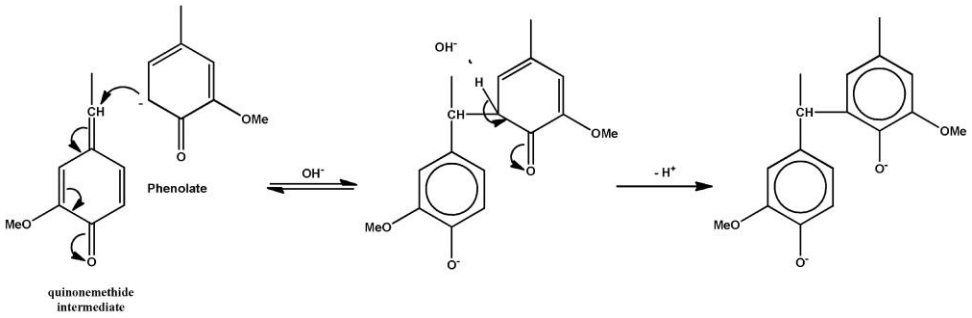

Figure 2.20 Lignin condensation under alkaline conditions (Elumalai & Pan, 2011)

Through reaction with a quinone methide intermediate, phenolic side chains can condensate via C-C bonds i.e. α-5 linkage. Lignin-carbohydrate complexes have also been theorized to be generated through peeling reaction-quinone methide intermediates (Gierer & Wannstrom, 1986).

2.3.3 Reduction Reactions

Sodium Dithionite Reactive and Nonreactive Species

Sodium dithionite will be one of the reducing agents this literature review will focus on, the other being sodium borohydride. Sodium dithionite is typically used for bleaching purposes when a 4-14 point increase in brightness is needed. It is considered a lignin-retaining bleaching agent due to its function. Sodium dithionite (and its reactive species), converts chromophores to their colorless forms without degrading the lignin itself (Ellis, 1996).

The main reactive species in sodium dithionite bleaching is the sulfur dioxide radical ion (Dence, 1996). The decomposition of dithionite to the sulfur dioxide radical is shown below in Reaction 2.1.

$$S_2O_4{}^{2-} \leftrightarrow 2SO_2{}^{\cdot-} \qquad \textit{Reaction 2.1}$$

Other reactive species include sulfur dioxide (SO_2), sulfur dioxide di-anion (SO_2^{2-}), and bisulfite (HSO_3^-) (Dence, 1996). Their decomposition reactions are shown below in Reaction 2.2 and 2.3.

$$2SO_2{}^{\cdot-} \rightarrow SO_2 + SO_2{}^{2-} \qquad \textit{Reaction 2.2}$$

$$S_2O_4{}^{2-} + 2H_2O \leftrightarrow 2HSO_3{}^{-} + 2H^+ + 2e^- \qquad \textit{Reaction 2.3}$$

There are other inorganic species that occur from the decomposition of sodium dithionite when it is exposed to oxygen including sulfite, sulfate, thiosulfate, and polythionate. These species do not have a major impact on the elimination of chromophoric systems in lignin (Dence, 1996). Sodium dithionite pulping brightens lignin and extractives, while cellulose and hemicellulose are generally unaffected.

Sodium Dithionite Reactions

The main reactive species, sulfur dioxide radical, can reduce quinone methide chromophores. Figure 2.21 shows this reaction pathway (Dence, 1996).

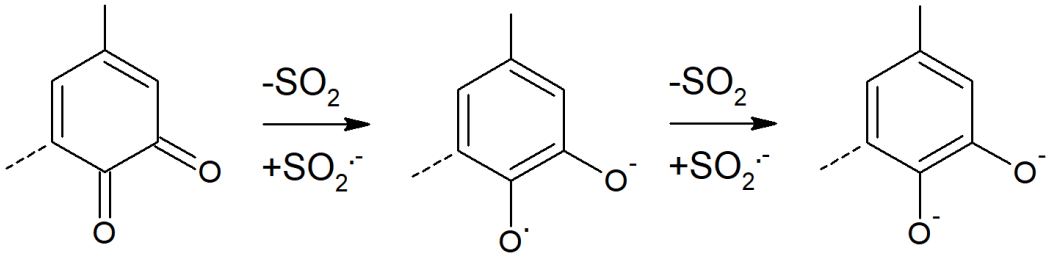

Figure 2.21 Quinone methide chromophore elimination by sulfur dioxide radical (Dence, 1996)

The sulfur dioxide radical breaks the quinone methide chromophore system, brightening the lignin fragment during bleaching. Along with the sulfur dioxide radical decomposition reaction, this pathway gives off sulfur dioxide. Decomposition must be limited by careful mill and environmental

control to prevent air from being introduced, speeding the reaction (Ellis, 1996).

Other lignin reactions occur mainly with bisulfite and dithionite species. These reactions are partial chromophore elimination reactions, focusing mostly on the top portion of lignin fragments. Figure 2.22 summarizes these reactions (Dence, 1996).

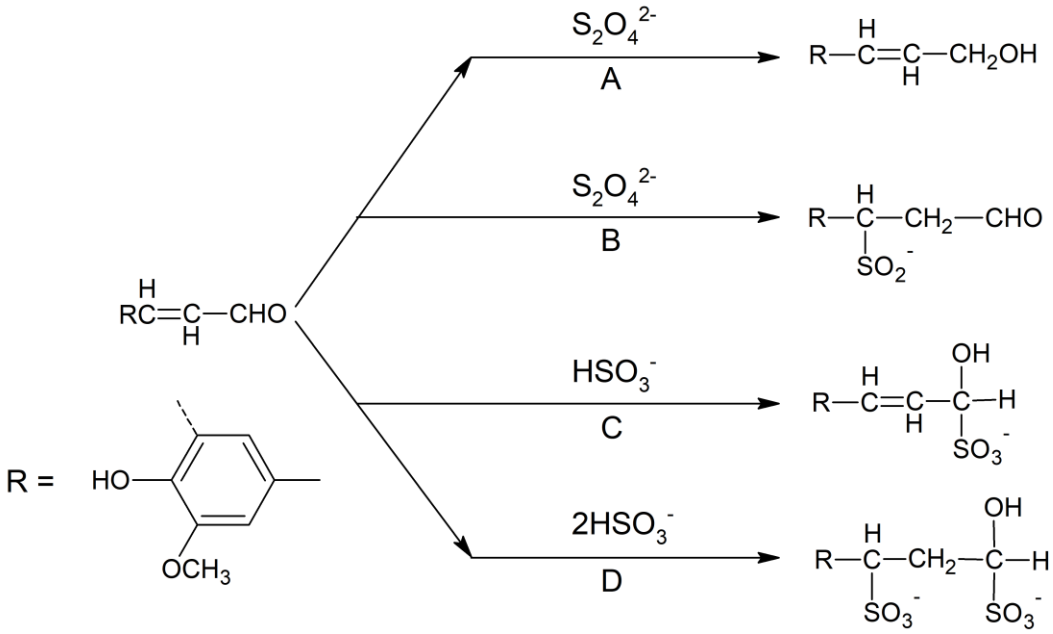

Figure 2.22 Partial chromophore elimination via dithionite and bisulfite reactions (Dence, 1996)

Reaction pathway A utilizes dithionite to react and interfere with the aldehyde group, whereas pathway B sees the attachment of a sulfur dioxide anion to the β-Carbon. Reaction pathways C and D see the

attachment of sulfur dioxide anions to both the aldehyde and α-Carbon groups, partially disrupting the chromophoric system.

Sodium dithionite, as previously mentioned, is a lignin-retaining bleaching agent that focuses on converting chromophores into their color-less forms or leucochromophores. However, this allows for the reoxidation of the leucochromophores into their quinonoid forms if reintroduced to oxygen or air (Dence, 1996).

Sodium Borohydride Reactions

Sodium borohydride, contrary to sodium dithionite, is a strong lignin-retaining bleaching agent, capable of reducing lignin or carbohydrate carbonyl aldehyde and ketone groups. The reducing species in sodium borohydride is a hydrogen anion. Figure 2.23 shows the simple reaction mechanism sodium borohydride uses on an aldehyde group.

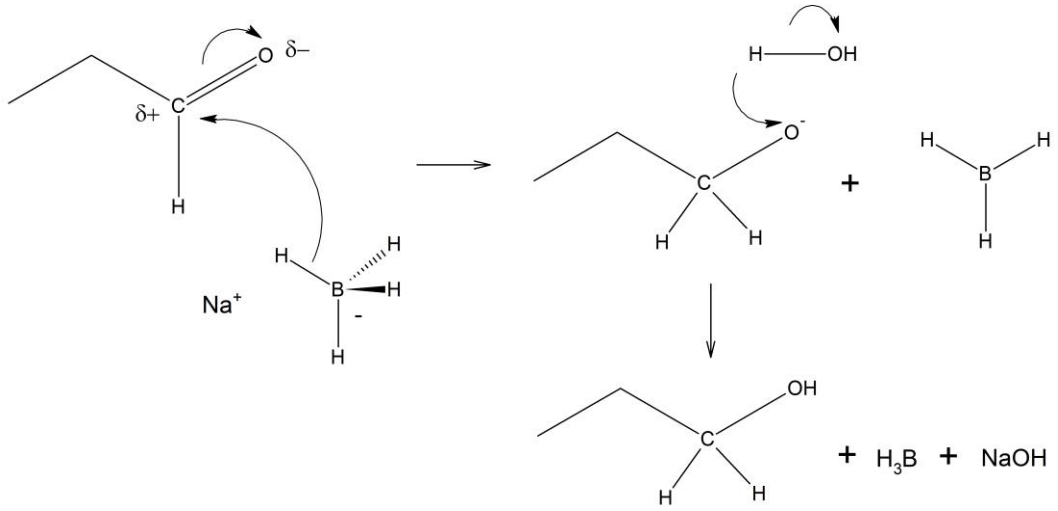

Figure 2.23 Aldehyde reduction by sodium borohydride

Ketone bonds are able to be reduced by similar mechanisms as aldehyde reduction. As shown, sodium hydroxide is a possible byproduct from this reduction reaction. Therefore, acid neutralization and alkalization could be a side-effect from reduction that could affect resulting bio-oil composition. Carboxylic acid groups are unable to be reduced due to the carbon being more electronegative than the attacking hydride. In bleaching practices, the reduction reaction disrupts chromophores especially in lignin, whitening the final product.

2.3.4 Thermal Degradation Reactions

Cellulose

The most prominent marker of thermal degradation in cellulose is a change in the degree of polymerization (DP). The DP of isolated cellulose remains steady up to 120°C, followed by a rapid decrease with increasing temperature (Fengel, 1967). Faster heating rates can decrease this minimum temperature of degradation (Roffael & Schaller, 1971). Moisture content also plays a major role in slowing the degradation of cellulose. High moisture content cellulose had a DP of about 200 units more compared to a low moisture content cellulose (Fengel & Wegener, 1983). Likely, the moisture content, with its high specific heat, slows the heating process, absorbing some of the thermal energy and hindering some degradation reactions.

Dehydration and oxidation reactions happen along with chain cleavage reactions at high temperatures. Oxidation of hydroxyl groups takes place when biomass is heated in air, resulting in an increase of carbonyl and carboxyl groups (Fengel & Wegener, 1983). At temperatures above 200°C, cellulose degrades rapidly to volatile products such as levoglucosan, other anhydroglucoses, and furan derivatives (Fengel & Wegener, 1983).

Shafizadeh and DeGroot characterized the following cellulose and generalized polysaccharide thermal degradation reactions (Shafizadeh & DeGroot, 1976):

- Depolymerization of polysaccharide by transglycosylation at 300°C into monomeric sugars and sugar derivatives, along with randomly linked oligosaccharides.
- Dehydration of cellulose into unsaturated compounds including 3-deoxyglucosenone, levoglucosenone, furfural, and furan derivatives.
- At relatively higher temperatures, sugar fission reactions yield carbonyl compounds that readily evaporate.
- Condensation of unsaturated products and side chain cleavages by free radical mechanisms yields highly reactive carbonaceous material composed of trapped free radicals.

These reactions, along with the following hemicellulose and lignin reactions below, assume pure feedstocks. As with any chemical or thermal degradation of biomass, intermolecular interactions will affect the overall reaction pathway.

Hemicellulose

Hemicellulose thermal degradation is similar to cellulose in terms of thermal degradation reactions. However, due to its inherent amorphous structure and diverse composition, hemicellulose has multiple avenues of degradation. Xylan degradation begins near 200°C with glycosidic linkage and pyranose C-C bond rupture. At 225°C, there is complete decomposition of the macrostructure. Finally, at 275–290°C, molecular fragments are dehydrated to furfural (Fengel & Wegener, 1983).

4-O-methylglucuronoxylan, as opposed to xylan, depolymerizes and dehydrates at temperatures of more than 150°C. Keto groups, γ-lactones, and furfural are formed by intramolecular dehydration and ester linkages via intermolecular dehydration (Fengel & Wegener, 1983). It is assumed that low-molecular weight products are formed from non-hydrolytic cleavage of glycosidic bonds by radical intermediates (Fengel, 1966). Carbon dioxide is produced in addition to the previously mentioned products at 200–300°C, signifying rapid degradation with increasing temperatures.

Lignin

While lignin is commonly seen as the most thermally stable of the three major biomass constituents, there are noticeable degradation effects at temperatures lower than 200°C. Non-hydrolyzable lignin residue increased with increasing temperatures up to 200°C (Kollmann & Fengel, 1965).

Temperatures up to 155°C did not affect the shape of fiber swelling in lignin. From 175–240°C lignin condensation increased with increasing temperature. At 260–280°C lignin condensation was accompanied by various changes that caused a decrease in the hydrophilic capacity of the lignin (Fengel & Wegener, 1983). Apart from the temperature, other factors play a role in lignin degradation such as moisture content. Higher moisture contents have been shown to decrease the softening temperature of periodate lignin (Fengel & Wegener, 1983).

Chemical and thermal reactions are integral to catalyzed hydrothermal liquefaction of biomass. Understanding the different degradation pathways allows for better control of bio-oil product formation.

Chapter 3 Materials, Methods, and Analysis

3.1 Materials Preparation

Corn stover and 2-year hybrid poplar supplied by the Bioproducts and Biosystems Engineering Department at the University of Minnesota were air dried and milled using a hammer mill with a 10 mesh screen. The ground biomass being used for trials was stored at room temperature in plastic bags, while excess material was stored at –20°C.

3.2 Biomass Characterization

Biomass composition was determined, following the lab procedures: NREL/TP-510-42618. Pre-HTL pH of biomass and solvent mixture was also determined using a Beckman Φ40 pH meter.

3.3 Integrated Catalysis Solvent Preparation

Sulfuric acid (Macron Fine Chemicals) and sodium hydroxide (Ward's Science) basic stock solutions were created for chemical catalysis. 0.5% and 1.5% w/v solutions of each were created via DI water dilution and designated 'dilute' and 'strong', respectively. Sodium dithionite (Fisher Chemical) dilute and strong solutions were prepared individually at the time of the experiment due to its inherent instability and sensitivity to air.

5% and 10% w/v solutions were created via DI water dilution and designated ‘dilute’ and ‘strong’, respectively for the sodium dithionite trials. In summation, a total of 6 different solutions were created for the integrated catalysis trials: dilute acid (0.5%), dilute base (0.5%), dilute reduction (5%), strong acid (1.5%), strong base (1.5%), and strong reduction (10%).

3.4 Reductive Pretreatment

As opposed to integrated catalysis, the reductive pretreatment methods reacted biomass before hydrothermally treated.

Sodium borohydride and sodium dithionite were the two reductive agents used in the pretreatment trials. For the sodium borohydride pretreatment, 3.00 ± 0.03 g of hybrid poplar was weighed and mixed into a small beaker with 10 mL of a 10% w/v solution of sodium borohydride and DI water. Tin foil was placed over the beaker and the mixture was allowed to react for 24–48 hrs to ensure complete reaction. The reacted biomass was filtered using a glass filter (VWR) and washed thoroughly with DI water. The washed biomass was allowed to air dry for 24–48 hrs. This biomass was then used in the hydrothermal liquefaction process, described below.

For the sodium dithionite pretreatment, 3.00 ± 0.03 g of hybrid poplar was weighed and poured into a Nitrogen flushed plastic bag which was quickly sealed. Then, 10 mL of a 10% w/v sodium dithionite/DI water solution was added to the Nitrogen flushed bag, which was, again, quickly sealed. The flushed bag was opened to let out enough Nitrogen to allow for “pinching” of the biomass to thoroughly mix the feedstock and reductive solution. The mixture was allowed to react in the Nitrogen flushed bag for 24–48 hrs to ensure complete reaction. The reacted biomass was then filter using a glass filter and washed with DI water, and allowed to air dry for 24–48 hrs. This biomass was then used in the hydrothermal liquefaction process, described below. For both sodium borohydride and sodium dithionite reductive pretreatments, two bio-oil generation trials were completed, but no yield analysis was completed due to time constraints.

3.5 Hydrothermal Liquefaction Equipment and Setup

An induction-based, batch reactor design was implemented for the hydrothermal liquefaction process. The LC Miller Dynaflux PR-15 induction heating system was used in conjunction with a Miller Coolmate 3 water cooling system and an Athena temperature controller system. The reactor chamber was a Parr Instruments 4740 high temperature/high

pressure vessel used with a Parr Instruments 4316 gauge block. Figure 3.1 and 3.2 show the system configuration with all previously mentioned components.

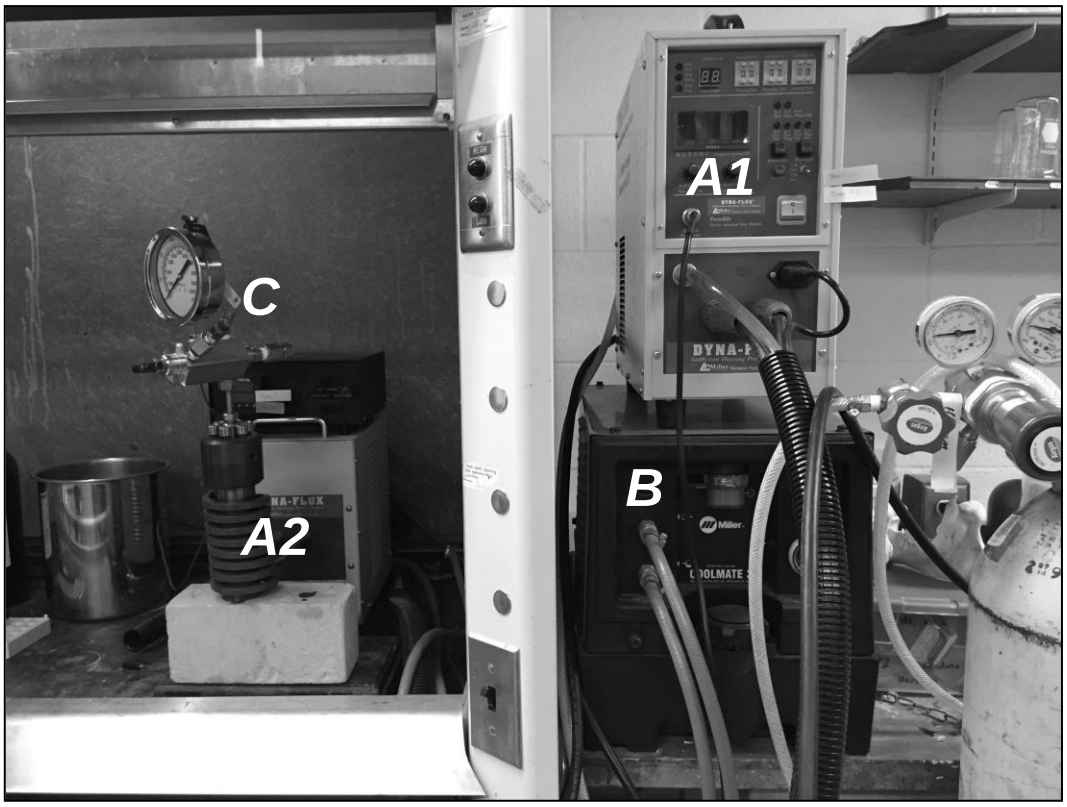

Figure 3.1 HTL System configuration from the front. (A1) Dynaflux PR-15 induction heating system controller. (A2) Dynaflux PR-15 induction heating system heating block. (B) Miller Coolmate 3 water cooling system. (C) Parr Instruments 4316 gauge block.

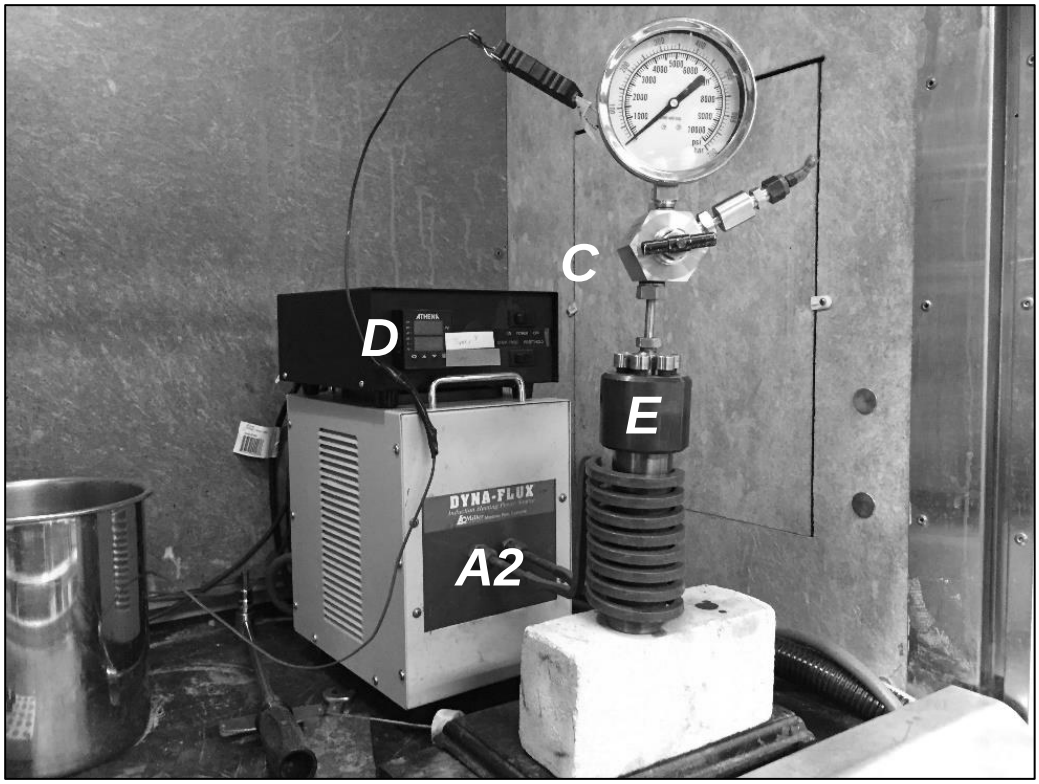

Figure 3.2 HTL system configuration from the side (zoomed in on A2). (D) Athena temperature controller. (E) Parr Instruments 4740 pressure vessel.

3.6 Hydrothermal Liquefaction

3.6.1 Integrated Catalysis

Integrated catalysis is defined as having the acidic, basic, or reductive solution in the reactor chamber during hydrothermal liquefaction process.

The empty pressure vessel was weighed and recorded for yield analysis trials (C_0). 3.00 ± 0.03 g of designated dry biomass (corn stover or hybrid poplar) was weighed and poured into the Parr 4740 pressure vessel. For

all control, acidic, and basic trials, 10 mL of designated solution was weighed and poured into the reactor chamber. The control trials used DI water as the solvent. For integrated catalysis reductive trials, 10 mL of DI water with either 0.53 or 1.11 g of sodium dithionite were added to the reactor. After solutions were added to the Parr chamber with the biomass, the mixture was stirred to ensure even distribution.

The chamber was then flushed for 60 seconds with industrial grade Nitrogen gas (University of Minnesota) to avoid combustion reactions due to high environmental oxygen content and promote liquefaction.

Immediately after chamber flushing, the chamber was closed using the default chamber assembly in conjunction with the Parr 4316 gauge block. The assembly was then placed inside the induction coil and heated to 100°C at a rate of 22 ± 2.5 °C/min.

The chamber was then held at ~100°C for 30 min to allow for the biomass and solution to react at an elevated temperature. While ideally the temperature would be held at a constant 100°C, the temperature fluctuated due to the induction heater turning on and off when the chamber temperature was below or above the target 100°C.

After 30 min, the chamber was heated to 350°C at a rate of 77 ± 4.3 °C/min. As soon as the thermocouple read 350°C the induction heater was turned off and the chamber was quenched in cool tap water for 10 min to ensure complete condensation of volatiles. Separate trials were completed to measure the pH after the 30 min 100°C catalysis and full 350°C liquefaction, designated Mid-HTL and Post-HTL, respectively. All integrated catalysis trials for both yield and compositional samples (described below) were done in triplicate.

3.6.2 Reductive Pretreatment

For reductive pretreatment trials, 3.00 ± 0.03 g of reduced biomass was added to the Parr pressure vessel and mixed with 10 mL DI water. The hydrothermal liquefaction process was identical to the integrated catalysis process.

3.7 Product Fractionation

The Parr reaction chamber, after hydrothermal liquefaction, contains four independent products: bio-oil, aqueous, solids, and gaseous phases. Measurements of each phase's abundance were done for the yield

analysis section using water assisted fractionation along with other methods. For compositional analysis trials, the bio-oil and aqueous phases were directly fractionated to provide pure products. These two method branches are explained below.

3.7.1 Yield Trials

Only the integrated catalysis trials, and not the reductive pretreatment trials, were analyzed for yield distribution due to time constraints. Integrated catalysis trials were much faster, whereas the pretreatments were time prohibitive. From the HTL process, the Parr reaction chamber was retrieved from the cool water quench and the pressure (gas phase) was released. The chamber was then dried, weighed, and weight was recorded (C_1).

Two extractions (50 mL and 65 mL) using HPLC grade chloroform (Fisher Chemical) were done to obtain the remaining contents from the Parr chamber (bio-oil, aqueous phase, and solids). These extractions entailed pouring the chloroform into the chamber and using a stainless steel mixer to stir the contents to disperse any sintered products into the solution. The contents of the chloroform extractions were poured through two layers of stainless-steel mesh (18 mesh) into a Boro 3.3 250mL separation funnel

of known weight (SF_0). The mesh layers were used to prevent too much solid particulate into the separation funnel which could cause clogging. The meshes were isolated under a fume hood to allow for chloroform evaporation.

A DI water extraction was also done to ensure all chloroform insoluble products were obtained from the Parr chamber. 70 mL of DI water was stirred in the Parr chamber and poured directly into the separation funnel. Two phases formed in the separation funnel: an organic, chloroform soluble phase, and an aqueous, chloroform insoluble phase. These two phases were allowed to fully separate for 30 min in the closed separation funnel.

After 30 min of separation, each phase was bled off into different beakers of known weight (B_0). The aqueous phase beaker was weighed immediately and recorded (B_1). The now empty separation funnel was allowed to dry for 10 min to evaporate excess chloroform, leaving behind only residual aqueous phase content. After the 10 min drying, the separation funnel was weighed and recorded (SF_1). $B_{0/1}$ and $SF_{0/1}$ were initially meant to quantify the aqueous and bio-oil phases separately. However, due to significant errors caused by the small sample sizes,

aqueous and bio-oil phases were combined into Total Liquid Yield to reduce error.

The Parr chamber was washed thoroughly with acetone (Fisher Chemical) to fully extract any residual solids still in the chamber. This acetone-solids mixture was filtered using a glass filter to determine solids content. The bio-oil and aqueous phase beakers obtained from the separation funnel were also filtered for solids. Residual solids from the dried separation funnel were extracted and filtered using acetone. After glass filtration, the filters (of known weight) were allowed to dry for 10 min to ensure no liquid content remained. The mesh used initially to filter large solid particulate, after ample time for chloroform evaporation, was scrapped of solids into a tared beaker. The filters and solid particulate were weighed and recorded, culminating in the solids phase yield (S_g).

Using the Equations 3.1–7, total liquid, solids, and gaseous percent yields were calculated from these fractionation measurements:

$$Initial\ Reactants\ (IR)\ g = Biomass\ wt. + Solution\ wt. \quad (3.1)$$

$$Pre\text{-}HTL\ Chamber\ (PHC)\ g = C_0 + IR \quad (3.2)$$

$$Total\ Liquid\ Yield\ \left(TLY_g\right)\ g = (C_1 - C_0) - S_g \quad (3.3)$$

$$Gaseous\ Yield\ (GY_g)\ g = PHC - C_1 \quad (3.4)$$

$$Solids\ Yield\ \% = {}^{S_g}/_{IR} \quad (3.5)$$

$$Total\ Liquid\ Yield\ \% = {}^{TLY_g}/_{IR} \quad (3.6)$$

$$Gaseous\ Yield\ \% = {}^{GY_g}/_{IR} \quad (3.7)$$

with C_0 – initial empty, dry Parr chamber, C_1 – Post-HTL surface dried Parr chamber with contents, and S_g – solids content (g) as determined by glass filtration and particulate weight in fractionation procedure.

The procedure and analysis utilized ensures minimal losses while considering most sources of product distribution i.e. separation funnel residue, etc.

3.7.2 Compositional and Aging Trials

Contrary to yield analysis trials, compositional (and aging) analysis trials were conducted to generate pure bio-oil and aqueous phases, with no dilution or filtration that could otherwise change compound distribution. Directly from the cool water quench the Parr chamber was opened, releasing the gaseous phase. Chloroform extraction of the Parr chamber used the same procedure as above. There was no water extraction for the compositional analysis trials. After chloroform extraction into the

separation funnel, the phases were allowed to fully separate for 30 min. After 30 min, a sample of each phase (organic and aqueous) was bled off and isolated into separate containers. The bio-oil sample was stored in a freezer at –20°C, while the aqueous phase sample was stored in a walk in cooler at ~4.4°C.

These bio-oil and aqueous phase samples were characterized via GC-MS and HPLC, respectively.

3.8 Bio-oil Composition Analysis

From the compositional trials completed during the experimental procedure section, bio-oil was characterized via Gas Chromatography-Mass Spectrometry (GC-MS) for molecular weight and elemental composition.

Using a 0.22 µm PES filter (Tisch Scientific), 0.75 mL of bio-oil was syringed into GC-MS vials. These vials were either stored at –20°C in the freezer or run the same day through an Agilent QTOF MassHunter GC-MS with a DB-5 column. Ramping temperatures of the GC-MS were 50–190°C at 5 °C/min then 190–320°C at 25 °C/min.

Spectra peak analysis was done with the Agilent B.07.00 Qualitative Analysis suite in conjunction with the NIST Mass Spectral Search Program Version 2.2. The spectra gleaned from the GC-MS was integrated and peaks were ordered by peak area. Due to the baseline shift caused by the increased ramping temperatures at and above 33 min, shown in Figure 3.3, peaks that were eluted after 33 min were excluded from all calculations i.e. calculating total peak area.

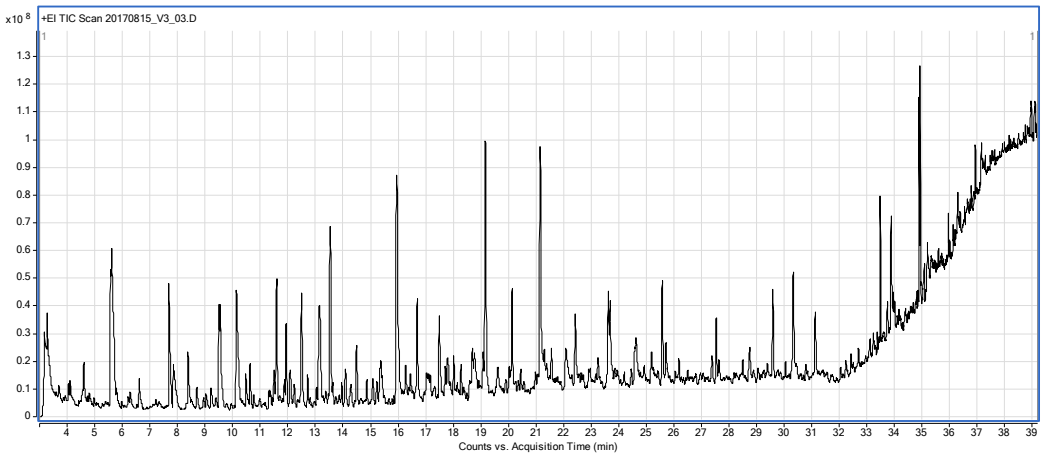

Figure 3.3 Spectra of control corn stover bio-oil

The 50 largest peaks for each compositional sample were computed using the analysis software, and the compounds were identified via the NIST library. Via the NIST library and analysis programs, peaks were assigned multiple compound probabilities and RMATCH scores. If the highest ranked i.e. most probable compound had a probability of less than 10%, had a low RMATCH score (<700), and low compound chemical formula

consensus among the other ranked compounds, that peak was discarded and excluded from all calculations, unless explicitly stated. Also, compound likelihood was another factor in determining the peak compound identity i.e. a fluorinated compound is much less likely than a phenolic compound.

From the list of the top 50 compounds in a given compositional sample, relative abundance of those compounds was calculated. Peak area % was determined by dividing the individual peak area by the sum of peak area in the spectra from 0 to 33 min. Weighted peak area % was determined by dividing the individual peak area % by the sum of the 50 peak area %s. With a weighted peak area %, molecular weight and elemental analyses were able to be completed. Example 3.1 shows the process of determining weighted peak area % using a 5 compound bio-oil. This process was used to determine molecular weight and the CHOS content of the bio-oil.

Example 3.1: *Total Spectra Area = 20 (from 0 to 33 min)*

Peak 1 – Furfural (MW: 96), Peak Area = 5, *Peak Area % = 25%*

Peak 2 – p-Cresol (MW: 108), Peak Area = 4, *Peak Area % = 20%*

Peak 3 – Phenol (MW: 94), Peak Area = 3, *Peak Area % = 15%*

Peak 4 – Creosol (MW: 138), Peak Area = 2, *Peak Area % = 10%*

Peak 5 – 2,4-Dimethylfuran (MW: 96), Peak Area = 1, *Peak Area % = 5%*

Total Peak Area % = 75%

Peak 1 – Weighted Peak Area % = 33%

Peak 2 – Weighted Peak Area % = 27%

Peak 3 – Weighted Peak Area % = 20%

Peak 4 – Weighted Peak Area % = 13%

Peak 5 – Weighted Peak Area % = 7%

Total Weighted Peak Area % = 100% (expected)

Peak 1 – Weighted MW = 31.7

Peak 2 – Weighted MW = 29.2

Peak 3 – Weighted MW = 18.8

Peak 4 – Weighted MW = 17.9

Peak 5 – Weighted MW = 6.7

Molecular Weight of Bio-oil = 104.3 (Similar method for CHOS Analysis)

3.9 Aqueous Phase Analysis

From the fractionation of the bio-oil, an undiluted aqueous phase was retrieved. Since fractionation into the two phases (organic and aqueous) is not a perfect system, an extra fractionation step was employed to further remove chloroform and organics. Aqueous phase samples were chosen from the lot of compositional trials and filter syringed into a separate vial using a 0.22 μm PES filter. 1 mL of chloroform was then syringed into the same beaker. Phase separation was immediate and apparent, thus the top, aqueous layer was syringed into HPLC compatible vials.

A Waters HPLC system was used with an Aminex HPX-87H Ion Exclusion Column, which is commonly applied for organic acid analysis. The internal and external heaters were set to 50°C and 55°C, respectively, with flow rate at 0.5 mL/min using 0.0100 Normal HPLC grade sulfuric acid (RICCA). Glacial acetic acid (Fisher Chemical) standards (3.94,11.82, 23.34, and 191.12 mg/mL) were created to provide reference points for calculating concentration.

3.10 Aging

Composition samples were chosen for aging analysis. Only hybrid poplar samples were used, as only hybrid poplar biomass utilized both the

integrated catalysis and reductive pretreatment methods. Aging analysis of 24 hr evaporation, 1 week, and 3 week samples were compared against the initial, compositional samples described in the previous subsection.

Using a 0.22 μm PES filter, 0.5 mL of bio-oil was syringed into a GC-MS compatible vial. The GC-MS vial was then placed under the fume hood for 24 hrs at room temperature to allow for the chloroform to evaporate off, thus starting the aging process. After 24 hrs, designated samples were taken and resolubilized with 0.75 mL of chloroform. These samples were stored in the freezer at –20°C. The 1 and 3 week samples were closed and allowed to age for the designated time, being resolubilized with 0.75 mL of chloroform at the end of their aging timeframe.

Aging samples were analyzed the same way with the same equipment as the compositional samples i.e. Agilent QTOF MassHunter GC-MS. Weighted molecular weight of each aged bio-oil was compared against the initial compositional sample molecular weight.

Chapter 4 Results and Discussion

One major point of discussion that should be addressed immediately is the exclusion of sodium dithionite integrated catalysis from most discussion until its designated section of this chapter i.e. yield, composition, and stability results. Sodium dithionite integrated catalysis, as will be discussed below, incorporated a large amount of sulfur into the resulting bio-oil. This would cause major issues with bio-oil value and should be taken as only an academic exercise, not a viable solution to increasing stability.

4.1 Biomass Characterization and Pre-HTL pH

Table 4.1 shows the major biomass constituents for both corn stover and 2-year hybrid poplar.

Table 4.1 Corn stover and hybrid poplar initial composition

Characteristic	Corn Stover	Hybrid Poplar
Cellulose %	32.23	31.03
Hemicellulose %	19.95	16.93
Lignin %	17.52	23.99
Moisture Content %	6.44	5.84
Ash Content %	6.48	2.15

As expected, corn stover had higher cellulose and hemicellulose content, due to it being an herbaceous-agricultural residue feedstock, while hybrid poplar was more abundant in lignin and less in ash content. These major components of biomass will play large roles in determining bio-oil yield, composition, and stability.

The pH of Pre-HTL biomass/solution mixtures was also measured for all trials. These measurements give insight to product formation and possible Post-HTL pH predictors. Table 4.2 shows the Pre-HTL pHs of the various treatments.

Table 4.2 Pre-HTL pH of all treatments

Treatment	Corn Stover pH	Hybrid Poplar pH
Control	5.29	4.77
0.5% Sulfuric Acid	2.59	2.81
0.5% Sodium Hydroxide	10.03	10.58
5% Sodium Dithionite	2.56	3.06
1.5% Sulfuric Acid	1.73	1.85
1.5% Sodium Hydroxide	11.25	12.05
10% Sodium Dithionite	2.39	2.79
10% Sodium Dithionite (PT)	-	5.85
10% Sodium Borohydride (PT)	-	9.94

As expected, acid and base treatments decreased and increased initial pH, respectively. The sodium dithionite (integrated catalysis) solution reduced the pH as well, nearing acid levels. Sodium borohydride pretreatment increased the Pre-HTL pH significantly due to the alkaline nature of the reducing agent. Sodium dithionite pretreatment also had a neutralization effect, increasing pH above the control. This is most likely due to the water wash accompanying the pretreatment. Mid- and Post-HTL pH values will be discussed in the Compositional Effects section of this chapter.

4.2 Effects of Integrated Catalysis on Bio-oil Yield

As discussed before, there are three phases that are produced from the HTL process: solids, liquids, and gases. Due to the small sample sizes of each trial, phase-specific bio-oil and aqueous yields were not able to be accurately measured. Using Equations 3.1-7, phase yields were calculated for each integrated catalysis treatment: control, 0.5% sulfuric acid, 0.5% sodium hydroxide, 1.5% sulfuric acid, and 1.5% sodium hydroxide for both corn stover and hybrid poplar.

Solids content is a strong indicator of condensation/polymerization reactions, as those compounds are less likely to volatilize during the HTL process. Figure 4.1 shows the solid phase yield of the integrated catalysis treatments with respect to the total initial reactants.

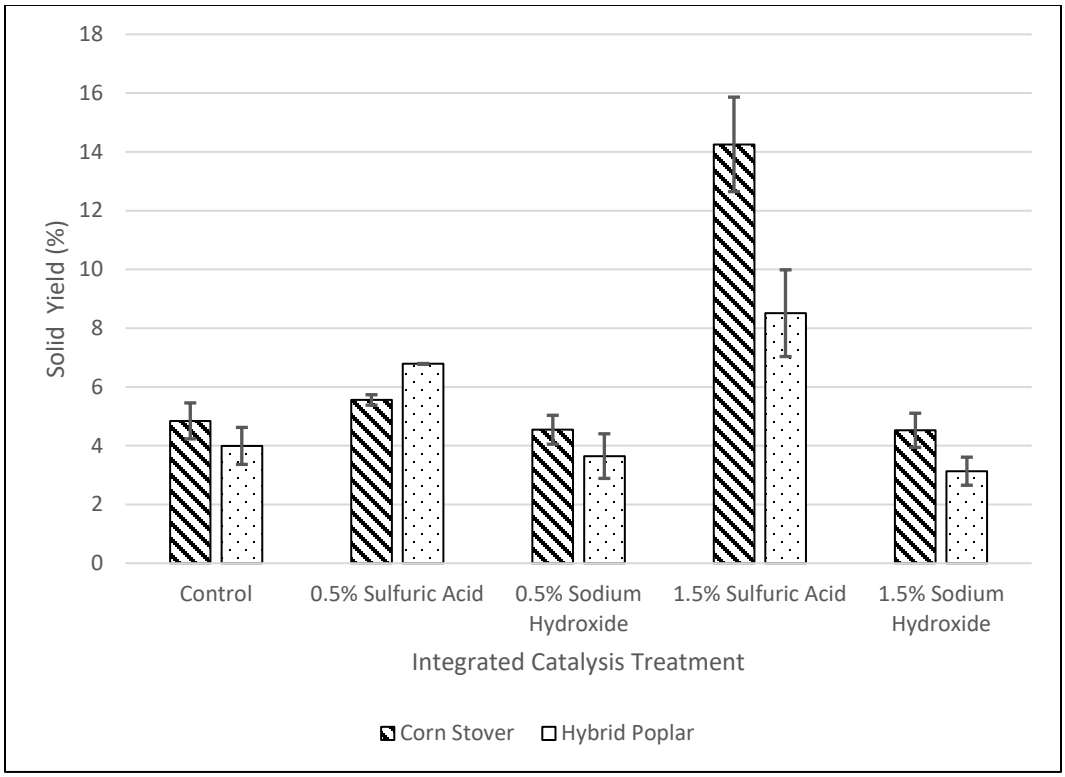

Figure 4.1 Solid phase yield (% from total initial reactants) of integrated catalysis treatments

As shown, expectedly 0.5% and 1.5% sulfuric acid catalysis increases the solid content of the HTL products. Lignin condensation reactions are much more likely to happen in strongly acidic environments. With the introduction of an acid medium in conjunction with the natural acidity of the biomass due to acetyl group cleavage, solids formation is heightened. 0.5% and 1.5% sodium hydroxide catalysis, on the other hand, appeared to show marginal decreases in solid content compared to the control. Basic solutions may provide a “buffer” to the acidity formed by acetyl

group cleavage. This would prevent highly increased condensation reactions due to acidity displayed in the acid trials. Nevertheless, the differences observed are not statistically significant.

Another point to be made is, with exception of the 0.5% sulfuric acid trial, hybrid poplar has lower average solid content. This is most likely due to the lower ash content in hybrid poplar compared to corn stover since ash content is linked to char formation during thermochemical conversion (Li, Thompson, & Thompson, 2016). Lower ash content means less solid formation, which can increase liquid yields from HTL.

Total liquid yield was calculated by subtracting the solid phase from the total products weighed (Equation 3.3). Figure 4.2 shows the total liquid yield with respect to the total initial reactants.

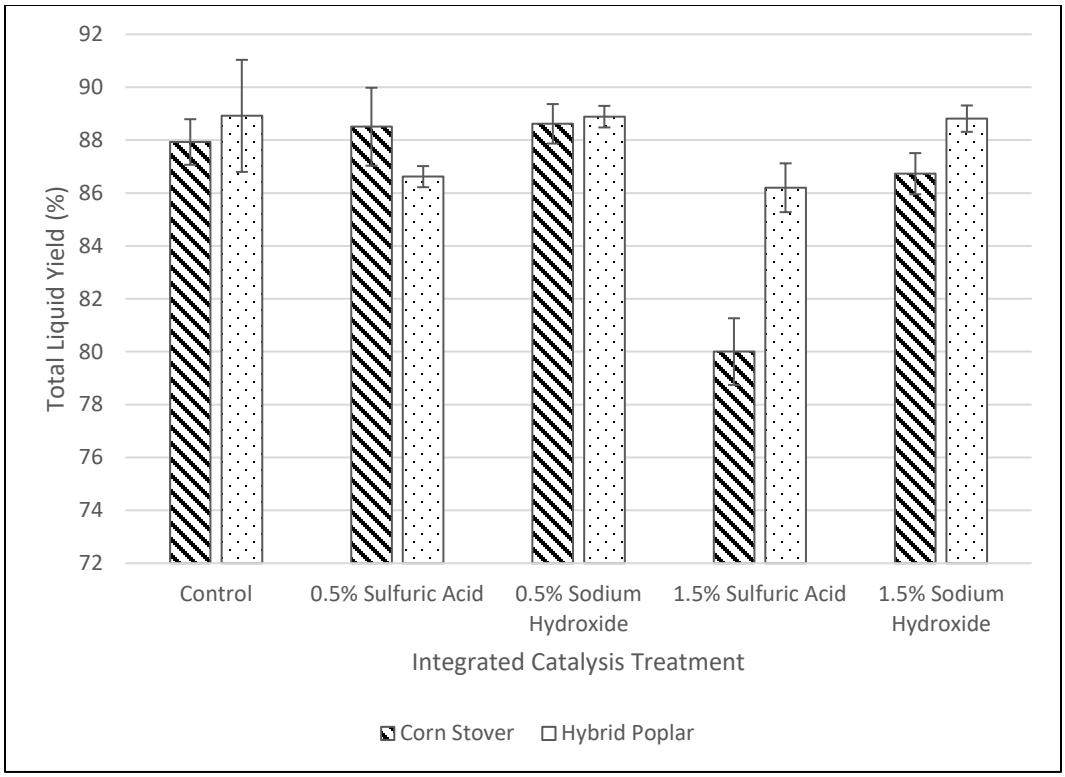

Figure 4.2 Total liquid yield (% from total initial reactants) of integrated catalysis treatments

Under control, 0.5% sulfuric acid, 0.5% sodium hydroxide, and 1.5% sodium hydroxide conditions, total liquid yield stays relatively stagnant. It seems the major factor in volatilizing biomass into a condensable state is the thermal treatment of HTL, which is a constant factor across all treatments. With 1.5% sulfuric acid conditions, the acidic environment can lead to condensation reactions, as previously stated, that can reduce condensable yields in favor of carbonized solids.

Hybrid poplar tends to have higher liquid yields compared to corn stover, which is expected sincer higher lignin content generally results in higher bio-oil yield. Due to the relatively large margin of error in our experimental setup, none of the differences are statistically significant, with the exception of the 1.5% sulfuric acid and 1.5% sodium hydroxide conditions. In both of these cases, hybrid poplar has higher liquid yields than corn stover. As mentioned before, decreased ash content in hybrid poplar leads to less solid formation, which allows for more condensable vapors to be formed during HTL. Due to acid condensation reactions, the overall liquid yield under 1.5% sulfuric acid conditions is lower than the control, while the liquid yield under 1.5% sodium hydroxide conditions is similar to that of the control.

The final phase calculation is gaseous yield. This value was calculated by subtracting Post-HTL products from the initial reactants (Equation 3.4). Figure 4.3 shows the gaseous phase yield % for the integrated catalysis treatments.

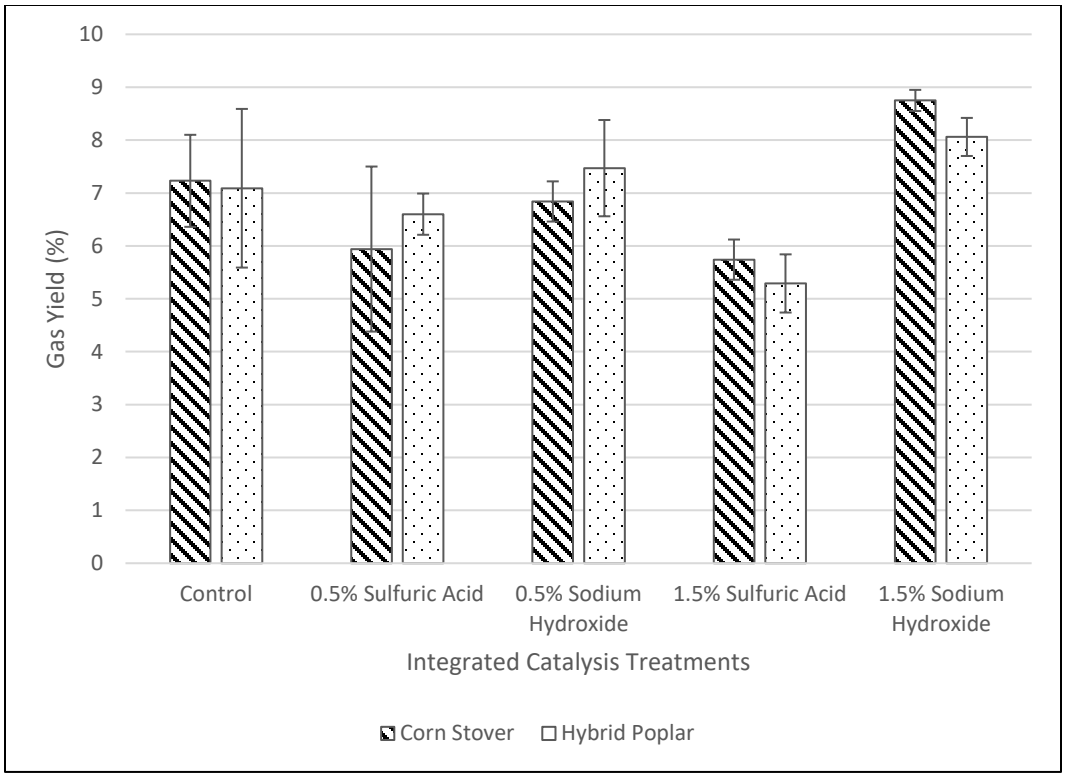

Figure 4.3 Gaseous phase yield (% from total initial reactants) for integrated catalysis treatments

Most gaseous yields are similar in quantity across treatments and biomass types. The most notable of gaseous yields is with the 1.5% sodium hydroxide treatment. Under alkaline conditions, polysaccharides undergo peeling reactions. However, with elevated temperatures such as those seen in HTL processing, biomass can also undergo alkaline random chain cleavage of carbohydrates. Under acidic conditions and HTL processing, there is a balance between polysaccharide chain cleavage/lignin volatilization and lignin condensation/polymerization reactions. Under

1.5% sodium hydroxide conditions, lignin condensation reactions would be limited compared to 1.5% sulfuric acid conditions. Therefore, volatilization reactions would generate a higher abundance of small, condensable vapors which could then undergo secondary reactions to gases. This would explain why sodium hydroxide catalyzed reactions have higher gas yields compared to sulfuric acid trials.

1.5% sulfuric acid integrated catalysis of biomass hydrothermal liquefaction is the only treatment that seems to have a significant impact on product phase distribution. Condensation reactions play a major role in determining solid phase yield, which, in turn, decreases total liquid yield. Most treatments, however, have very similar product phase distributions.

4.3 Compositional Effects

Through GC-MS analysis the composition of both the integrated catalysis and reductive pretreatment bio-oils was derived. Mid- and Post-HTL pH values were also measured as possible stability indicators. Three major compositional summaries were created to characterize the bio-oil: Mid- and Post-HTL pH values, a list of major chemical compounds found in each bio-oil, and an overall CHOS elemental analysis. Bio-oil molecular

weight, which was mostly used for comparison with aged bio-oil, was also derived from the GC-MS analysis. The aqueous phase of the HTL process was also analyzed through HPLC to find relative acetic acid contents of the various treatments.

4.3.1 Bio-oil Composition

Mid- and Post-HTL pH

Table 4.3 and 4.4 show the Mid-HTL and Post-HTL pH values of the integrated catalysis and reductive pretreatments, respectively.

Table 4.3 Mid-HTL pH of the integrated catalysis and reductive pretreatments

Treatment	Corn Stover pH	Hybrid Poplar pH
Control	5.58	3.39
0.5% Sulfuric Acid	3.17	3.19
0.5% Sodium Hydroxide	10.03	10.58
1.5% Sulfuric Acid	2.19	3.03
1.5% Sodium Hydroxide	10.18	9.43
10% Sodium Dithionite (PT)	-	4.99
10% Sodium Borohydride (PT)	-	8.24

Table 4.4 Post-HTL pH of the integrated catalysis and reductive pretreatments

Treatment	Corn Stover pH	Hybrid Poplar pH
Control	3.76	3.56
0.5% Sulfuric Acid	3.45	3.46
0.5% Sodium Hydroxide	4.16	3.93
1.5% Sulfuric Acid	3.16	3.30
1.5% Sodium Hydroxide	4.51	3.99
10% Sodium Dithionite (PT)	-	4.06
10% Sodium Borohydride (PT)	-	3.75

As expected, acid and base catalyzed HTL yield more acidic and more basic bio-oil, respectively compared to the control. For acid integrated catalysis, higher yields in compounds such as furfural, furan derivatives, and organic acids can lead to highly acidic, highly unstable bio-oils. Whereas in alkaline integrated catalysis, the base will neutralize these species generated through the release of acid groups from hemicellulose and cellulose. The higher pH suppresses furan formation, yielding a more basic bio-oil.

Another point to be made is the pHs of the reductive pretreatments. Mid-HTL pH values show a shift from their relatively basic Pre-HTL pHs,

symbolizing the formation of acidic species. While sodium borohydride pretreated biomass has a significant drop in pH (>1), sodium dithionite has a pH drop of less than one. Post-HTL pH values continue this trend of acid suppression, yielding more basic bio-oils than the control for both pretreatments. The reductive pretreatment with water washing and the resultant higher initial pH, either by alkalization from sodium borohydride or neutralization from sodium dithionite, is the most likely cause for the more basic product bio-oil.

Major Chemical Compounds

The top 5 largest relative compounds from each bio-oil were listed with their weighted peak area. Constitutional isomer compounds were included to account for small GC-MS discrepancies i.e. phenol, 2-methyl was combined with phenol, 3-methyl. This list contains 16 compounds that constitute the most relatively abundant molecules in both the integrated catalysis and reductive pretreatment bio-oils (excluding reductive integrated catalysis). Table 4.5 shows the major chemical compounds found in all treatments.

Table 4.5 Major compounds (% relative abundance) of integrated catalysis and reductive pretreatment bio-oil (±0.56%)

Family	Compound	C-CS	C-HP	DA-CS	DA-HP	DB-CS	DB-HP	SA-CS	SA-HP	SB-CS	SB-HP	SDT	SBH
F	Furfural	7.30	4.62	6.14	5.24	5.16	4.33	10.26	7.14	-	-	4.32	-
F	2-Furancarboxaldehyde, 5-methyl	3.95	2.35	6.12	4.08	1.24	1.46	9.61	5.84	-	-	3.69	3.13
F	2,4-Dimethylfuran	5.54	5.62	5.42	3.78	7.31	4.91	3.58	4.94	6.41	4.93	3.26	8.93
F	1,2-Cyclopentanedione, 3-methyl	2.80	2.52	2.86	2.16	2.48	3.01	2.29	2.30	2.27	4.12	4.92	5.26
P	Phenol, 2,6-dimethyl	10.03	4.92	8.36	5.07	7.41	5.03	6.04	5.49	9.13	1.76	1.42	3.25
P	Phenol, 2,6-dimethoxy	6.61	5.34	4.92	6.89	5.51	3.40	3.80	7.65	3.26	4.35	3.55	2.62
P	Phenol, 2-methoxy	5.68	5.22	3.24	4.79	5.49	6.90	5.06	3.24	4.44	3.91	3.36	3.16
P	Phenol	4.35	5.15	4.12	4.22	4.92	4.79	5.62	7.20	4.93	6.62	5.75	6.22
P	Creosol	3.73	6.18	3.56	6.10	4.39	6.51	3.32	4.51	8.63	3.29	1.05	2.84
P	Phenol, 2-methyl	6.53	5.99	6.61	6.22	7.34	8.09	8.00	4.64	5.85	8.58	7.08	6.40
P	1,2-Benzenediol, 3-methoxy	0.73	2.85	1.58	3.62	0.86	2.15	1.53	2.32	2.94	3.67	-	-
L	Phenol, 4-ethyl-2-methoxy	6.36	3.47	4.40	5.53	3.60	2.41	3.66	2.53	6.87	4.31	3.00	3.90
L	Phenol, 4-methoxy-3-(methoxymethyl)	1.74	2.46	1.98	3.45	1.41	5.36	2.32	4.76	-	1.76	-	-
L	Eugenol	2.52	4.02	2.88	3.53	3.99	5.69	-	-	2.74	4.70	7.80	8.52
L	Phenol, 2,6-dimethoxy-4-(2-propenyl)	2.16	5.48	1.52	2.75	2.57	5.47	-	-	1.94	7.44	7.62	8.14
L	Benzenemethanol, 2,5-dimethoxy-, acetate	1.43	2.21	1.58	2.51	1.63	1.84	2.42	4.76	1.03	2.12	3.26	2.74

C – Control; DA – 0.5% Sulfuric Acid; DB – 0.5% Sodium Hydroxide; SA – 1.5% Sulfuric Acid; SB – 1.5% Sodium Hydroxide; CS – Corn Stover; HP – Hybrid Poplar; Reductive Pretreatments: SDT – 10% Sodium Dithionite; SBH – 10% Sodium borohydride Families: F – Furan Derivative; P – Phenol Derivative; L – Larger Aromatic Fragments

There are many conclusions that can be drawn from these results on a compound-by-compound or molecular family basis. The main effects of the treatments and biomass types will be discussed as such.

Furfural and Furan Derivatives

The most abundantly clear trend that can be seen is the formation of furfural and furan derivatives. Furfural forms from 5-carbon sugars, typically from hemicellulose, under acidic conditions (see Biomass Primary Reactions). Furan derivatives, for the purpose of our discussion, are considered closely related compounds that structurally resemble furan with slight to moderate modifications i.e. methyl or hydroxyl additions etc. These structural similarities are illustrated in Figure 4.4.

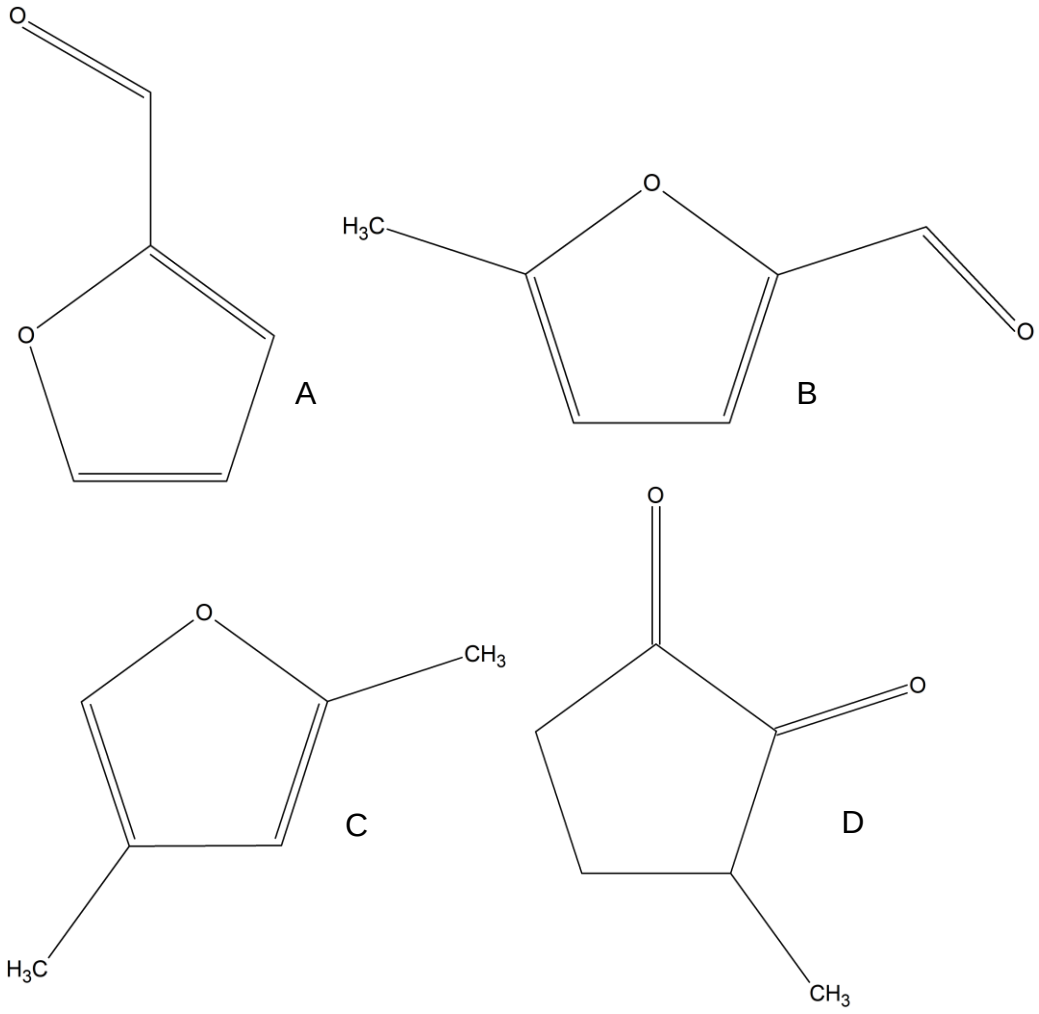

Figure 4.4 Furan derivative structures: A – Furfural; B – 2-Furancarboxaldehyde, 5-methyl; C – 2,4-Dimethylfuran; D – 1,2-Cyclopentanedione, 3-methyl

Due to the greater cellulose and hemicellulose content of corn stover compared to hybrid poplar, it is expected that the furfural and furan content is higher in corn stover. This trend stays relatively consistent across all treatments and individual furan compounds.

Not surprisingly, for both hybrid poplar and corn stover species, 0.5% and 1.5% sulfuric acid integrated catalysis increased furan derivatives. Notably, furfural [A] increased markedly in the 1.5% sulfuric acid catalyzed treatment by about 3% for each biomass. 5-Furancarboxaldehyde, 5-methyl [B] is another furan derivative that shows large increases for both biomasses under acid catalyzed conditions. Along with water, heightened temperatures, and free H^+ ions from both sulfuric acid and the natural acidity formed by acetyl group cleaving, biomass hemicellulose and cellulose hydrolyze and reform into furan compounds, especially furfural [A] and 2-Furancarboxyaldehyde, 5-methyl [B].

Alkaline integrated catalysis trials show the opposite trends with furan formation. Furfural [A] and 2-Furancarboxyaldehyde, 5-methyl [B] are decreased in 0.5% sodium hydroxide trials, and dropping to trace amounts in 1.5% sodium hydroxide trials. They are most likely present in some form, but are not part of the 50 largest peaks when analyzing the bio-oil through GC-MS. This reduction in two major furan derivatives signifies a hindrance of acid-catalyzed reactions such as furfural [A] formation from xylose. The alkaline environment from the sodium hydroxide neutralizes the acetic acid and organic acids from the biomass and bio-oil, respectively. This deters furan formation. This claim is corroborated by the

Post-HTL pH of the 0.5% and 1.5% sodium hydroxide integrated catalysis bio-oils, all of which were higher pH than the control bio-oil.

The reductive pretreatments also have interesting effects on the formation of furfural and furan derivatives. Only the sodium borohydride pretreatment significantly affected furfural [A] content. Sodium dithionite is a lignin-retaining reducing agent that does not greatly effect carbohydrates in biomass. Also, the acidity of the treated biomass remained relatively low compared to the alkaline integrated catalysis or sodium borohydride HTL process. Therefore, furfural is not hindered to the same degree as the other more significant treatments.

While sodium borohydride can effect some aspects of carbohydrates i.e. reducing end groups, the effect of these reactions would most likely be insignificant. The main effect the sodium borohydride pretreatment had was the alkalization of the feedstock, as seen by Pre-, Mid-, and Post-HTL pH values. This alkalization reduced furfural [A] formation.

Other furan derivatives such as 2,4-Dimethylfuran [C] and 1,2-Cyclopentanedione, 3-methyl [D] have other trends that are worth discussion. Sodium borohydride pretreatment greatly increases both of the

aforementioned compounds. Compared to furfural [A] and 2-Furancarboxaldehyde, 5-methyl [B], these compounds are lower in relative oxygen content i.e. more carbon and hydrogen or less oxygen. This could be due to the reduction of carbohydrates and prospective aldehyde-ketone groups in the biomass during the pretreatment.

Phenol and Phenolic Derivatives

Phenols are aromatic, conjugated structures that are derived from the lignin in biomass and are a major constituent of bio-oil. Figure 4.5 shows the phenolic structures that were main constituents in the bio-oils.

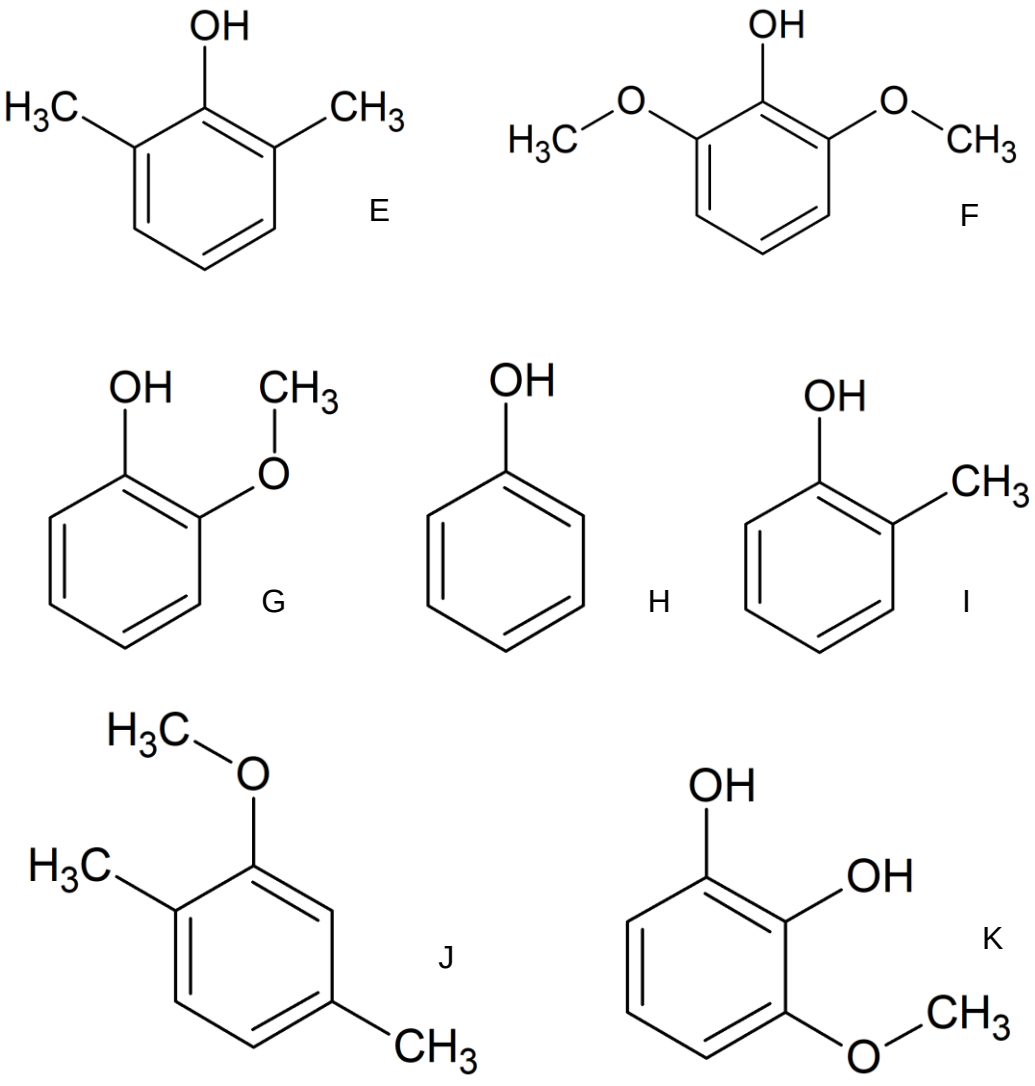

Figure 4.5 Phenol derivative structures: E – Phenol, 2,6-dimethyl; F – Phenol, 2,6-dimethoxy; G – Phenol, 2-methoxy; H – Phenol; I – Phenol, 2-methyl; J – Creosol; K – 1,2-Benzenediol, 3-methyl

Phenolic compounds come from the S, G, and H lignin units that are degraded during HTL. Taking into account the following section of Lignin Fragments, hybrid poplar bio-oil has more *relative* phenolic content than

corn stover, which is expected due to hybrid poplar's higher lignin content. This is not to say the *quantity* of phenolics in the bio-oil is necessarily higher, but simply that the ratio of phenolics to other compound types such as furans is higher in hybrid poplar.

In addition, there are certain phenolic species that have higher relative abundance in corn stover than hybrid poplar. H lignin units are scarce in hardwood such as hybrid poplar, while being more abundant in corn stover and other like herbaceous biomass. Phenol, 2,6-dimethyl [E] is a possible fragment from an H lignin unit due to the single hydroxyl group. With these assumptions, it is expected and shown that the relative concentration of Phenol, 2,6-dimethyl [E] is much higher in corn stover than hybrid poplar. Conversely, creosol [J] and 1,2-Benzenediol, 3-methoxy [K] are likely derivatives from G and S lignin units, respectively, due to the location of their methoxy and hydroxyl groups. These species have higher relative abundance in hybrid poplar than corn stover.

Most integrated catalysis treatments did not have a significant effect on the relative abundance of phenolic derivatives in the resulting bio-oil. The clearest interaction between integrated catalysis and the formation of phenolic derivatives is the phenol [H] content of 1.5% sulfuric acid

catalysis. In both cases of corn stover and hybrid poplar, phenol [H] content increases under 1.5% sulfuric acid conditions. Most likely, the acid environment is cleaving lignins into lignin fragments, which are cleaved into phenolic derivatives such as creosol [J], which are finally degraded to the smallest base unit of a simple phenol [H].

The reductive pretreatments, contrary to the integrated catalysis, had a much larger effect on phenolic relative abundance. The most likely cause of overall small phenolic compound loss is due to the pretreatment washing. While sodium borohydride and sodium dithionite do react with lignin, they are both lignin-retaining agents and therefore would most likely not have a significant impact on phenolic decrease.

Larger Aromatic Fragments

Larger aromatic fragments are larger lignin compounds comparatively to the phenolic derivatives. Structures commonly have α and β-carbons, along with some γ-carbon structures. The compounds for large aromatic fragments are shown in Figure 4.6.

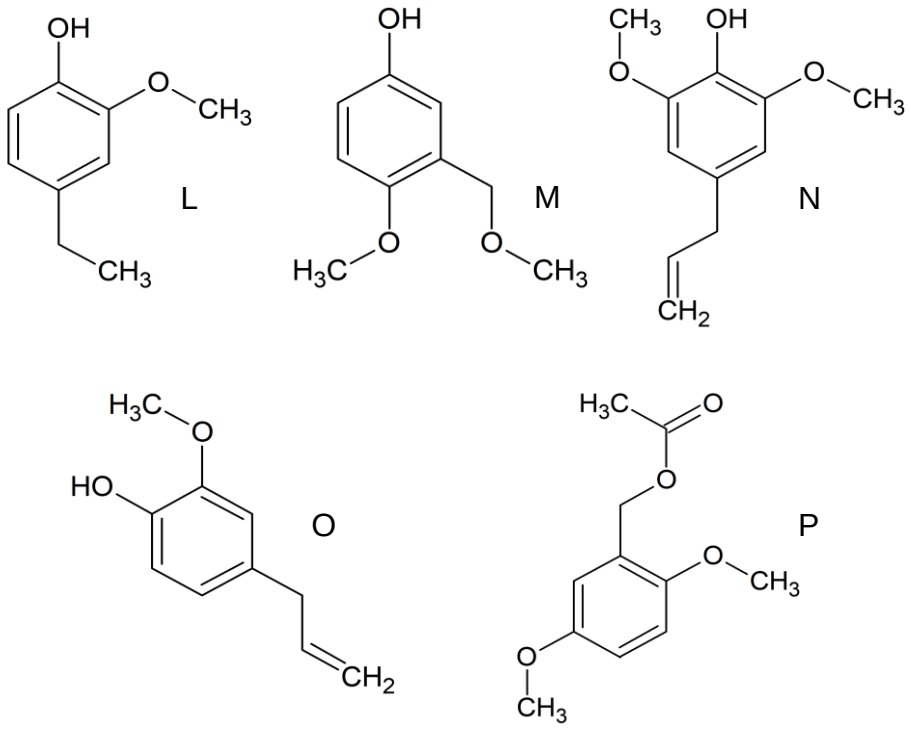

Figure 4.6 Large aromatic fragment structures: L – Phenol, 4-ethyl-2-methoxy; M – Phenol, 4-methoxy-3-(methoxymethyl); N – Phenol, 2,6-dimethoxy-4-(2-propenyl); O – Eugenol; P – Benzenemethanol, 2,5-dimethoxy-, acetate

As with phenolic derivatives, large aromatic fragments are more relatively abundant in hybrid poplar bio-oil compared to corn stover. Most large aromatic fragments have multiple methoxy and hydroxyl groups, suggesting that they are derived from G and S lignin units rather than H lignin units, supporting the trend of high lignin fragment abundance in a lignin-rich, hardwood feedstock's bio-oil.

1.5% sulfuric acid integrated catalysis greatly decreased eugenol [O] and Phenol, 2-6-dimethoxy-4-(2-propenyl) [N] relative abundance. Both of these large aromatic fragments have double bonded γ-carbons instead of an aldehyde group. This signifies that the acid environment hinders the formation of a double bonded γ-carbon. However, the acidic conditions did favor the formation of Benzenemethanol, 2,5-dimethoxy-, acetate [P], which includes an ester group, likely caused by acid assisted esterification.

Both sodium dithionite and sodium borohydride reduce lignin during pretreatment via negatively charged ions (bisulfite or hydrogen anion). These species can interact with aldehyde or hydroxymethyl groups on the γ-carbon of lignin, promoting the formation of a double bonded γ-carbon. Neutralization and alkalization effects from the pretreatments also reduces the acidity of the resulting bio-oil, corroborated by the more alkaline Mid- and Post-HTL pH values for the pretreatments.

Reductive pretreatments also stifle Phenol, 4-methoxy-3-(methoxymethyl) [M], which has a non-reducible ether bond. The reductive pretreatments therefore hindered the formation of this specific carbonyl group. Benzene methanol, 2,5-dimethoxy-, acetate [P] formation, on the other hand, was

not deterred during HTL. It is likely that Phenol, 4-methoxy-3-(methoxymethyl) [M] is formed by some intermediate that is effected by the pretreatments, whereas Benzene methanol, 2,5-dimethoxy-, acetate [P] is overall unaffected by the pretreatments.

CHOS Elemental Analysis

The elemental composition of the resulting bio-oil, unlike specific compounds, does not dramatically change between the control, integrated catalysis, and reductive pretreatment processes. Figure 4.7 and 4.8 show the effects of the different treatments on CHOS elemental composition of corn stover and hybrid poplar derived bio-oil.

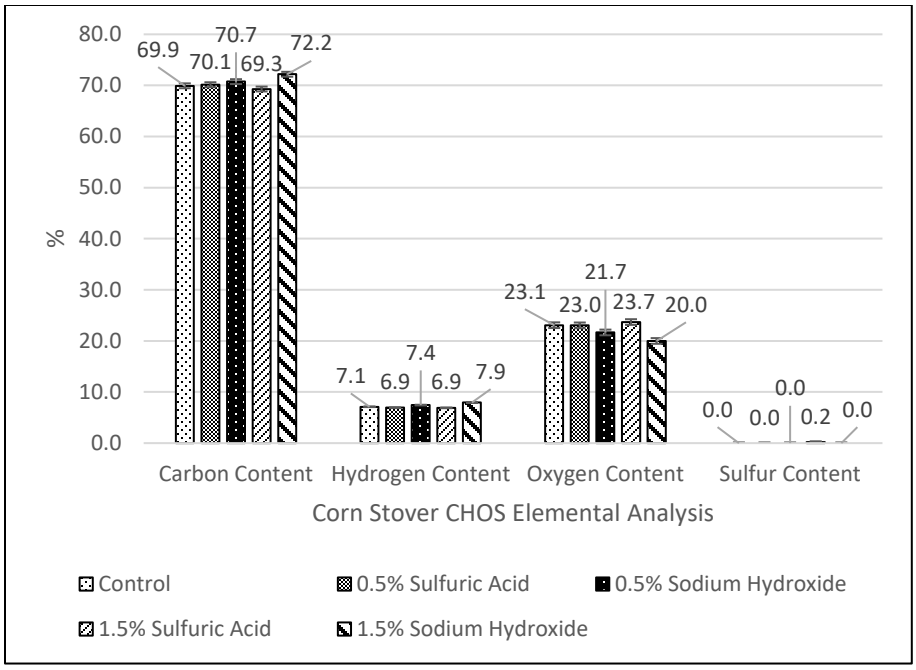

Figure 4.7 Corn stover CHOS Elemental Analysis

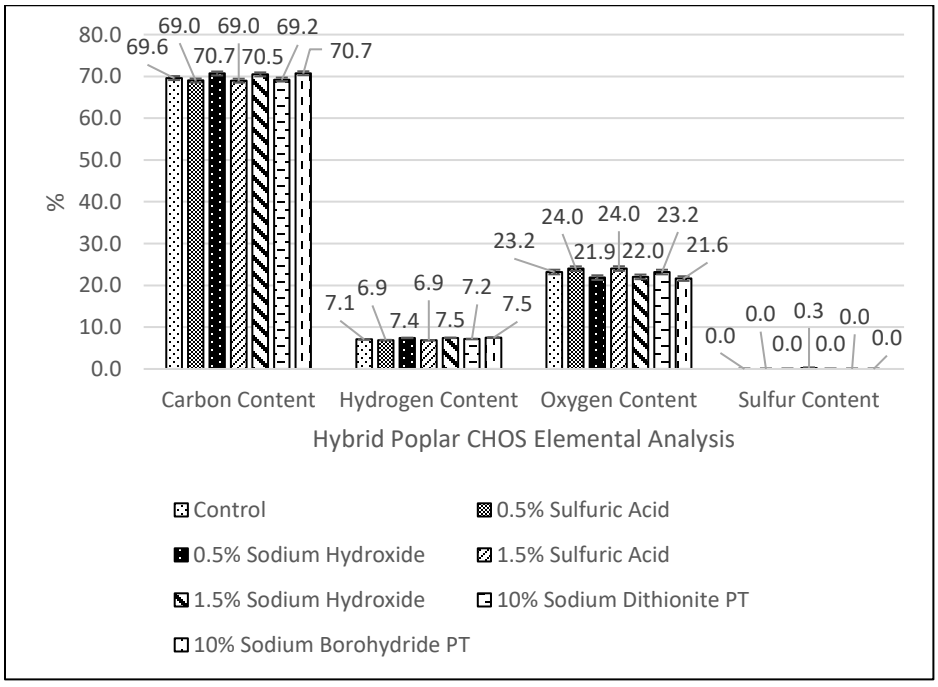

Figure 4.8 Hybrid poplar CHOS Elemental Analysis

The main elemental compositions of the feedstock to bio-oil are relatively unchanged due to the conditions that all of the main reactants for both integrated catalysis and reductive pretreatment trials are inside the pressurized vessel when undergoing hydrothermal liquefaction. There is very little difference in corn stover bio-oil elemental composition compared to hybrid poplar.

Carbon and hydrogen contents were the most stagnant over the different treatments, whereas oxygen content was more affected. Oxygen content is an important marker in determining possible stability enhancements of the bio-oil. On average, acidic integrated catalysis had slightly higher oxygen content compared with the control, while alkaline integrated catalysis had slightly lower oxygen content. This is corroborated by the low and high pH values for acidic and alkaline bio-oils, respectively. Sodium borohydride reduced oxygen content more than the other treatments, signifying that reduction of biomass is a possible means to decreasing oxygen content in the resulting bio-oil, albeit by a very small margin.

Sulfur content was seen to increase marginally in 1.5% sulfuric acid trials of both corn stover and hybrid poplar. Sulfur content will play a much

larger role in evaluating the reduction integrated catalysis trials, discussed later.

4.3.2 Aqueous Phase Composition

Acetic acid of the aqueous phase, formed during HTL, was analyzed via HPLC for all treatments. This analysis was designed to more fully explain the mechanism of furan derivative formation and bio-oil pH. Figure 4.9 shows the results of the acetic acid concentration analysis.

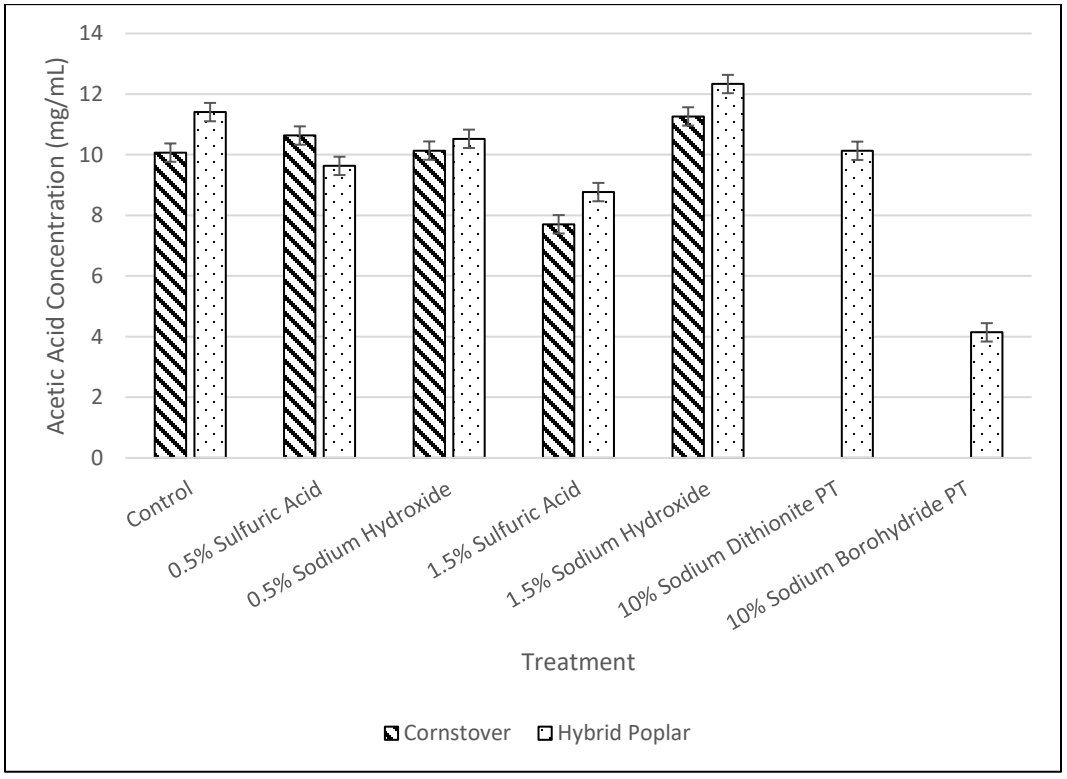

Figure 4.9 Acetic acid concentration (mg/mL) of HTL aqueous phase from all treatments

Acid integrated catalysis was shown to have lower acetic acid concentration compared to the control, whereas alkaline trials had higher acetic acid concentrations. Alkaline conditions serve as a catalyst to cleaving acetyl groups from hemicellulose, while acidic conditions either hinder acetic acid formation or cause secondary reactions, lowering resulting acetic acid concentrations. Whereas sodium dithionite pretreatment has relatively the same concentration of acetic acid as untreated hybrid poplar, most likely due to sodium dithionite's inactivity with carbohydrates and only neutralization effects from washing, sodium borohydride pretreatment greatly reduced acetic acid concentration, corroborating a higher pH for resulting bio-oil. This sodium borohydride reduction of acetic acid is most likely caused by the reduction of aldehyde and ketone groups that could be the building blocks for the carboxylic acids, as well as alkalization effects and subsequent washing from the pretreatment itself.

Relative abundance of acetic acid is another factor to consider, especially if acetic acid can be used as a value-added byproduct. The area % of the acetic acid peak obtained from HPLC analysis marks the relative abundance of the species compared to the other compounds within the

aqueous phase. Table 4.6 shows the relative abundance % of acetic acid in the aqueous phase from all trials.

Table 4.6 Relative abundance % of acetic acid in aqueous phase from all trials (±0.99%)

Treatment	Corn Stover	Hybrid Poplar
Control	34.99	32.59
0.5% Sulfuric Acid	24.36	38.80
0.5% Sodium Hydroxide	24.35	27.20
1.5% Sulfuric Acid	23.38	28.26
1.5% Sodium Hydroxide	18.41	18.19
10% Sodium Dithionite (PT)	-	22.55
10% Sodium Borohydride (PT)	-	11.90

Control trials have the highest relative abundance of acetic acid in the aqueous phase, signifying low secondary reactions. Acid trials, on average, have higher acetic acid relative abundance than their alkaline counterpart. The aqueous phase of alkaline trials is a more diverse mixture of many compounds compared to acidic trials, which have a consolidation of only a few, main chemicals. Both pretreatments also have low acetic acid relative abundance compared to control conditions.

Finally, Post-HTL bio-oil pH was plotted against acetic acid concentration in Figure 4.10.

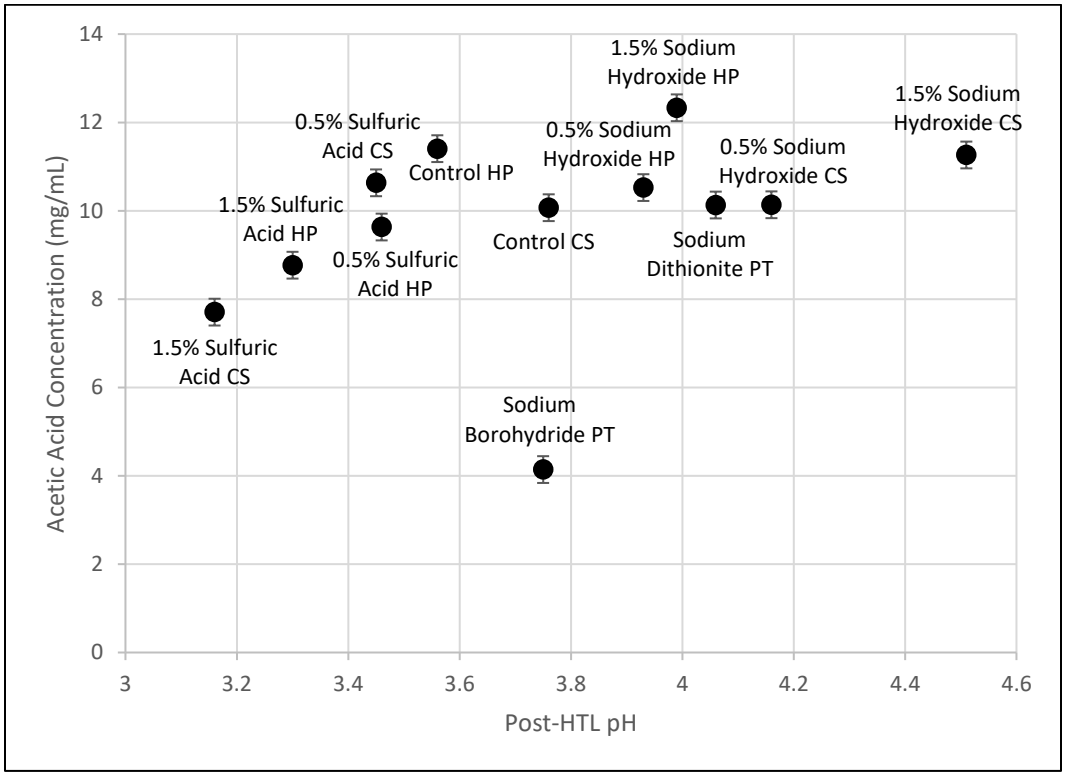

Figure 4.10 Post-HTL bio-oil pH vs acetic acid concentration (mg/mL)

As mentioned before, a more alkaline environment generally increases acetic acid formation in the aqueous phase i.e. more cleavage of acetyl groups, whereas acidic treatments hinder acetic acid formation in the aqueous phase. Sodium borohydride seems to be the outlier, most likely due to the alkalinity of the pretreatment combined with the pretreatment

wash, which would severely reduce the overall acetyl groups in the initial feedstock for HTL processing.

4.4 Aging Effects

Stability is the final major factor to be discussed about the effects of chemical treatments on bio-oil quality. Stability, in this instance, is the ability of the bio-oil to not change over time. Repolymerization and condensation reactions form C-C bonds with phenols and furans, increasing viscosity and reducing the quality and value of the bio-oil. Initial composition and aged samples were analyzed for their relative abundance of the 50 largest spectra peaks. Molecular weight of the bio-oil was then calculated from the weighted values. Table 4.7 summarizes the bio-oil average molecular weight values over various timeframes (hybrid poplar bio-oil only).

Table 4.7 Average molecular weight values over time for hybrid poplar bio-oil (±1.18)

Treatment	Initial	24 hour	1 week	3 week
Control	138.9	144.9	147.5	147.1
0.5% Sulfuric Acid	140.6	145.8	145.3	-
0.5% Sodium Hydroxide	138.8	143.6	144.2	-
1.5% Sulfuric Acid	134.0	144.3	143.5	146.6
1.5% Sodium Hydroxide	137.1	139.3	140.3	140.8
10% Sodium Dithionite (PT)	145.8	152.6	148.5	151.0
10% Sodium Borohydride (PT)	143.1	147.3	149.0	150.1

1.5% sulfuric acid catalyzed bio-oil saw the largest increase in molecular weight, which is to be expected due to the low pH and higher oxygen content. Condensation reactions are a concern with lignin and lignin fragments under acidic conditions. In comparison, 1.5% sodium hydroxide and reduction pretreatment bio-oil species both did not increase as much over time. It is also worth noting that the bulk of aging progression happens within the first 24 hours of the process.

The trend of pH being a marker for bio-oil molecular weight increase also corroborates the changes seen in the sodium dithionite and sodium borohydride pretreatment trials as well. Both of these treatments had

higher Mid- and Post-HTL pH values compared to the control, and subsequently have either comparable or slightly smaller increases in bio-oil molecular weight. Figure 4.11 and 4.12 show the trend of molecular weight increase values vs. Mid and Post-HTL pH, respectively.

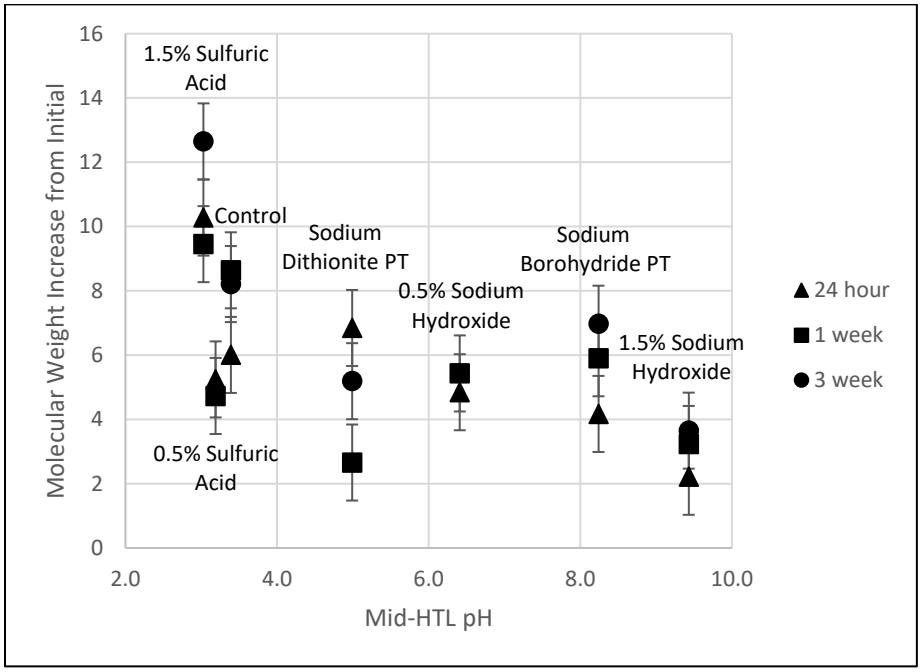

Figure 4.11 Molecular weight increase vs. Mid-HTL pH

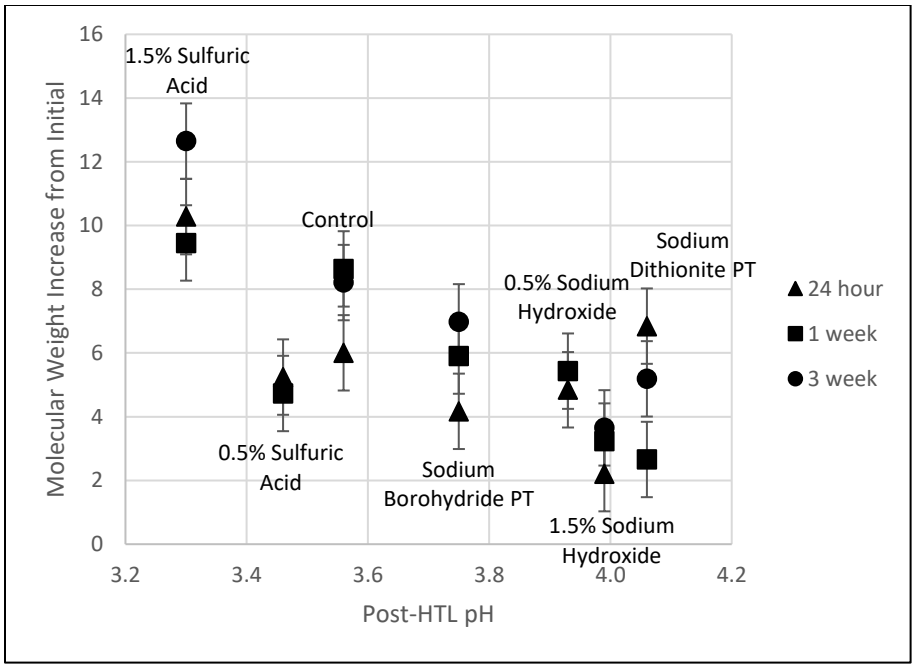

Figure 4.12 Molecular weight increase vs. Post-HTL pH

As the trend suggests, a lower Mid- or Post-HTL pH increases instability and bio-oil molecular weight increases i.e. viscosity over time. Some bio-oil had an unexpected drop in molecular weight increase from 24 hour to 1 week aging. This could be caused by either precipitation of solids from the chloroform solution or by GC-MS analysis errors. However, the trend remains true that higher Mid- and Post-HTL pH is related to more stability.

As expected, acid and base catalyzed HTL involves relatively more acidic and basic Mid- and Post-HTL products, as stated above. Sodium borohydride and sodium dithionite pretreated products had more alkaline

relative products compared to the control and thus had more molecular weight stability. Initial pHs from the pretreatments resulted in more alkaline or neutral feedstocks that allowed for pH buffering during HTL, resulting in less unstable acidic products i.e. furfural, assumed organic acids. This stabilized the resultant bio-oil.

Acidic bio-oil is less stable due to the low pH which catalyzes condensation and repolymerization reactions, increasing viscosity. Higher pH bio-oil have reduced condensation reactions and thus more stability. Therefore, alkaline catalyzed and reduced pretreatment bio-oil production techniques seem to have a more stable resulting bio-oil than acid catalyzed or control bio-oil. In all, while the trend seems inherently true, the data presented in Figure 4.11 and Figure 4.12 is not clear in statistical significance.

Another measure of bio-oil stability can be determined by the chemical diversity of the bio-oil itself, compared to the pH. As condensation and polymerization reactions occur, relative abundance of some species decreases, either being utilized in the reaction, or simply becoming less abundant in the process. In either case, a more chemically diverse aged bio-oil can be considered unchanged or less aged than a less chemically

diverse aged bio-oil. Chemical diversity was determined by calculating the total peak area % from the first 50 bio-oil compounds of each bio-oil, regardless of individual peak composition. A higher total peak area %, the less chemically diverse the bio-oil and vice versa. Figure 4.13 shows the total peak area % of the first 50 compounds of initial and aged bio-oils compared to the Post-HTL pH.

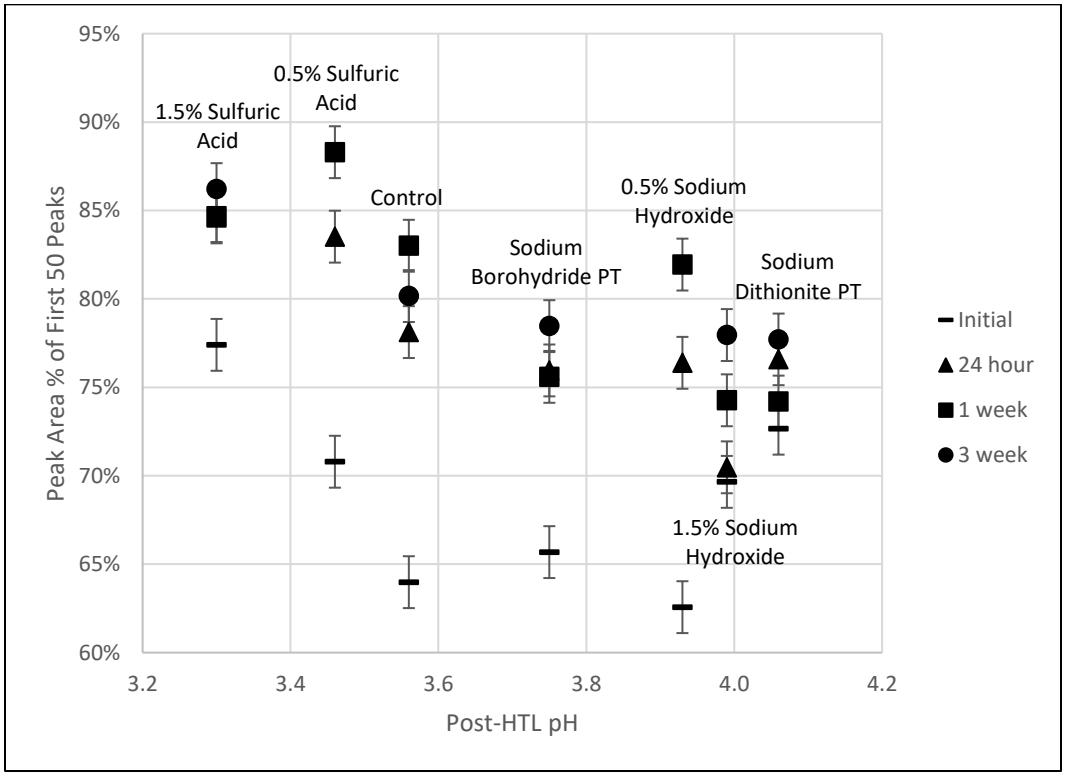

Figure 4.13 Total peak area % of first 50 compounds of initial and aged bio-oil compared to Post-HTL pH

As shown, more acidic bio-oils have greater total peak area %s than more alkaline bio-oils, signifying that they are less chemically diverse and

therefore possibly more unstable. While all bio-oils increased in total peak area % from the initial to aged bio-oil, illustrating the aging process, final aged peak area % show a general trend of more chemical diversity over time for more alkaline bio-oils i.e. alkaline bio-oils lose less of the smaller chemical peaks over time compared to acidic bio-oils. This corroborates the molecular weight increase data that shows similar stabilizing trends with more basic bio-oil. As with the previous data, statistical significance is low in this data set due to overlapping data ranges.

4.5 Effects of Sodium Dithionite Integrated Catalysis

As stated above, reduction integrated catalysis resulted in a non-applicable technique and was difficult to analyze or make conclusions regarding yield, composition, and stability. This was most likely due to the high sulfur content, which adds a dimension of difficulty when concluding things such as molecular weight over time. Therefore, most of the results of the thesis research regarding reduction integrated catalysis have been isolated to this specific section.

4.5.1 Effects of Reduction Catalysis on Yield

Yields with respect to initial reactants of reduction integrated catalysis are shown in Figure 4.14-16 for solids, total liquid, and gaseous phases, respectively.

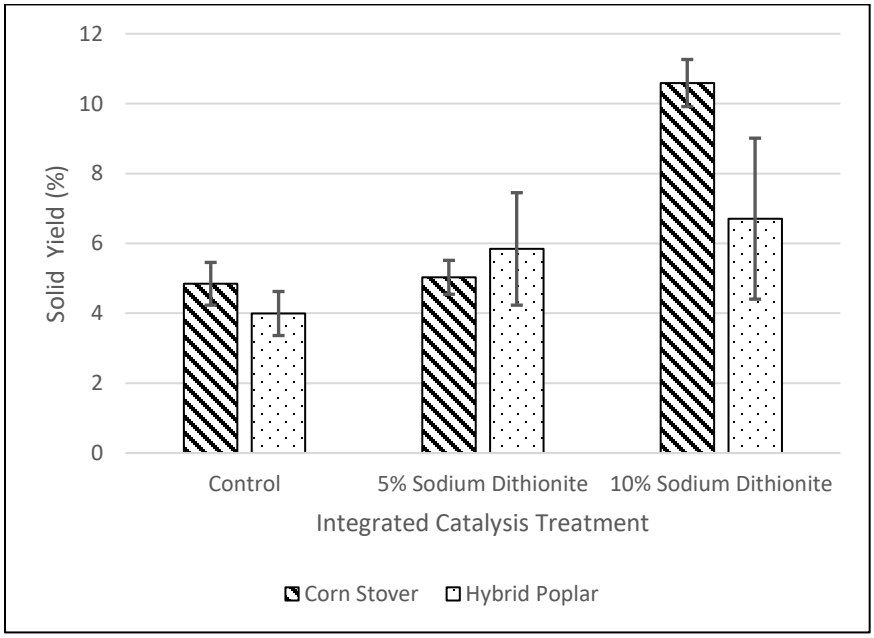

Figure 4.14 Solid phase yield (% from total initial reactants) of reduction integrated catalysis trials

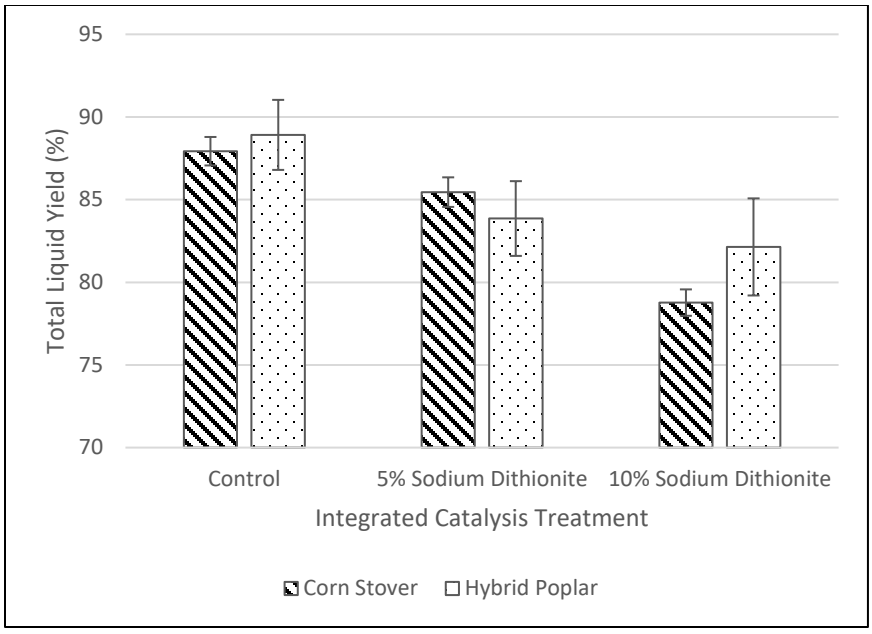

Figure 4.15 Total liquid yield (% from total initial reactants) of reduction integrated catalysis trials

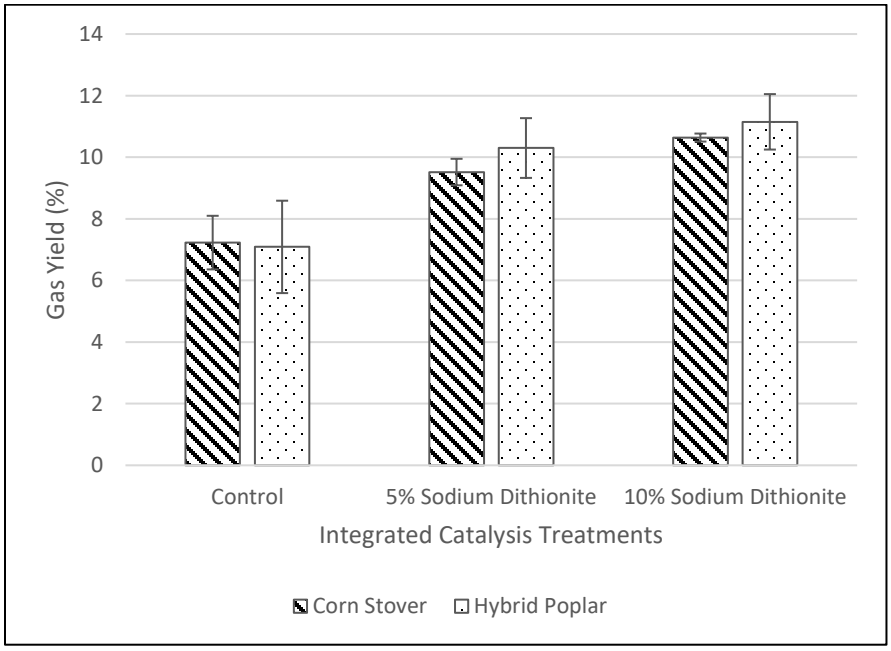

Figure 4.16 Gaseous phase yield (% from total initial reactants) for reduction integrated catalysis trials

The solids phase increased from control to 5% and 10% sodium dithionite integrated catalysis. Sodium dithionite is a lignin-retaining reduction agent, and therefore does not degrade the entire lignin structure to a soluble form i.e. phenol derivatives and lignin fragments on its own. The overall macro structure of the lignin is retained. Lignin-bound sulfur and free sulfur in the reaction vessel can both potentially influence the overall reactions during the HTL process.

Liquid yield suffered under the result of elevated solids and gaseous phases. Biomass degradation to a volatile form was not optimal with dithionite in the system. Sodium dithionite most likely either degraded into a gaseous form (in the presence of oxygen) or slightly modified the biomass lignin with sodium dioxide di-anion/bisulfite addition, increasing both gaseous and solid phases, respectively. These reactions resulted in reduced volatilization during HTL, decreasing the total liquids yield.

Finally, as mentioned above, degradation of sodium dithionite solution to a gaseous form was most likely cause of increased gaseous phase yield with increasing reducing agent concentration. This is opposed to the control, which only utilized DI water as the HTL solvent. The control

gaseous phase was most likely composed mainly of water vapor, H_2, and CO_2. The reduction integrated catalysis gaseous phase most likely also contained sulfur gases such as sulfur dioxide and hydrogen sulfide. This is corroborated by the pungent smell the resulting HTL products had during the reduction integrated catalysis trials.

4.5.2 Compositional Effects

Bio-Oil Composition

Table 4.8 and 4.9 show the Mid- and Post-HTL pH values of control and reduction integrated catalysis trials, respectively.

Table 4.8 Mid-HTL pH of control and reduction integrated catalysis trials

Treatment	Corn Stover pH	Hybrid Poplar pH
Control	5.58	3.39
5% Sodium Dithionite	3.50	3.18
10% Sodium Dithionite	3.64	3.39

Table 4.9 Post-HTL pH of control and reduction integrated catalysis trials

Treatment	Corn Stover pH	Hybrid Poplar pH
Control	3.76	3.56
5% Sodium Dithionite	3.88	3.86
10% Sodium Dithionite	4.31	3.46

Integrated sodium dithionite catalysis decreases the pH initially. Then, during the process of liquefaction, the pH slowly rises for both corn stover and hybrid poplar at 5% and 10% sodium dithionite concentrations. Sodium dithionite generates acidic species which most likely causes this drop in pH. As the species react with the biomass during the liquefaction process, the pH increases.

Table 4.10 shows an extended table of major compounds formed from reduction integrated catalysis. An additional family of sulfur derivatives was added to show how sulfur becomes a major component only under these specific conditions.

Table 4.10 Major compounds (% relative abundance) of reduction integrated catalysis bio-oil (±0.56%)

Family	Compound	C-CS	C-HP	DR-CS	DR-HP	SR-CS	SR-HP
F	Furfural	7.30	4.62	2.87	2.89	-	-
F	2-Furancarboxaldehyde, 5-methyl	3.95	2.35	-	-	-	-
F	2,4-Dimethylfuran	5.54	5.62	5.69	2.27	3.90	4.17
F	1,2-Cyclopentanedione, 3-methyl	2.80	2.52	1.09	1.09	-	-
P	Phenol, 2,6-dimethyl	10.03	4.92	6.05	5.28	6.06	2.06
P	Phenol, 2,6-dimethoxy	6.61	5.34	4.02	1.44	3.82	4.66
P	Phenol, 2-methoxy	5.68	5.22	5.49	-	5.19	-
P	Phenol	4.35	5.15	5.49	6.01	3.94	5.23
P	Creosol	3.73	6.18	2.08	5.30	-	1.02
P	Phenol, 2-methyl	6.53	5.99	7.11	7.03	6.06	5.84
P	1,2-Benzenediol, 3-methoxy	0.73	2.85	2.96	3.42	1.50	2.62
L	Phenol, 4-ethyl-2-methoxy	6.36	3.47	5.24	2.76	3.17	1.99
L	Phenol, 4-methoxy-3-(methoxymethyl)	1.74	2.46	5.44	3.93	1.77	1.91
L	Eugenol	2.52	4.02	1.99	2.74	3.75	6.59
L	Phenol, 2,6-dimethoxy-4-(2-propenyl)	2.16	5.48	3.82	6.99	1.58	4.88
L	Benzenemethanol, 2,5-dimethoxy-, acetate	1.43	2.21	1.73	2.08	1.71	3.51
S	Thiophene, 2,3,4-trimethyl	-	-	-	4.35	0.89	5.02

C – Control; DR – 5% Sodium Dithionite; SR – 10% Sodium Dithionite; CS – Corn Stover; HP – Hybrid Poplar; Families: F – Furan Derivative; P – Phenol Derivative; L – Large Aromatic Fragments; S – Sulfur Derivatives

Sodium dithionite integrated catalysis has some major impacts on specific compound formation, most prevalently on the furfural and furan derivative family. Furfural, 2-Furancarboxaldehyde, 5-methyl, and 1,2-Cyclopentanedione, 3-methyl were greatly reduced in the 10% sodium dithionite integrated catalysis trials for both corn stover and hybrid poplar

feedstocks. This signifies that these smaller furans are most likely being converted into some other type of compound, such as Thiophene, 2,3,4-trimethyl [Q] seen in Figure 4.17.

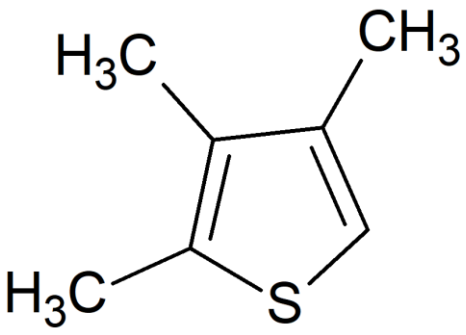

Q

Figure 4.17 Sulfur Derivatives structures: Q – Thiophene, 2,3,4-trimethyl

Phenol derivatives were also reduced, most likely caused by more sulfur addition and slight degradation during the HTL process, whereas larger aromatic fragments were mostly unchanged. As mentioned before, sodium dithionite is a lignin-retaining reducing agent. Chromophoric systems are modified via a reversible addition reaction with bisulfite and sodium dioxide di-anion. Small lignin systems could be more susceptible to chromophoric degradation by sulfur addition than larger phenolic groups. This would explain why small phenolic derivatives are effected moreso than large aromatic fragments.

Figure 4.18 and 4.19 show the CHOS elemental analysis of the reduction integrated catalysis trials for corn stover and hybrid poplar.

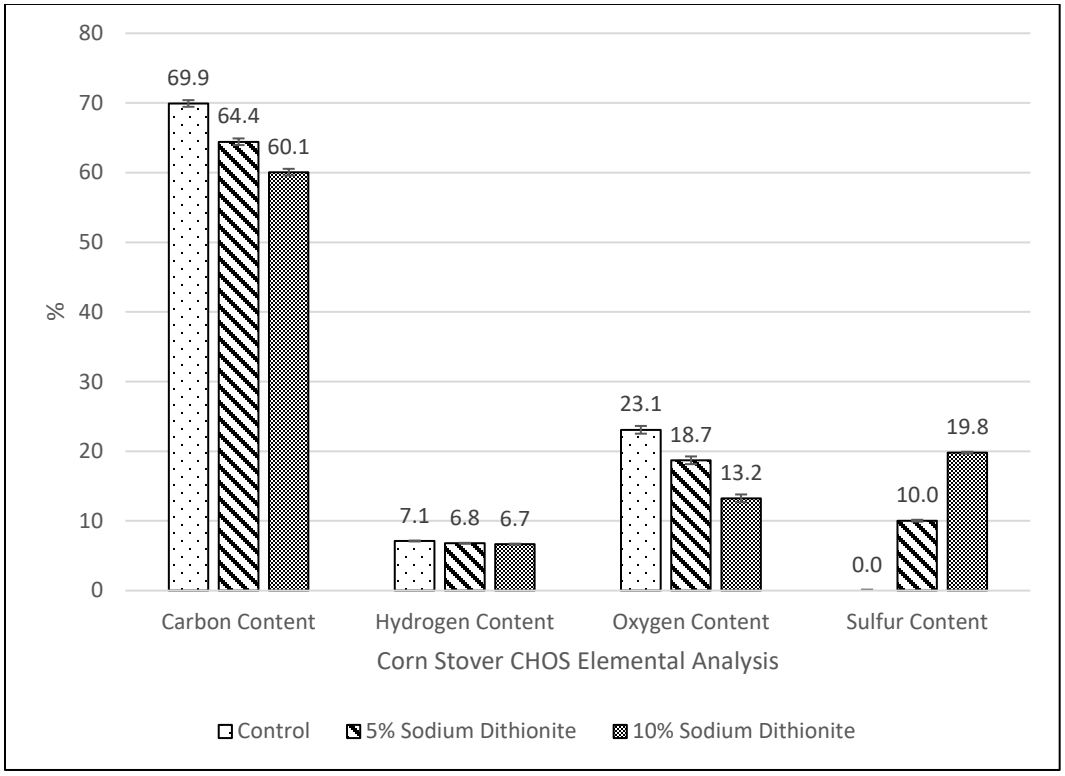

Figure 4.18 Corn stover CHOS Elemental Analysis of reduction integrated catalysis trials

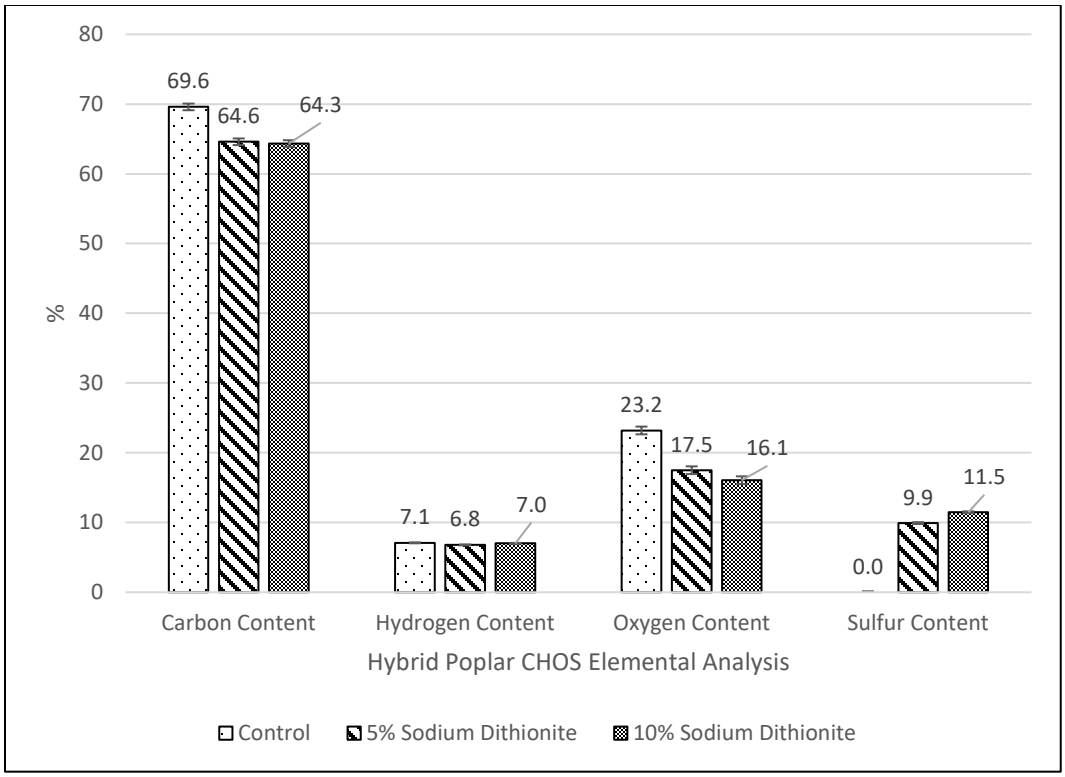

Figure 4.19 Hybrid poplar CHOS Elemental Analysis of reduction integrated catalysis trials

As shown, for both corn stover and hybrid poplar bio-oil, carbon and oxygen content decreased with dramatically increasing sulfur content. This is due to sulfur addition reactions during the HTL process that creates many sulfur derivatives from what are usually furan and phenolic derivatives i.e. furfural to Thiophene, 2,3,4-trimethyl. While the CHOS analysis seems to indicate decreased oxygen content, which could indicate a more stable bio-oil, it is more likely that the sulfur addition reactions are only decreasing the relative abundance of oxygen rather

than the absolute amount due to the way CHOS was calculated. Therefore, it can be surmised that reduction integrated catalysis may not have the stability enhancements expected from other integrated or pretreated trials.

Aqueous Phase Composition

Figure 4.20 shows the acetic acid concentration of reduction integrated catalysis trials.

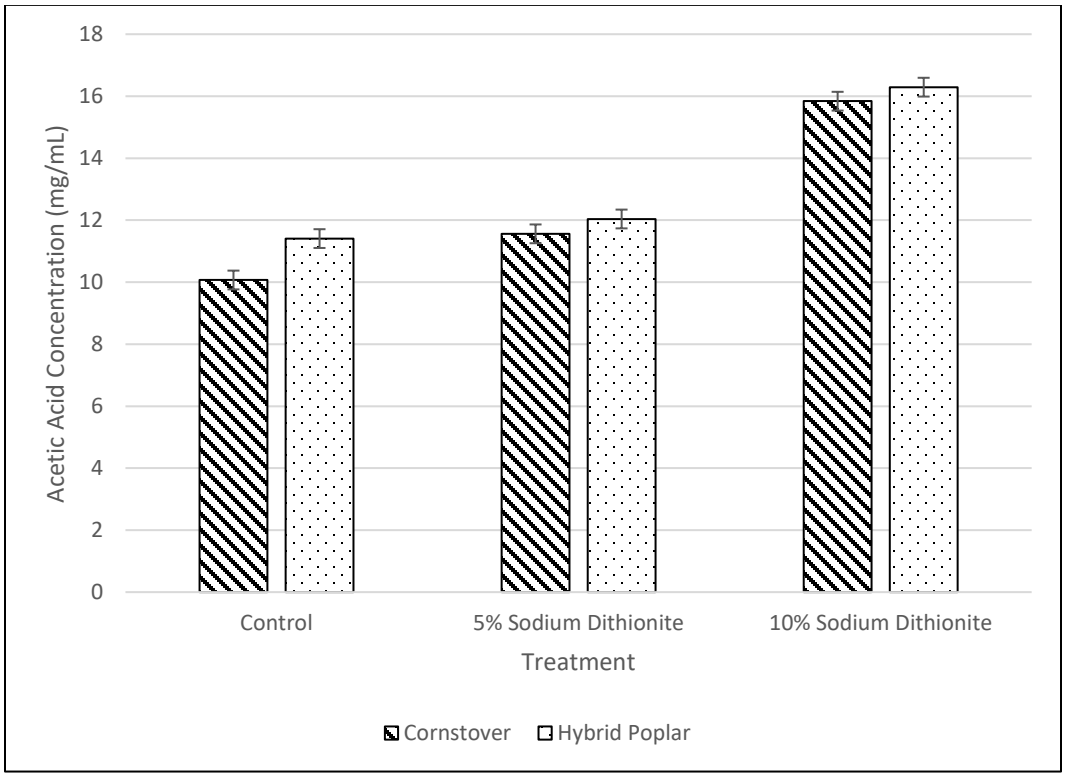

Figure 4.20 Acetic acid concentration (mg/mL) of reduction integrated catalysis trials

As shown, acetic acid concentration increases with increasing sodium dithionite concentration, which is to say sodium dithionite addition to biomass under high temperature and pressure conditions must have a beneficial effect for the formation of acetic acid.

Table 4.11 shows the acetic acid relative abundance % of reduction integrated catalysis.

Table 4.11 Relative abundance % of acetic acid in aqueous phase from reduction integrated catalysis (±0.99%)

Treatment	Corn Stover	Hybrid Poplar
Control	34.99	32.59
5% Sodium Dithionite	16.27	17.53
10% Sodium Dithionite	10.98	12.49

Similarly again to the alkaline integrated catalysis trials, reduction integrated catalysis yields a reduced relative abundance of acetic acid in the aqueous phase. Due to its unique, dark visual appearance, the other compounds in the aqueous phase are likely chromophores i.e. phenol and phenolic derivatives that were degraded from the HTL process. The alkaline integrated catalysis also had a diverse array of compounds in the

aqueous phase, suggesting, again, that the mechanism for acetic acid formation is similar.

Figure 4.21 plots Post-HTL pH against acetic acid concentrations of the reductive integrated catalysis trials.

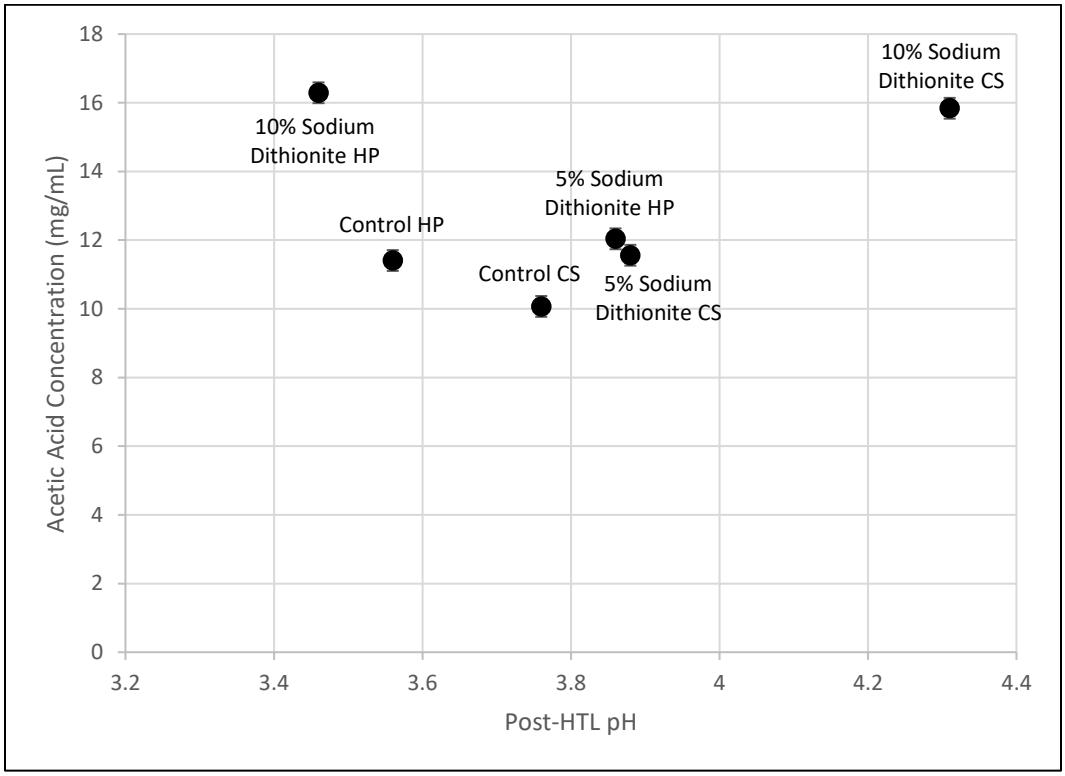

Figure 4.21 Post-HTL pH vs acetic acid concentration (mg/mL) of reduction integrated catalysis trials

As with most of the reductive integrated catalysis data, not much can be concluded from the information. The pH of the bio-oil does not seem to

correspond in any significant way to the concentration of acetic acid in the aqueous phase of the reductive integrated catalysis trials.

4.5.3 Aging Effects

The final aspect to be analyzed from the reduction integrated catalysis trials is the stability. As mentioned before, the stability effects might have been manipulated greatly from the introduction of sulfur compounds. With that assumption in mind, Table 4.12 shows the molecular weight values of the reduction integrated catalysis trials over time.

Table 4.12 Average molecular weight values over time for hybrid poplar reduction integrated catalysis bio-oil (±1.18)

Treatment	Initial	24 hour	1 week	3 week
Control	138.9	144.9	147.5	147.1
5% Sodium Dithionite	138.9	150.4	152.6	-
10% Sodium Dithionite	144.7	146.3	145.7	146.8

As shown, the 5% sodium dithionite reduction trials had much less stability compared to the 10% sodium dithionite reduction trial. When analyzing the individual compounds for the 5% sodium dithionite reduction trial, many of the small, sulfur compounds found in the initial bio-oil are not present in the aged bio-oil, likely caused by condensation reactions. This could be

the main cause for the large increase in molecular weight. In comparison, the 10% sodium dithionite trial retains many of the small sulfur compounds, and thusly increases less over time.

There is an unexpected reversal in pH stability marker trends when analyzing the reduction integrated catalysis bio-oils vs Post-HTL pH. Figure 4.22 and 4.23 show the molecular weight increase over time vs Mid- and Post-HTL pH, respectively.

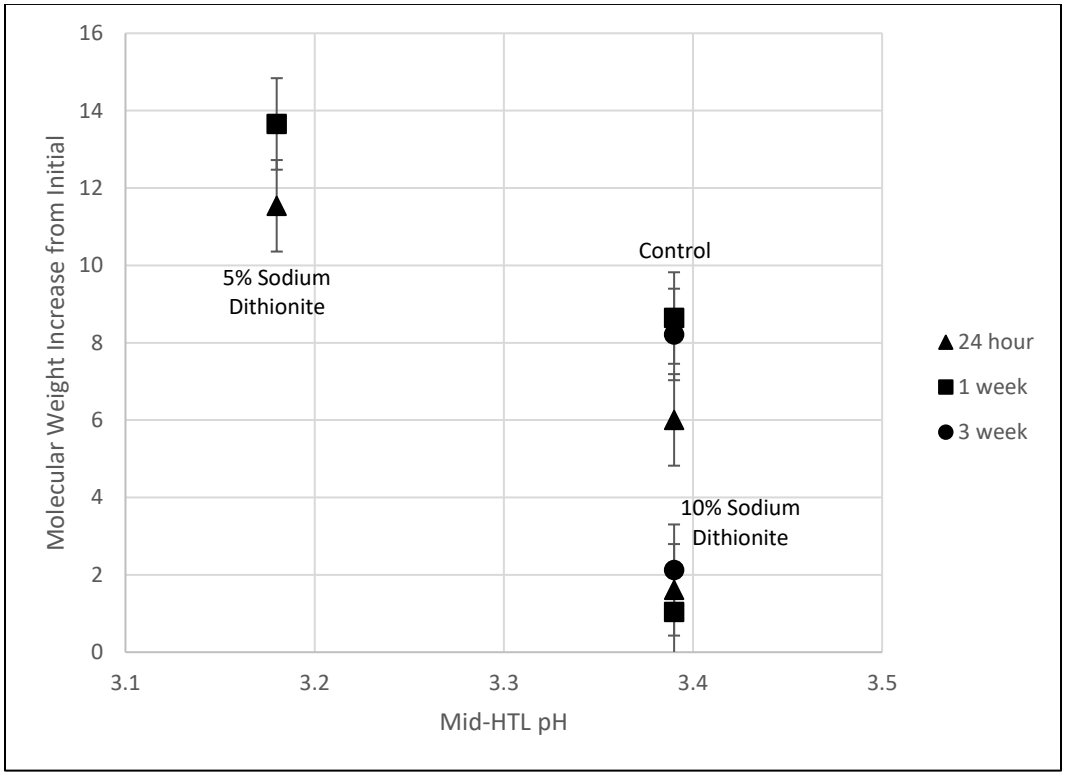

Figure 4.22 Molecular weight increase vs Mid-HTL pH of reduction integrated catalysis trials

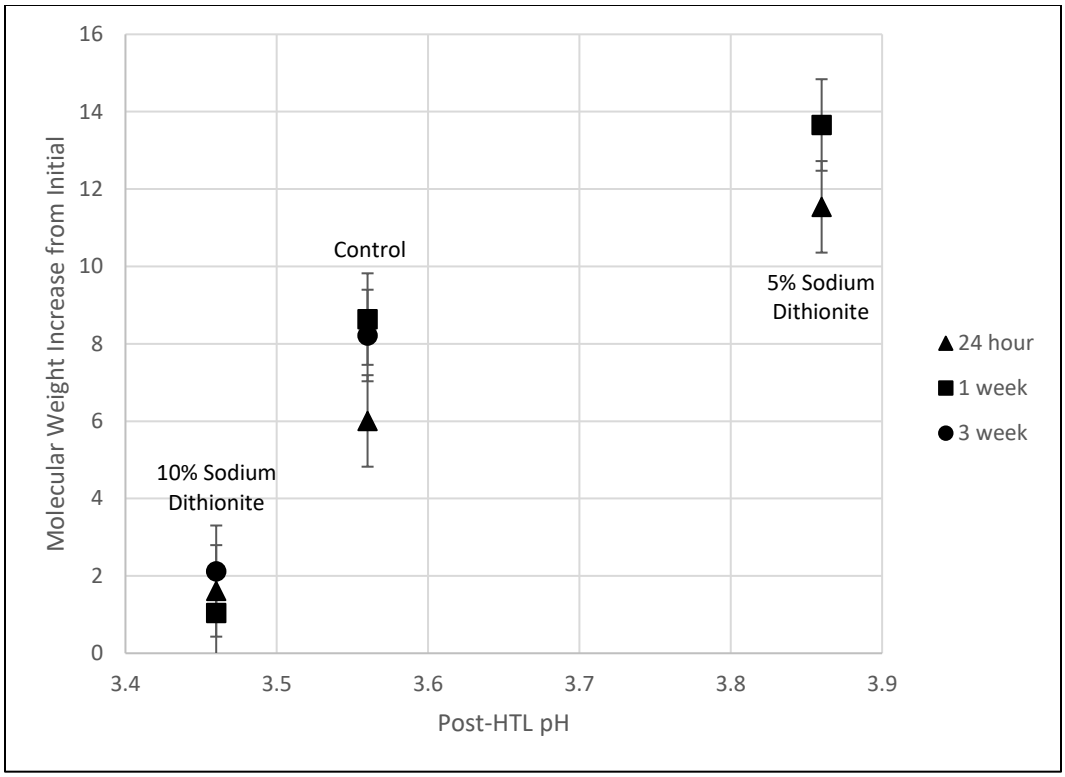

Figure 4.23 Molecular weight increase vs Post-HTL pH of reduction integrated catalysis trials

While Mid-HTL pH seems to have a similar trend of bio-oil stability with increasing pH, Post-HTL pH values seems to show a reversal of this trend. It is likely due to the addition of sulfur that cause the shown trends. These effects make it difficult to compare these trials to the other integrated catalysis and reductive pretreatment trials. While the acidic and alkaline integrated catalysis trials have solutions that are integrated into the resulting bio-oil, these solutions are much more inert compared to sodium dithionite, as seen with the similar compound distributions and the

lack of unique, solvent-specific products i.e. sulfur derivatives for sodium dithionite.

Total peak area % of the first 50 bio-oil compounds also shows a reversal in stability trends. Figure 4.24 shows the total peak area % of the first 50 compounds of initial and aged bio-oil vs Post-HTL pH.

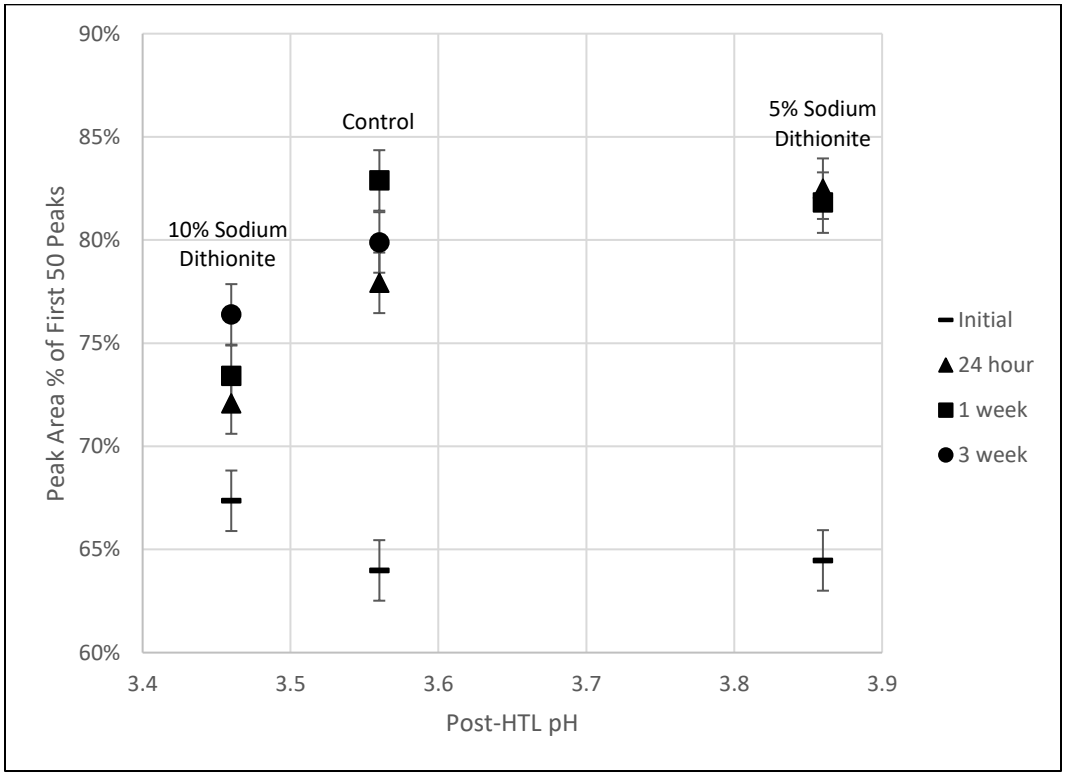

Figure 4.24 Total peak area % of first 50 compounds of initial and aged reduction integrated catalysis bio-oil compared to Post-HTL pH

Again, sulfur addition reactions may be playing some role in skewing data to show a reversal in stability trends compared to the other integrated and

pretreated bio-oils. While initial total peak area %s seem to follow similarly to the established trend, aged bio-oil does not follow the trend, likely due to an unknown phenomena.

Chapter 5 Conclusion

Biomass hydrothermal liquefaction is a complicated process that utilizes both thermal and chemical degradation to produce a complex, viscous bio-oil product. Both integrated catalysis and reductive pretreatment methods influenced in some way the yield, composition, and stability of the bio-oil.

Acidic integrated catalysis, as expected, produced high levels of solids via condensation reactions at the expense of decreasing condensable volatiles and thus liquid yield. Compositionally, acidic bio-oil was relatively much higher in furan derivatives, signifying possibly a higher value bio-oil as these compounds can be used in some capacity as platform chemicals. However, there is a tradeoff of bio-oil intrinsic value and bio-oil yield. This balance needs to be considered when designing bio-oil production. Stability over time of the acidic bio-oil was also much lower than the control bio-oil, most likely due to continuing condensation and repolymerization reactions, marked by the low Mid- and Post-HTL pHs of the bio-oil. A decrease in low-abundance chemicals over time also signaled low bio-oil stability.

Alkaline integrated catalysis saw comparable liquid yield with the control bio-oil. However, compositionally there were many noticeable differences between the two. Furfural and furan derivatives decreased under alkaline conditions, signifying there is some product inhibition. Most likely, the alkaline conditions neutralize a significant amount of organic acid species, which are probable to be the main drivers of furan formation. This mechanism is corroborated by the increased Mid- and Post-HTL pHs of the alkaline bio-oil. While high value platform chemicals such as furfural are decreased in alkaline bio-oil, the higher pH leads to greater bio-oil stability. Over time, alkaline integrated catalysis bio-oil increased in molecular weight less than the control and acidic bio-oils and had more chemical diversity.

Reductive pretreatment methods with sodium dithionite and sodium borohydride resulted in many interesting effects on bio-oil composition and stability. Furan derivatives decreased markedly under both sodium borohydride and sodium dithionite reductive pretreatment conditions. With sodium borohydride pretreatment, alkalization increased Pre-HTL pH, inhibiting furan formation. Sodium dithionite pretreatment neutralized the Pre-HTL pH, also slightly inhibiting furan formation. Lignin fragment species e.g. Eugenol, increased greatly with reductive pretreatment, likely

caused by conversion of carbonyl groups on the γ-carbon of lignin to OH groups. Subsequently, these groups would be prone to removal via water formation during the HTL process. Overall, resulting Mid- and Post-HTL pH of the reductive pretreatment bio-oil was greater than the control, signifying possible stability enhancements. Resulting bio-oil stability was comparable or slightly greater than the control according to the molecular weight increase over time and chemical diversity markers, suggesting the possibility that a reductive pretreatment or similar processes could potentially increase downstream bio-oil stability.

Reductive integrated catalysis with sodium dithionite did not produce results that are comparable to the other integrated catalysis and reductive pretreatment methods. The addition of sulfur compounds into the bio-oil creates difficulties when analyzing for stability and composition. Solid and gaseous content increased with increasing integrated reducing agent solution concentration. Sodium dithionite is a lignin-retaining reducing agent and therefore does not necessarily destabilize the macro-structure for assisted volatilization during the HTL process. As for gaseous content, sodium dithionite is a relatively unstable reducing agent that degrades when in aqueous solution. Therefore, one cause of increased gaseous content is the degradation of sodium dithionite. Compositionally, the

reductive integrated catalysis yielded sulfur compounds, and, as a result, shifted the ratio of carbon and oxygen lower. However, as previously stated, it is likely that the carbon and oxygen content did not decrease in absolute abundance, but rather only in relative abundance.

In all, reductive pretreatment of biomass could be used for higher yield production of double bonded γ-carbon products such as Eugenol, which can be used for perfumes and flavorings. By increasing its abundance in bio-oil, the overall product value is increased, leading to possible further development of the technologies employed in thermochemical conversion. Moreover, reductive pretreatment methods could lead to greater bio-oil stability, even further increasing its value as an efficient energy carrier or viable biomass densification medium.

Bio-oil stability and chemical composition are the two most important factors when determining its value. Further research must be done to both optimize high-value chemical production and inherent stability to create a more profitable bio-oil product. Inert pH and oxygen controllers with buffers or pretreatments could be possible avenues to efficiently address these two factors. As with most biomass related research, further development must also be made on understanding and optimizing the

hydrothermal liquefaction process to increase bio-oil yield and throughput. Continuous reactors are more cost effective than batch reactors, which is one area that HTL will need to progress quickly in. While future biomass-related technologies may seem distant, as global demand for energy and chemicals increase, with greater understanding of our impact on the climate, the green sector will expand, and, with it, a sustainable future will be finally within our collective grasp.

Bibliography

(1) Akhtar, J., & Amin, N. (2011). A review on process conditions for optimum bio-oil yield in hydrothermal liquefaction of biomass. *Renewable and Sustainable Energy Reviews*, 1615-1624.

(2) Azadi, P., Malina, R., Barrett, S., & Kraft, M. (2017). The evolution of the biofuel science. *Renewable and Sustainable Energy Reviews*, 1479-1484.

(3) Boerjan, W., Ralph, J., & Baucher, M. (2003). Lignin Biosynthesis. *Annual Review of Plant Biology*, 519-546.

(4) Braimakis, K., Atsonios, K., Panopoulos, K. D., Karellas, S., & Kakaras, E. (2014). Economic evalution of decentralized pyrolysis for the production of bio-oil as an energy carrier for improved logistics towards a large centralized gasification plant. *Renewable and Sustainable Energy Reviews*, 57-72.

(5) Bridgwater, A. (2012). Review of fast pyrolysis of biomass and product upgrading. *Biomass and Bioenergy*, 68-94.

(6) Caretto, A., & Perosa, A. (2013). Upgrading of Levulinic Acid with Dimethylcarbonate as Solvent/Reagent. *ACS Sustainable Chemistry and Engineering*, 989-994.

(7) Carpenter, D., Westover, T. L., Stefan, C., & Jablonski, W. (2014). Biomass feedstocks for renewable fuel production: a review of the impacts of feedstock and pretreatment on the yield and product distribution of fast pyrolysis bio-oils and vapors. *Green Chemistry*, 384-406.

(8) Chiappe, C., Rodriguez Douton, M. J., Mezzetta, A., Guazzelli, L., Pomelli, C. S., Assanelli, G., & de Angelis, A. R. (2018). Exploring and exploiting different catalytic systems for the direct conversion of cellulose into levulinic acid. *New Journal of Chemistry*, 1845-1852.

(9) Demirbas, A. (2011). Competitive liquid biofuels from biomass. *Applied Energy*, 17-28.

(10) Dence, C. W. (1996). Chemistry of Mechanical Pulp Bleaching. In C. W. Dence, & D. W. Reeve, *Pulp Bleaching: Principles and Practice* (pp. 161-182). Atlanta: TAPPI Press.

(11) Dimitriadis, A., & Bezergianni, S. (2017). Hydrothermal liquefaction of various biomass and waste feedstocks for biocrude production: A

state of the art review. *Renewable and Sustainable Energy Reviews*, 113-125.

(12) Ellis, M. E. (1996). Hydrosulfite (Dithionite) Bleaching. In C. W. Dence, & D. W. Reeve, *Pulp Bleaching: Principles and Practice* (pp. 491-512). Atlanta: TAPPI Press.

(13) Elumalai, S., & Pan, X. J. (2011). Chemistry and Reactions of Forest Biomass in Biorefining. In J. Zhu, X. Zhang, & X. Pan, *Sustainable Production of Fuels, Chemicals, and Fibers from Forest Biomass* (pp. 109-144). Washington DC: OUP USA.

(14) Fengel, D. (1966). Die Hemicellulosen in unbehandeltem und in thermisch behandeltem Fichtenholz. *Holz als Roh-und Werkstoff*, 98-109.

(15) Fengel, D. (1967). Das Verhalten der Cellulose im Fichtenholz bei thermischer Behandlung. *Holz als Roh-und Werkstoff*, 102-11.

(16) Fengel, D., & Wegener, G. (1983). *Wood: chemistry, ultrastructure, reactions.* Berlin: Walter de Gruyter.

(17) Gierer, J., & Wannstrom, S. (1986). Formation of Ether Bonds between Lignins and Carbohydrates during Alkaline Pulping Processes. *Holzforschung*, 347-352.

(18) Gollakota, A., Kishore, N., & Gu, S. (2018). A review on hydrothermal liquefaction of biomass. *Renewable and Sustainable Energy Reviews*, 1378-1392.

(19) Goudriaan, F., & Peferoen, D. (1990). Liquid Fuels From Biomass Via A Hydrothermal Process. *Chemical Engineering Science*, 2729-2734.

(20) Hashaikeh, R., Fang, Z., Butler, I., Hawari, J., & Kozinski, J. (2007). Hydrothermal dissolution of willow in hot compressed water as a model for biomass conversion. *Fuel*, 1614-1622.

(21) Jindal, M. K., & Jha, M. K. (2016). Hydrothermal liquefaction of wood: a critical review. *Reviews in Chemical Engineering*, 459-488.

(22) Kabyemela, B. M., Takigawa, M., Adschiri, T., Malaluan, R. M., & Arai, K. (1998). Mechanism and Kinetics of Cellobiose Decomposition in Sub- and Supercritical Water. *Industrial and Engineering Chemistry Research*, 357-361.

(23) Keegstra, K. (2010). Plant Cell Walls. *Plant Physiology*, 483-486.

(24) Khampuang, K., Boreriboon, N., & Prasassarakich, P. (2015). Alakali catalyzed liquefaction of corncob in supercritical ethanol-water. *Biomass and Bioenergy*, 460-466.

(25) Kollmann, F., & Fengel, D. (1965). Anderungen der chemischen Zusammensetzung von Holz durch thermische Behandlung. *Holz als Roh-und Werkstoff*, 461-468.

(26) Kumar, M., Oyedun, A. O., & Kumar, A. (2018). A review on the current status of various hydrothermal technologies on biomass feedstock. *Renewable and Sustainable Energy Reviews*, 1742-1770.

(27) Li, C., Thompson, V. S., & Thompson, D. N. (2016). Impact of feedstock quality and variation on biochemical and thermochemical conversion. *Renewable and Sustainable Energy Reviews*, 525-536.

(28) Li, F., Hu, Z., & Xiao, B. (2017). Bio-oil Production by Thermochemical Catalytic Liquefaction of Bloom-Forming Cyanobacteria: Optimization Using Response Surface Methodology (RSM). *Energy and Fuels*, 13733-13742.

(29) Meng, J., Moore, A., Tilotta, D., Kelley, S., & Park, S. (2014). Toward Understanding of Bio-Oil Aging: Accelerated Aging of Bio-Oil Fractions. *ACS Sustainable Chemistry and Engineering*, 2011-2018.

(30) Mohan, D., Pittman, Jr., C. U., & Steele, P. H. (2006). Pyrolysis of Wood/Biomass for Bio-oil: A Critical Review. *Energy and Fuels*, 848-889.

(31) Plomion, C., Leprovost, G., & Stokes, A. (2001). Wood Formation in Trees. *Plant Physiology*, 1513-1523.

(32) Qian, Y., Zuo, C., Tan, J., & He, J. (2007). Structural analysis of bio-oils from sub-and supercritical water liquefaction of woody biomass. *Energy*, 196-202.

(33) Ramirez, J. A., Brown, R. J., & Rainey, T. J. (2015). A Review of Hydrothermal Liquefaction Bio-Crude Properties and Prospects for Upgrading to Transportating Fuels. *Energies*, 6765-6794.

(34) Roffael, E., & Schaller, K. (1971). EinfluB thermischer Behandlung auf Cellulose. *Holz als Roh-und Werkstoff*, 275-278.

(35) Shafizadeh, F., & DeGroot, W. F. (1976). Combustion Characteristics of Cellulosic Fuels. In F. Shafizadeh, K. V. Sarkanen, & D. A. Tillman, *Thermal Uses and Properties of Carbohydrates and Lignins* (pp. 1-17). New York: Academic Press.

(36) Somerville, C. (2006). Cellulose Synthesis in Higher Plants. *Annual Review of Cell and Developmental Biology*, 53-78.

(37) Vassilev, S. V., Baxter, D., Andersen, L. K., Vassileva, C. G., & Morgan, T. J. (2012). An overview of the organic and inorganic phase composition of biomass. *Fuel*, 1-33.

(38) Wang, D., Montane, D., & Chornet, E. (1996). Catalytic steam reforming of biomass-derived oxygenates: acetic acid and hydroxyacetaldehyde. *Applied Catalysis*, 245-270.

(39) Wang, Z., Xu, J., & Cheng, J. J. (2011). Modeling Biochemical Conversion of Lignocellulosic Materials for Sugar Production: A Review. *Bioresources*, 5282-5306.

(40) Williams, C. L., Westover, T. L., Emerson, R. M., Tumuluru, J. S., & Li, C. (2016). Sources of Biomass Feedstock Variability and the Potential Impact on Biofuels Production. *BioEnergy Research*, 1-14.

(41) Xian, L., Zhao, Z., Xu, G., Han, S., & Yu, H. (2017). Progress on upgrading methods of bio-oil: A review. *International Journal of Energy Research*, 1798-1816.

(42) Xiu, S., & Shahbazi, A. (2012). Bio-oil production and upgrading research: A review. *Renewable and Sustainable Energy Reviews*, 4406-4414.

(43) Xu, C., & Lad, N. (2008). Production of Heavy Oils with High Caloric Values by Direct Liquefaction of Woody Biomass in Sub/Near-critical Water. *Energy and Fuels*, 635-642.

(44) Xue, Y., Chen, H., Zhao, W., Yang, C., Ma, P., & Han, S. (2016). A review on the operating conditions of producing bio-oil from hydrothermal liquefaction of biomass. *International Journal Of Energy Research*, 865-877.

(45) Ye, L., Zhang, J., Zhao, J., & Tu, S. (2014). Liquefaction of bamboo shoot shell for the production of polyols. *Bioresource Technology*, 147-153.

(46) Yoon, S.-Y., Han, S.-H., & Shin, S.-J. (2014). The effect of hemicelluloses and lignin on acid hydrolysis of cellulose. *Energy*, 19-24.

(47) Zhang, B., Keitz, M. v., & Valentas, K. (2008). Thermal Effects on Hydrothermal Biomass Liquefaction. *Applied Biochemistry and Biotechnology*, 143-150.

(48) Zhong, C., & Wei, X. (2004). A comparative experimental study on the liquefaction of wood. *Energy*, 1731-1741.